

Supplementary Information

Divergent Response of Homologous ATP Sites to Stereospecific Ligand Fluorination for Selectivity Enhancement

Alpesh Patel, Ari Hardianto, Shoba Ranganathan, Fei Liu*

*Department of Chemistry and Biomolecular Sciences, Macquarie University, Sydney, New South
Wales, Australia, 2109*

I. Synthesis of (-)-balanol **1** and balanoids **1a–1e**.

A. General information. (S2)

B. Synthesis and characterization of the final balanol **1** and balanoids **1a–1e**. (S2–S11)

C. References. (S11)

D. NMR spectra of **1**, **3a–3e**, **3.1a–3.1e**, and **1a–1e**. (S12–S43)

II. Binding affinity measurements.

A. Binding assay for balanol and balanoids. (S44–S45)

B. Full set of binding constants and curves measured for balanol **1** and balanoids **1a–1e** against PKA/C isozymes. (S45–S49)

III. Docking analysis.

A. Development of docking protocols using the balanol-PKA X-ray crystal structure (pdb code:1BX6). (S50–S52)

B. Construction of the PKC ϵ structural homology model. (S52–S56)

C. Docking simulation of balanoids to PKA/C using optimised docking simulation procedure. (S56–S64)

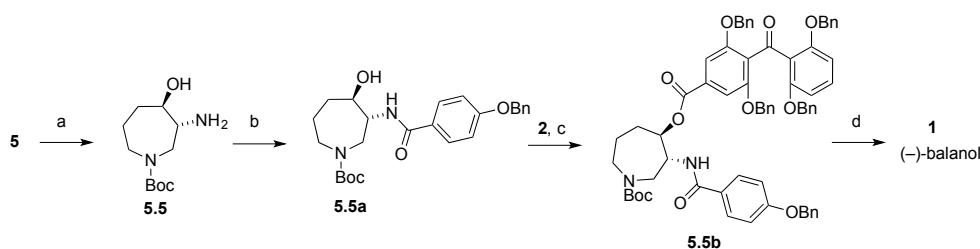
D. References. (S65)

I. Synthesis of (-)-balanol **1** and balanoids **1a–1e**.

A. General information.

All reactions were conducted under N₂ atmosphere. Unless otherwise specified, all reagents were purchased from Sigma–Aldrich and used without further purification. CH₂Cl₂ was obtained from a solvent purification system (Innovative Technology SPS400) and stored over MS 4Å beads. Acetone, EtOAc and petroleum ether were distilled before use. Petroleum ether refers to the fraction collected between 60 °C and 80 °C. THF was distilled from Na–benzophenone and stored over MS 4Å beads. ¹H NMR spectra were recorded at 25 °C on either a Bruker DRX600K or DPX400 NMR spectrometer and are reported in ppm using the specified solvent as the internal standard (CDCl₃ at 7.26 ppm, (CD₃)₂SO at 2.50 ppm, CD₃CN at 1.94 ppm). ¹³C NMR spectra are reported in ppm using the specified solvent as the internal standard (CDCl₃ at 77.16 ppm, (CD₃)₂SO at 39.52 ppm, CD₃CN at 1.32 and 118.26 ppm).

B. Synthesis and characterization of the final balanol **1** and balanoids **1a–1e**.



Scheme S1.1. Synthesis of balanol **1**. *Reagents and conditions:* (a) H₂, Pd/C, triflic acid, MeOH, 14 h, 25 °C; (b) Et₃N, 4-benzyloxybenzoyl chloride, 2 h, 25 °C, 52% over two steps; (c) 2-chloro-1-methylpyridinium iodide, DMAP, NEt₃, DCM, 8 h, 25 °C, 75%; (d) i) H₂, Pd/C, THF, H₂O, AcOH, 25 °C, 10 h; ii) TFA, neat, 5 min., 25 °C, 70%.

The benzophenone (**2**) and azepane fragment **5** were synthesized as described previously.^[1] The coupling of benzophenone (**2**) and azepane (**5.5a**) fragments was successfully accomplished via esterification using the Mukaiyama procedure to afford the fully protected balanol progenitor **5.5b** in 75% yield (Scheme S1.1). The universal benzyl deprotection was achieved by mild palladium-catalyzed hydrogenolysis of **5.5b** in acidic media to obtain the Boc protected balanol as a yellow solid, which was subjected to purification by reverse phase HPLC. The Boc deprotection was readily achieved by treatment with neat TFA to furnish balanol (**1**) in 70% yield, which exhibited characterization data consistent with that from previous reports.

2-(2,6-dihydroxy-4-(((3R,4R)-3-(4-hydroxybenzamido)azepan-4-yloxy)carbonyl) benzoyl)-3-hydroxybenzoic acid (1**)**

$[\alpha]_D^{20} = -109.3$ (*c* 0.12, MeOH); $^1\text{H NMR}$ (400 MHz, $(\text{CD}_3)_2\text{SO}$) δ 11.67 (s, 2H), 9.88 (brs, 1H), 9.06 (brs, 1H), 8.98 (brs, 1H), 8.51 (d, $J = 7.91$ Hz, 1H), 7.64 (d, $J = 8.87$ Hz, 2H), 7.37 (dd, $J = 7.78, 1.01$ Hz, 1H), 7.27 (t, $J = 7.90$ Hz, 1H), 7.05 (dd, $J = 8.00, 1.01$ Hz, 1H), 6.78 (d, $J = 8.66$ Hz, 2H), 6.78 (s, 2H), 5.29–5.23 (m, 1H), 4.53–4.45 (m, 1H), 3.39–3.25 (m, 2H), 3.20–3.11 (brs, 2H), 2.17–2.08 (m, 1H), 2.03–1.79 (m, 3H); $^{13}\text{C NMR}$ (100 MHz, $(\text{CD}_3)_2\text{SO}$) δ 201.6, 166.9, 166.2, 164.2, 161.5, 160.5, 153.3, 135.5, 132.5, 129.3, 129.0, 128.9, 124.4, 120.0, 119.7, 114.9, 113.5, 107.3, 75.9, 50.8, 46.0, 45.9, 28.2; MS (ESI): m/z , 551.17 [$\text{M}^+ + \text{H}$].

(3*R*,4*R*)-3-(4-(benzyloxy)benzamido)-4-hydroxyazepane-1-carboxylic acid-*tert*-butyl ester (5.5a)

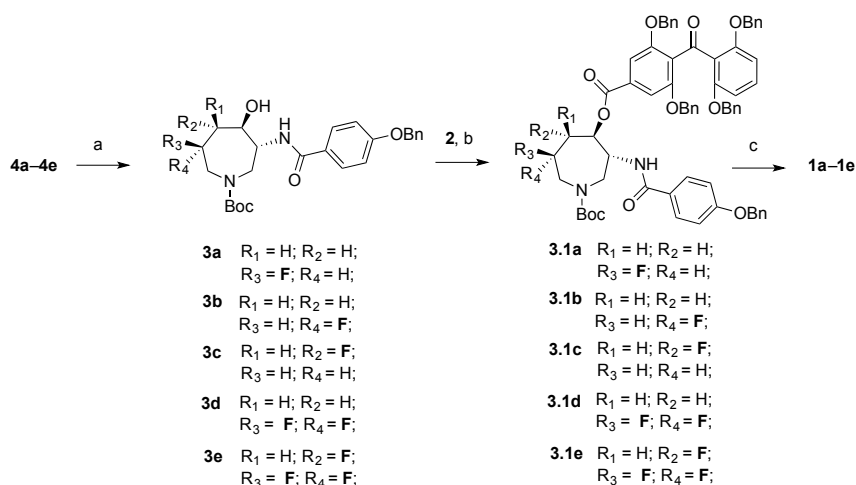
A solution of compound **5** (20 mg, 58.1 μmol) and trifluoromethanesulfonic acid (4 μL , 58.1 μmol) in MeOH (1.21 mL) was treated with Pd/C (5% w/w). The resulting suspension was stirred under H_2 (1 atm) for 14 h. The reaction mixture was then filtered through a pad of Celite which was rinsed with MeOH (1 mL \times 5). The solvent was evaporated under reduced pressure to yield the desired amine **5.5** which was used in the next step without further purification. 4-benzyloxybenzoyl chloride (15.6 mg, 68.1 μmol) was added to the solution of amine **5.5** and Et_3N (64 μL , 681 μmol) in CH_2Cl_2 (0.81 mL) under N_2 atmosphere. The reaction mixture was stirred for 2 h at 25 $^\circ\text{C}$ before it was quenched by the addition of MeOH (0.15 mL) and pyridine (0.15 mL). The volatiles were evaporated under vacuum and the residue was dissolved in EtOAc. The organic phase was successively washed with aqueous 2 *N* HCl, water, aqueous saturated NaHCO_3 , and brine. The organic layer was then dried (Na_2SO_4) before vacuum evaporation to obtain the crude mixture, which was purified by flash chromatography (petroleum ether/ethyl acetate, 1/1) to afford azepane **5.5a** (15.6 mg, 52% over two steps) as a colourless oil with NMR, optical rotation and mass spectra matching to those reported previously.^[1] R_f (petroleum ether/EtOAc, 1/1) 0.33; $[\alpha]_D^{20} = -4.1$ (*c* 0.8, CH_2Cl_2); $^1\text{H NMR}$ (400 MHz, CD_2Cl_2) δ 8.96 (d, $J = 4.98$ Hz, 1H), 7.90 (d, $J = 8.71$ Hz, 2H), 7.51–7.36 (m, 5H), 7.08 (d, $J = 8.71$ Hz, 2H), 5.17 (s, 2H), 4.11–4.02 (m, 3H), 3.82–3.75 (m, 1H), 3.33 (dd, $J = 15.46, 4.90$ Hz, 1H), 2.79 (ddd, $J = 13.88, 12.30, 3.50$ Hz, 1H), 1.95–1.63 (m, 4H), 1.54 (s, 9H); $^{13}\text{C NMR}$ (100 MHz, CD_2Cl_2) δ 168.5, 162.0, 157.7, 137.0, 129.4, 129.0, 128.5, 128.0, 126.5, 115.0, 81.0, 78.0, 70.5, 61.2, 50.7, 50.1, 33.1, 28.5, 27.5; MS (ESI): m/z , 441.23 [$\text{M}^+ + \text{H}$].

(3*R*,4*R*)-*tert*-butyl-3-(4-(benzyloxy)benzamido)-4-(3,5-bis(benzyloxy)-4-(2-(benzyloxy)-6-(benzyloxycarbonyl)benzoyl)benzoyloxy)azepane-1-carboxylate (5.5b)

A suspension of hydroxyazepane benzamide **5.5a** (15.6 mg, 35.4 μmol), benzophenone **2** (24.0 mg, 35.4 μmol) and 2-chloro-1-methylpyridinium iodide (11.8 mg, 46.0 μmol) in CH_2Cl_2 (0.35 mL) was treated with Et_3N (9.9 μL , 70.8 μmol) and allowed to stir for 30 min at 25 $^\circ\text{C}$. The reaction

mixture was then reacted with 4-dimethylaminopyridine (2.2 mg, 17.7 μmol) and was allowed to stir for 8 h at 25 °C before vacuum evaporation to obtain the crude mixture for purification by flash chromatography (petroleum ether/ethyl acetate, 3/2) to afford the fully protected balanol **5.5b** (29.2 mg, 75%) as a colourless oil with NMR, optical rotation and mass spectra matching to those reported previously.^[2] R_f (petroleum ether/EtOAc, 3/2) 0.31; $[\alpha]_D^{20} = -61.1$ (c 0.7, CH_2Cl_2); ^1H NMR (400 MHz, CDCl_3) δ 8.03 (d, $J = 7.60$ Hz, 1H), 7.77 (d, $J = 8.56$ Hz, 2H), 7.42–7.03 (m, 27H), 6.93 (brd, $J = 8.82$ Hz, 3H), 6.82 (d, $J = 7.92$ Hz, 2H), 5.11 (s, 2H), 5.05 (s, 2H), 4.84 (s, 4H), 4.67 (s, 2H), 4.13–3.94 (m, 2H), 3.35 (dd, $J = 15.66, 5.77$ Hz, 1H), 2.89–2.79 (m, 1H), 2.09–1.69 (m, 6H), 1.57 (s, 9H); ^{13}C NMR (100 MHz, CDCl_3) δ 191.7, 167.5, 166.4, 165.8, 161.4, 158.1, 156.4, 136.5, 135.9, 135.8, 132.9, 130.6, 129.0, 128.8, 128.4, 128.3, 128.0, 127.9, 127.6, 127.5, 127.4, 122.1, 115.5, 114.7, 107.1, 81.0, 77.9, 70.6, 70.1, 67.2, 53.7, 50.3, 49.8, 28.6; MS (ESI): m/z , 1101.24 [$\text{M}^+ + \text{H}$].

A solution of fully protected balanol **5.5b** (20.0 mg, 18.2 μmol) in THF/AcOH/Water (16/4/1) at 25 °C was treated with Pd/C (10% w/w) and stirred under H_2 atmosphere (1 atm) for 10 h at 25 °C before it was filtered through a pad of celite and vacuum evaporated to obtain the crude mixture. The crude was then chromatographed on a Phenomenex Gemini C18 column (150 \times 21.20 mm) eluting with MeCN/water/TFA (from 35:65:0.1 to 39:61:0.1 over 25 min; flow rate: 8.80 mL/min; retention time 19.5 min) to provide boc-protected balanol as a pale yellow solid powder. The compound was treated with TFA (1 mL) at 25 °C for 5 min before TFA was vacuum evaporated. The reaction flask was kept under high vacuum (0.005 Torr, 25 °C) for 3 h to remove traces of TFA, and the pale yellow film obtained was characterized as balanol (**1**) (7.0 mg, 70%) with NMR, optical rotation and mass spectra matching to those reported previously.^[3] $[\alpha]_D^{20} = -109.3$ (c 0.12, MeOH); ^1H NMR (400 MHz, $(\text{CD}_3)_2\text{SO}$) δ 11.67 (s, 2H), 9.88 (brs, 1H), 9.06 (brs, 1H), 8.98 (brs, 1H), 8.51 (d, $J = 7.91$ Hz, 1H), 7.64 (d, $J = 8.87$ Hz, 2H), 7.37 (dd, $J = 7.78, 1.01$ Hz, 1H), 7.27 (t, $J = 7.90$ Hz, 1H), 7.05 (dd, $J = 8.00, 1.01$ Hz, 1H), 6.78 (d, $J = 8.66$ Hz, 2H), 6.78 (s, 2H), 5.29–5.23 (m, 1H), 4.53–4.45 (m, 1H), 3.39–3.25 (m, 2H), 3.20–3.11 (brs, 2H), 2.17–2.08 (m, 1H), 2.03–1.79 (m, 3H); ^{13}C NMR (100 MHz, $(\text{CD}_3)_2\text{SO}$) δ 201.6, 166.9, 166.2, 164.2, 161.5, 160.5, 153.3, 135.5, 132.5, 129.3, 129.0, 128.9, 124.4, 120.0, 119.7, 114.9, 113.5, 107.3, 75.9, 50.8, 46.0, 45.9, 28.2; MS (ESI): m/z , 551.17 [$\text{M}^+ + \text{H}$].



Scheme S1.2. Synthesis of balanoids **1a–1e**. *Reagents and conditions:* (a) i) H₂, Pd/C, triflic acid, MeOH, 14 h, 25 °C; ii) Et₃N, 4-benzyloxybenzoyl chloride, 2 h, 25 °C; (b) 2-chloro-1-methylpyridinium iodide, DMAP, NEt₃, DCM, 8 h, 25 °C; (c) i) H₂, Pd/C, THF, H₂O, AcOH, 25 °C, 10 h; ii) TFA, neat, 5 min., 25 °C.

The azepanes **4a–4e** were prepared as described previously^[4] and subjected to the same coupling protocol that used in the total synthesis of (–)-balanol (**1**). The palladium catalyzed hydrogenation in acidic conditions followed by amidation to afforded the azepane benzamides (**3a–3e**) which were then coupled with benzophenone (**2**) to furnish the fluorinated, fully protected balanoids (**3.1a–3.1e**). Finally, removal of both the benzyl and Boc groups furnished the fluorinated balanol analogues (**1a–1e**) in fair yields (Scheme S1.2).

(3*R*,4*R*,6*S*)-3-(4-(benzyloxy)benzamido)-6-fluoro-4-hydroxyazepane-1-carboxylic acid-*tert*-butyl ester (**3a**)

The procedure for the synthesis of **5.5a** was followed: yield 50% over two steps; colourless oil; R_f (petroleum ether/EtOAc, 1/1) 0.34; [α]_D²⁰ = +19.7 (*c* 1.4, CH₂Cl₂); IR (film) ν_{max} (cm⁻¹): 3500–3100 (br), 1673, 1634, 1607, 1508, 1243, 1200, 1178, 1134, 1049, 849, 799, 721; ¹H NMR (400 MHz, CDCl₃) δ 8.76 (d, *J* = 5.34 Hz, 1H), 7.84 (d, *J* = 8.78 Hz, 2H), 7.45–7.31 (m, 5H), 7.02 (d, *J* = 8.76 Hz, 2H), 5.52 (brs, 1H), 5.12 (s, 2H), 4.70–4.50 (m, ¹*J*_{HF} = 45.93 Hz, 1H), 4.37 (dd, *J* = 13.54, 5.55 Hz, 1H), 4.18–4.09 (m, 2H), 3.79 (dd, *J* = 11.03, 6.67 Hz, 1H), 3.33 (dd, *J* = 15.74, 5.47 Hz, 1H), 2.88–2.78 (m, 1H), 2.37 (dd, *J* = 15.24, 15.15 Hz, 1H), 2.23–2.12 (m, 1H), 1.49 (s, 9H); ¹³C NMR (100 MHz, CDCl₃) δ 168.8, 161.9, 157.2, 136.5, 129.3, 128.8, 128.3, 127.6, 125.6, 114.9, 87.6 (d, ¹*J*_{CF} = 176.82 Hz), 82.0, 73.7 (d, ³*J*_{CF} = 14.86 Hz), 70.3, 60.2, 53.3 (d, ²*J*_{CF} = 34.19 Hz), 50.4, 39.5 (d, ²*J*_{CF} = 19.96 Hz), 28.4; HRMS (ESI): [M + H]⁺, *m/z* calcd for C₂₅H₃₂FN₂O₅ 459.2295, found 459.2299.

(3R,4R,6R)-3-(4-(benzyloxy)benzamido)-6-fluoro-4-hydroxyazepane-1-carboxylic acid-*tert*-butyl ester (3b)

The procedure for the synthesis of **5.5a** was followed: yield 48% over two steps; colourless oil; R_f (petroleum ether/EtOAc, 1/1) 0.35; $[\alpha]_D^{20} = -38.8$ (c 0.9, CH_2Cl_2); IR (film) ν_{max} (cm^{-1}): 3500–3100 (br), 1673, 1634, 1607, 1508, 1243, 1200, 1178, 1134, 1049, 849, 799, 721; ^1H NMR (400 MHz, CDCl_3) δ 8.99 (d, $J = 4.88$ Hz, 1H), 7.85 (d, $J = 8.79$ Hz, 2H), 7.44–7.30 (m, 5H), 7.01 (d, $J = 8.83$ Hz, 2H), 5.11 (s, 2H), 4.87–4.72 (m, $^1J_{\text{HF}} = 45.06$ Hz, 1H), 4.43 (dd, $J = 15.94, 15.28$ Hz, 1H), 4.27–4.06 (m, 3H), 3.21 (dd, $J = 15.48, 5.38$ Hz, 1H), 2.98 (dd, $J = 15.81, 2.02$ Hz, 1H), 2.39–1.97 (m, 2H), 1.47 (s, 9H); ^{13}C NMR (100 MHz, CDCl_3) δ 168.8, 161.9, 157.8, 135.8, 129.3, 128.8, 128.3, 127.6, 125.8, 114.8, 88.7 (d, $^1J_{\text{CF}} = 178.54$ Hz), 81.7, 72.0 (d, $^3J_{\text{CF}} = 6.67$ Hz), 70.2, 60.2, 54.4 (d, $^2J_{\text{CF}} = 22.99$ Hz), 50.1, 37.4 (d, $^2J_{\text{CF}} = 20.06$ Hz), 28.4; HRMS (ESI): $[\text{M} + \text{H}]^+$, m/z calcd for $\text{C}_{25}\text{H}_{32}\text{FN}_2\text{O}_5$ 459.2295, found 459.2300.

(3R,4S,5S)-3-(4-(benzyloxy)benzamido)-5-fluoro-4-hydroxyazepane-1-carboxylic acid-*tert*-butyl ester (3c)

The procedure for the synthesis of **5.5a** was followed: yield 48% over two steps; colourless oil; R_f (petroleum ether/EtOAc, 1/1) 0.34; $[\alpha]_D^{20} = +44.5$ (c 1.2, CH_2Cl_2); IR (film) ν_{max} (cm^{-1}): 3500–3100 (br), 1673, 1634, 1607, 1508, 1243, 1200, 1178, 1134, 1049, 849, 799, 721; ^1H NMR (400 MHz, CDCl_3) δ 8.36 (d, $J = 4.83$ Hz, 1H), 7.79 (d, $J = 8.28$ Hz, 2H), 7.43–7.30 (m, 5H), 6.99 (d, $J = 8.93$ Hz, 2H), 5.10 (s, 2H), 4.81–4.62 (dt, $J = 45.88$ ($^1J_{\text{HF}}$), 9.43, 9.0 Hz, 1H), 4.20–3.89 (m, 3H), 3.28–3.20 (m, 1H), 3.06–2.95 (m, 2H), 2.28–2.14 (m, 1H), 2.07–1.93 (m, 1H), 1.48 (s, 9H); ^{13}C NMR (100 MHz, CDCl_3) δ 168.8, 162.2, 157.3, 136.7, 129.6, 129.1, 128.6, 127.9, 125.8, 115.1, 92.2 (d, $^1J_{\text{CF}} = 172.0$ Hz), 81.8, 78.6 (d, $^2J_{\text{CF}} = 20.9$ Hz), 70.5, 57.7 (d, $^3J_{\text{CF}} = 7.41$ Hz), 47.8, 44.7 (d, $^3J_{\text{CF}} = 14.77$ Hz), 33.1 (d, $^2J_{\text{CF}} = 21.8$ Hz), 28.7; HRMS (ESI): $[\text{M} + \text{H}]^+$, m/z calcd for $\text{C}_{25}\text{H}_{32}\text{FN}_2\text{O}_5$ 459.2295, found 459.2297.

(5R,6R)-6-(4-(benzyloxy)benzamido)-3,3-difluoro-5-hydroxyazepane-1-carboxylic acid-*tert*-butyl ester (3d)

The procedure for the synthesis of **5.5a** was followed: yield 55% over two steps; colourless oil; R_f (petroleum ether/EtOAc, 1/1) 0.34; $[\alpha]_D^{20} = -27.4$ (c 1.0, CHCl_3); IR (film) ν_{max} (cm^{-1}): 3500–3100 (br), 2360, 1716, 1683, 1652, 1630, 1613, 1518, 1249, 1210, 1171, 1139, 1049, 840, 793, 726, 608; ^1H NMR (400 MHz, CDCl_3) δ 8.84 (d, $J = 5.25$ Hz, 1H), 7.85 (d, $J = 8.70$ Hz, 2H), 7.45–7.31 (m, 5H), 7.03 (d, $J = 8.58$ Hz, 2H), 5.38 (brs, 1H), 5.13 (s, 2H), 4.43 (dd, $J = 14.99, 13.34$ Hz, 1H), 4.21–4.09 (m, 2H), 4.03 (dd, $J = 9.97, 7.34$ Hz, 1H), 3.32 (dd, $J = 15.78, 5.26$ Hz, 1H), 3.09 (dd, $J = 31.99, 14.94$ Hz, 1H), 2.49–2.24 (m, 2H), 1.51 (s, 9H); ^{13}C NMR (100 MHz, CDCl_3) δ 168.8,

161.9, 157.2, 136.5, 129.3, 128.8, 128.3, 127.6, 125.6, 121.7 (d, $^1J_{\text{CF}} = 238.33$ Hz), 114.9, 82.5, 72.1 (dd, $J = 11.18$ ($^2J_{\text{CF}}$), 3.82 ($^3J_{\text{CF}}$) Hz), 70.3, 60.0, 55.7 (dd, $J = 41.22$ ($^2J_{\text{CF}}$), 28.80 ($^3J_{\text{CF}}$) Hz), 50.1, 41.2 (t, $^2J_{\text{CF}} = 23.80$ Hz), 28.3; HRMS (ESI): $[M + H]^+$, m/z calcd for $\text{C}_{25}\text{H}_{31}\text{F}_2\text{N}_2\text{O}_5$ 477.2201, found 477.2203.

(4*R*,5*S*,6*R*)-6-(4-(benzyloxy)benzamido)-3,3,4-trifluoro-5-hydroxyazepane-1-carboxylic acid-*tert*-butyl ester (3e)

The procedure for the synthesis of **5.5a** was followed: yield 58% over two steps; white crystals; R_f (petroleum ether/EtOAc, 1/1) 0.37; $[\alpha]_{\text{D}}^{20} = -11.4$ (c 1.0, CHCl_3); IR (film) ν_{max} (cm^{-1}): 3500–3100 (br), 2360, 1716, 1683, 1652, 1630, 1613, 1518, 1249, 1210, 1171, 1139, 1049, 840, 793, 726, 608; ^1H NMR (600 MHz, CDCl_3) δ 8.44 (d, $J = 4.87$ Hz, 1H), 7.82 (d, $J = 8.66$ Hz, 2H), 7.45–7.32 (m, 5H), 7.03 (d, $J = 8.59$ Hz, 2H), 5.45 (s, 1H), 5.12 (s, 2H), 4.68 (dddd, $J = 46.57$ ($^1J_{\text{HF}}$), 18.31, 9.42, 1.57 Hz, 1H), 4.47–4.39 (m, 1H), 4.30–4.24 (m, 1H), 4.21–4.10 (m, 2H), 4.34–4.23 (m, 2H), 1.51 (s, 9H); ^{13}C NMR (150 MHz, CDCl_3) δ 168.6, 162.0, 156.7, 136.4, 129.3, 128.8, 128.4, 127.6, 125.4, 121.7 (dd, $J = 252.11$ ($^1J_{\text{CF}}$), 18.99 ($^3J_{\text{CF}}$) Hz), 114.9, 90.3 (dt, $J = 193.17$ ($^1J_{\text{CF}}$), 22.29 ($^2J_{\text{CF}}$) Hz), 82.9, 73.2 (d, $^2J_{\text{CF}} = 16.55$ Hz), 70.3, 57.6 (d, $^3J_{\text{CF}} = 5.71$ Hz), 52.4 (dd, $J = 37.68$ ($^2J_{\text{CF}}$), 27.76 ($^2J_{\text{CF}}$) Hz), 48.9, 28.3; HRMS (ESI): $[M + H]^+$, m/z calcd for $\text{C}_{25}\text{H}_{30}\text{F}_3\text{N}_2\text{O}_5$ 495.2107, found 495.2104.

(3*R*,4*R*,6*S*)-3-(4-(benzyloxy)benzamido)-4-(3,5-bis(benzyloxy)-4-(2-(benzyloxy)-6-(benzyloxycarbonyl)benzoyl)benzoyloxy)-6-fluoroazepane-1-carboxylic acid-*tert*-butyl ester (3.1a)

The procedure for the synthesis of **5.5b** was followed: yield 70%; colourless oil; R_f (petroleum ether/EtOAc, 3/2) 0.33; $[\alpha]_{\text{D}}^{20} = +34.3$ (c 0.9, CH_2Cl_2); IR (film) ν_{max} (cm^{-1}): 3365, 2390, 2324, 2288, 1715, 1688, 1666, 1652, 1638, 1585, 1493, 1129, 978, 919, 613; ^1H NMR (400 MHz, CDCl_3) δ 7.90 (d, $J = 7.08$ Hz, 1H), 7.75 (d, $J = 8.56$ Hz, 2H), 7.43–7.30 (m, 7H), 7.26–7.14 (m, 15H), 7.09–7.02 (m, 5H), 6.98–6.89 (m, 3H), 6.81 (d, $J = 7.55$ Hz, 2H), 5.09 (s, 2H), 5.05 (s, 2H), 4.95–4.77 (m, 1H), 4.81 (s, 2H), 4.80 (s, 2H), 4.67 (s, 2H), 4.32 (dd, $J = 14.63$, 6.70 Hz, 1H), 4.15 (d, $J = 15.24$ Hz, 1H), 3.54–3.44 (m, 1H), 3.39 (dd, $J = 15.67$, 4.98 Hz, 1H), 2.89 (dd, $J = 24.21$, 11.39 Hz, 1H), 2.46–2.30 (m, 2H), 1.55 (s, 9H); ^{13}C NMR (100 MHz, CDCl_3) δ 192.0, 167.8, 166.5, 165.8, 161.9, 158.4, 157.4, 156.7, 136.7, 136.6, 136.2, 136.1, 133.2, 132.9, 132.7, 130.9, 129.3, 129.1, 128.8, 128.7, 128.6, 128.3, 128.2, 127.9, 127.8, 127.6, 127.5, 126.8, 122.4, 115.7, 115.1, 107.4, 104.3, 87.8 (d, $^1J_{\text{CF}} = 177.72$ Hz), 82.2, 72.6 (d, $^3J_{\text{CF}} = 7.78$ Hz), 70.9, 70.5, 67.5, 67.3, 53.5, 53.1 (d, $^2J_{\text{CF}} = 34.37$ Hz), 51.6, 34.4 (d, $^2J_{\text{CF}} = 20.91$ Hz), 28.7; HRMS (ESI): $[M + H]^+$, m/z calcd for $\text{C}_{68}\text{H}_{64}\text{FN}_2\text{O}_{12}$ 1119.4443, found 1119.4413.

(3R,4R,6R)-3-(4-(benzyloxy)benzamido)-4-(3,5-bis(benzyloxy)-4-(2-(benzyloxy)-6-(benzyloxycarbonyl)benzoyl)benzoyloxy)-6-fluoroazepane-1-carboxylic acid-*tert*-butyl ester (3.1b)

The procedure for the synthesis of **5.5b** was followed: yield 72%; colourless oil; R_f (petroleum ether/EtOAc, 3/2) 0.31; $[\alpha]_D^{20} = -67.5$ (c 0.6, CH_2Cl_2); IR (film) ν_{max} (cm^{-1}): 3365, 2390, 2324, 2288, 1715, 1688, 1666, 1652, 1638, 1585, 1493, 1129, 978, 919, 613; ^1H NMR (400 MHz, CDCl_3) δ 8.21–7.62 (m, 3H), 7.57–7.67 (m, 32H), 5.24–2.76 (m, 16H), 2.70–1.93 (m, 3H), 1.51 (s, 9H); ^{13}C NMR (150 MHz, $(\text{CD}_3)_2\text{CO}$) δ 190.8, 168.2, 167.0, 166.0, 162.6, 162.3, 162.2, 157.6, 155.6, 138.0, 137.9, 136.8, 132.6, 132.5, 130.0, 130.0, 129.8, 129.3, 129.1, 129.0, 128.9, 128.8, 128.5, 122.6, 116.2, 115.3, 115.2, 92.2 (d, $^1J_{\text{CF}} = 169.37$ Hz), 81.6, 80.6, 76.3, 71.8, 71.5, 70.7, 70.6, 67.5, 60.0, 54.0, 53.2, 50.5, 46.7, 46.1, 39.7 (d, $^2J_{\text{CF}} = 21.27$ Hz), 28.6, 28.4; HRMS (ESI): $[\text{M} + \text{H}]^+$, m/z calcd for $\text{C}_{68}\text{H}_{64}\text{FN}_2\text{O}_{12}$ 1119.4443, found 1119.4447.

(3R,4S,5S)-3-(4-(benzyloxy)benzamido)-4-(3,5-bis(benzyloxy)-4-(2-(benzyloxy)-6-(benzyloxycarbonyl)benzoyl)benzoyloxy)-5-fluoroazepane-1-carboxylic acid-*tert*-butyl ester (3.1c)

The procedure for the synthesis of **5.5b** was followed: yield 67%; colourless oil; R_f (petroleum ether/EtOAc, 3/2) 0.34; $[\alpha]_D^{20} = +54.9$ (c 1.0, CH_2Cl_2); IR (film) ν_{max} (cm^{-1}): 3365, 2390, 2324, 2288, 1715, 1688, 1666, 1652, 1638, 1585, 1493, 1129, 978, 919, 613; ^1H NMR (600 MHz, CDCl_3) δ 7.76–7.66 (m, 2H), 7.42–6.79 (m, 32H), 5.17–4.87 (m, 5H), 4.81–4.56 (m, 6H), 4.00–3.12 (m, 6H), 2.32–2.16 (m, 2H), 1.56 (s, 9H); ^{13}C NMR (150 MHz, CDCl_3) δ 192.3, 167.5, 166.2, 165.7, 161.9, 158.1, 156.6, 155.1, 136.4, 135.9, 135.7, 132.2, 131.1, 130.7, 129.0, 128.8, 128.6, 128.5, 128.4, 128.1, 128.0, 127.8, 127.7, 127.6, 127.4, 122.2, 115.4, 115.2, 114.9, 114.8, 107.2, 103.9, 91.1 (d, $^1J_{\text{CF}} = 175.6$ Hz), 81.8, 81.3 (d, $^2J_{\text{CF}} = 16.36$ Hz), 76.1, 70.9, 70.7, 70.2, 51.2, 47.8, 46.3, 41.5, 37.3, 32.1, 28.5; HRMS (ESI): $[\text{M} + \text{H}]^+$, m/z calcd for $\text{C}_{68}\text{H}_{64}\text{FN}_2\text{O}_{12}$ 1119.4443, found 1119.4425.

(5R,6R)-6-(4-(benzyloxy)benzamido)-5-((3,5-bis(benzyloxy)-4-(2-(benzyloxy)-6-(benzyloxy) carbonyl)benzoyl)benzoyloxy)-3,3-difluoroazepane-1-carboxylic acid-*tert*-butyl ester (3.1d)

The procedure for the synthesis of **5.5b** was followed: yield 70%; colourless oil; R_f (petroleum ether/EtOAc, 3/2) 0.33; $[\alpha]_D^{20} = -74.9$ (c 0.6, CH_2Cl_2); IR (film) ν_{max} (cm^{-1}): 3370, 2383, 2322, 2282, 1711, 1687, 1652, 1649, 1631, 1581, 1484, 1122, 999, 921, 627; ^1H NMR (400 MHz, CDCl_3) δ 8.03–7.94 (m, 1H), 7.84–7.76 (m, 2H), 7.46–6.82 (m, 32 H), 5.50 (t, $J = 7.42$ Hz, 1H), 5.13 (s,

2H), 5.09 (s, 4H), 4.81 (s, 4H), 4.68–4.58 (m, 1H), 4.50–4.34 (m, 1H), 4.19 (d, $J = 14.98$ Hz, 1H), 3.44 (dd, $J = 15.13, 4.88$ Hz, 1H), 3.30 (dd, $J = 15.12, 4.22$ Hz, 1H), 2.76–2.47 (m, 2H), 1.56 (s, 9H); ^{13}C NMR (100 MHz, CDCl_3) δ 191.7, 167.5, 166.5, 161.7, 158.1, 157.1, 136.5, 135.9, 135.8, 132.3, 130.7, 129.1, 128.8, 128.6, 128.4, 127.8, 127.6, 127.2, 126.3, 122.2, 115.4, 114.9, 107.2, 82.4, 76.1, 70.7, 70.6, 70.2, 67.2, 55.7 (d, $^2J_{\text{CF}} = 27.60$ Hz), 53.4, 50.6, 36.3 (d, $^2J_{\text{CF}} = 27.70$ Hz), 28.3; HRMS (ESI): $[\text{M} + \text{H}]^+$, m/z calcd for $\text{C}_{68}\text{H}_{63}\text{F}_2\text{N}_2\text{O}_{12}$ 1137.4349, found 1137.4318.

(4*R*,5*S*,6*R*)-6-(4-(benzyloxy)benzamido)-5-((3,5-bis(benzyloxy)-4-(2-(benzyloxy)-6-((benzyloxy)carbonyl)benzoyl)benzoyl)oxy)-3,3,4-trifluoroazepane-1-carboxylic acid-*tert*-butyl ester (3.1e)

The procedure for the synthesis of **5.5b** was followed: yield 74%; colourless oil; R_f (petroleum ether/EtOAc, 3/2) 0.36; $[\alpha]_{\text{D}}^{20} = -57.1$ (c 0.9, CH_2Cl_2); IR (film) ν_{max} (cm^{-1}): 3378, 2388, 2343, 2267, 1721, 1689, 1659, 1641, 1639, 1587, 1489, 1129, 987, 926, 607; ^1H NMR (400 MHz, CDCl_3) δ 7.78–7.64 (m, 2H), 7.43–6.76 (m, 32H), 5.74–5.60 (m, 1H), 5.11 (s, 2H), 5.06 (s, 2H), 4.97–4.75 (m, 1H), 4.76 (s, 4H), 4.74 (s, 2H), 4.45–4.30 (m, 1H), 4.06 (brd, $J = 14.54$ Hz, 1H), 4.00–3.82 (m, 1H), 3.58–3.34 (m, 2H), 1.56 (s, 9H); ^{13}C NMR (100 MHz, CDCl_3) δ 191.8, 167.6, 166.3, 161.8, 158.1, 156.2, 136.4, 135.9, 129.0, 128.8, 128.6, 128.4, 128.1, 127.9, 127.8, 127.6, 127.3, 126.4, 122.2, 115.2, 114.9, 107.3, 89.4 (d, $^1J_{\text{CF}} = 217.71$ Hz), 82.6 (d, $^2J_{\text{CF}} = 24.57$ Hz), 78.3, 70.9, 70.6, 70.2, 67.4, 67.3, 51.8 (d, $^3J_{\text{CF}} = 9.44$ Hz), 30.4, 28.3; HRMS (ESI): $[\text{M} + \text{H}]^+$, m/z calcd for $\text{C}_{68}\text{H}_{62}\text{F}_3\text{N}_2\text{O}_{12}$ 1155.4255, found 1155.4226.

2-(4-(((3*R*,4*R*,6*S*)-6-fluoro-3-(4-hydroxybenzamido)azepan-4-yl)oxy)carbonyl)-2,6-dihydroxybenzoyl)-3-hydroxybenzoic acid (1a)

The procedure for the synthesis of **1** was followed: yield 64%; yellow film; retention time 20.0 min (Phenomenex Gemini C18 column (150 × 21.20 mm); MeCN/water/TFA (from 35:65:0.1 to 44:56:0.1 over 30 min; flow rate: 8.80 mL/min); $[\alpha]_{\text{D}}^{20} = +82.1$ (c 0.5, MeOH); IR (film) ν_{max} (cm^{-1}): 3400–2800 (br), 2360, 2340, 1717, 1683, 1652, 1646, 1635, 1489, 1102, 991, 922, 632; ^1H NMR (600 MHz, $(\text{CD}_3)_2\text{SO}$) δ 11.63 (s, 2H), 10.00 (s, 1H), 9.83 (s, 1H), 9.24 (brs, 1H), 8.46 (d, $J = 8.00$ Hz, 1H), 7.62 (d, $J = 8.74$ Hz, 2H), 7.35 (d, $J = 7.80$ Hz, 1H), 7.26 (t, $J = 7.90$ Hz, 1H), 7.04 (d, $J = 8.13$ Hz, 1H), 6.77 (d, $J = 8.60$ Hz, 2H), 6.76 (s, 2H), 5.36–5.31 (m, 1H), 5.29–5.17 (m, $^1J_{\text{HF}} = 44.09$ Hz, 1H), 4.57–4.51 (m, 1H), 3.50–3.31 (m, 4H), 2.57–2.42 (m, 2H); ^{13}C NMR (150 MHz, $(\text{CD}_3)_2\text{SO}$) δ 201.5, 166.9, 166.1, 164.1, 161.4, 160.4, 153.2, 135.3, 132.4, 129.2, 128.9, 128.8, 124.5, 120.0, 119.6, 114.8, 113.5, 107.3, 86.2 (d, $^1J_{\text{CF}} = 172.92$ Hz), 71.5, 50.8, 49.2 (d, $^2J_{\text{CF}} = 25.48$ Hz), 47.7, 33.9 (d, $^2J_{\text{CF}} = 22.28$ Hz); HRMS (ESI): $[\text{M} + \text{H}]^+$, m/z calcd for $\text{C}_{28}\text{H}_{26}\text{FN}_2\text{O}_{10}$ 569.1571, found 569.1575.

2-(4-(((3*R*,4*R*,6*R*)-6-fluoro-3-(4-hydroxybenzamido)azepan-4-yl)oxy)carbonyl)-2,6-dihydroxybenzoyl)-3-hydroxybenzoic acid (1b)

The procedure for the synthesis of **1** was followed: yield 69%; yellow film; retention time 27.4 min (Phenomenex Gemini C18 column (150 × 21.20 mm); MeCN/water/TFA (from 5:95:0.1 to 55:45:0.1 over 30 min; flow rate: 8.80 mL/min); $[\alpha]_{\text{D}}^{20} = -77.9$ (*c* 0.4, MeOH); IR (film) ν_{max} (cm^{-1}): 3400–2800 (br), 2360, 2340, 1717, 1683, 1652, 1646, 1635, 1489, 1102, 991, 922, 632; ^1H NMR (600 MHz, $(\text{CD}_3)_2\text{SO}$) δ 11.67 (s, 2H), 10.07 (brs, 1H), 9.87 (s, 1H), 9.34 (brs, 2H), 8.55 (d, $J = 8.47$ Hz, 1H), 7.61 (d, $J = 8.69$ Hz, 2H), 7.36 (d, $J = 7.61$ Hz, 1H), 7.27 (t, $J = 8.01$ Hz, 1H), 7.04 (d, $J = 8.01$ Hz, 1H), 6.78 (d, $J = 8.66$ Hz, 2H), 6.76 (s, 2H), 5.55 (ddd, $J = 10.33, 9.93, 2.02$ Hz, 1H), 5.33–5.21 (m, $^1J_{\text{HF}} = 47.37$ Hz, 1H), 4.59–4.53 (m, 1H), 3.58 (dd, $J = 17.42, 15.96$ Hz, 1H), 3.52–3.40 (m, 2H), 3.30 (dd, $J = 14.14, 7.39$ Hz, 1H), 2.57–2.52 (m, 1H), 2.39–2.27 (m, 1H); ^{13}C NMR (150 MHz, $(\text{CD}_3)_2\text{SO}$) δ 201.6, 166.9, 166.3, 164.0, 161.5, 160.6, 153.2, 135.3, 132.4, 129.2, 128.9, 128.8, 124.2, 120.0, 119.6, 114.9, 113.5, 107.4, 86.0 (d, $^1J_{\text{CF}} = 169.84$ Hz), 70.1, 50.5, 50.3 (d, $^2J_{\text{CF}} = 24.68$ Hz), 47.1, 32.3 (d, $^2J_{\text{CF}} = 19.15$ Hz); HRMS (ESI): $[\text{M} + \text{H}]^+$, m/z calcd for $\text{C}_{28}\text{H}_{26}\text{FN}_2\text{O}_{10}$ 569.1571, found 569.1577.

2-(4-(((3*R*,4*S*,5*S*)-5-fluoro-3-(4-hydroxybenzamido)azepan-4-yl)oxy)carbonyl)-2,6-dihydroxybenzoyl)-3-hydroxybenzoic acid (1c)

The procedure for the synthesis of **1** was followed: yield 72%; yellow film; retention time 21.2 min (Phenomenex Gemini C18 column (150 × 21.20 mm); MeCN/water/TFA (from 35:65:0.1 to 44:56:0.1 over 30 min; flow rate: 8.80 mL/min); $[\alpha]_{\text{D}}^{20} = +58.7$ (*c* 0.2, MeOH); IR (film) ν_{max} (cm^{-1}): 3400–2800 (br), 2360, 2340, 1717, 1683, 1652, 1646, 1635, 1489, 1102, 991, 922, 632; ^1H NMR (600 MHz, CD_3CN) δ 10.69 (brs, 1H), 8.00 (d, $J = 6.91$ Hz, 1H), 7.68 (d, $J = 8.06$ Hz, 2H), 7.51 (d, $J = 7.62$ Hz, 1H), 7.33 (t, $J = 7.95$ Hz, 1H), 7.11 (d, $J = 7.62$ Hz, 1H), 7.02 (s, 2H), 6.83 (d, $J = 8.06$ Hz, 2H), 5.49 (t, $J = 7.98$ Hz, 1H), 5.29–5.16 (m, $^1J_{\text{HF}} = 43.56$ Hz, 1H), 4.41 (brs, 1H), 3.71–3.64 (m, 2H), 3.59–3.54 (m, 1H), 3.42–3.34 (m, 1H), 2.63–2.46 (m, 2H); ^{13}C NMR (150 MHz, $(\text{CD}_3)_2\text{SO}$) δ 202.5, 169.5, 167.5, 162.5, 161.6, 160.5, 153.7, 137.1, 130.6, 130.6, 130.4, 125.5, 122.3, 121.2, 116.1, 109.2, 103.7, 86.9 (d, $^1J_{\text{CF}} = 167.92$ Hz), 71.2 (d, $^2J_{\text{CF}} = 19.71$ Hz), 53.0, 50.6, 50.3, 35.3 (d, $^2J_{\text{CF}} = 24.12$ Hz); HRMS (ESI): $[\text{M} + \text{H}]^+$, m/z calcd for $\text{C}_{28}\text{H}_{26}\text{FN}_2\text{O}_{10}$ 569.1571, found 569.1567.

2-(4-(((3*R*,4*R*)-6,6-difluoro-3-(4-hydroxybenzamido)azepan-4-yl)oxy)carbonyl)-2,6-dihydroxybenzoyl)-3-hydroxybenzoic acid (1d)

The procedure for the synthesis of **1** was followed: yield 75%; yellow film; retention time 27.5 min (Phenomenex Gemini C18 column (150 × 21.20 mm); MeCN/water/TFA (from 30:70:0.1 to 70:30:0.1 over 50 min; flow rate: 8.80 mL/min); $[\alpha]_D^{20} = -98.4$ (*c* 0.7, MeOH); IR (film) ν_{\max} (cm^{-1}): 3400–2800 (br), 2363, 2341, 1711, 1687, 1652, 1649, 1631, 1484, 1122, 999, 921, 627; ^1H NMR (600 MHz, $(\text{CD}_3)_2\text{SO}$) δ 11.68 (s, 2H), 10.09 (brs, 1H), 9.89 (s, 1H), 8.54 (d, $J = 8.13$ Hz, 1H), 7.63 (d, $J = 8.58$ Hz, 2H), 7.37 (d, $J = 7.63$ Hz, 1H), 7.28 (t, $J = 7.99$ Hz, 1H), 7.05 (d, $J = 8.16$ Hz, 1H), 6.78 (d, $J = 8.64$ Hz, 2H), 6.78 (s, 2H), 5.45–5.41 (m, 1H), 4.59–4.54 (m, 1H), 3.77–3.68 (m, 2H), 3.52–3.47 (m, 1H), 3.39–3.33 (m, 1H), 2.83–2.74 (m, 2H); ^{13}C NMR (150 MHz, $(\text{CD}_3)_2\text{SO}$) δ 201.6, 167.0, 166.3, 164.0, 161.5, 160.6, 153.3, 135.1, 132.5, 129.3, 129.0, 128.9, 124.3, 121.8 (d, $^1J_{\text{CF}} = 243.01$ Hz), 120.0, 119.7, 115.0, 113.6, 107.5, 69.4, 51.7 (t, $^2J_{\text{CF}} = 38.37$ Hz), 50.6, 48.1, 37.1 (t, $^2J_{\text{CF}} = 25.41$ Hz); HRMS (ESI): $[\text{M} + \text{H}]^+$, *m/z* calcd for $\text{C}_{28}\text{H}_{25}\text{F}_2\text{N}_2\text{O}_{10}$ 587.1477, found 587.1467.

2-(2,6-dihydroxy-4-((((3R,4S,5R)-5,6,6-trifluoro-3-(4-hydroxybenzamido)azepan-4-yl)oxy)carbonyl)benzoyl)-3-hydroxybenzoic acid (1e)

The procedure for the synthesis of **1** was followed: yield 68%; yellow film; retention time 27.6 min (Phenomenex Gemini C18 column (150 × 21.20 mm); MeCN/water/TFA (from 30:70:0.1 to 70:30:0.1 over 50 min; flow rate: 8.80 mL/min); $[\alpha]_D^{20} = -64.6$ (*c* 0.4, MeOH); IR (film) ν_{\max} (cm^{-1}): 3400–2800 (br), 2360, 2346, 1719, 1667, 1659, 1640, 1639, 1480, 1129, 987, 946, 607; ^1H NMR (600 MHz, $(\text{CD}_3)_2\text{SO}$) δ 11.68 (s, 2H), 10.01 (brs, 1H), 9.86 (s, 1H), 8.48 (d, $J = 8.05$ Hz, 1H), 7.57 (d, $J = 8.46$ Hz, 2H), 7.36 (d, $J = 7.80$ Hz, 1H), 7.28 (t, $J = 7.97$ Hz, 1H), 7.05 (d, $J = 7.95$ Hz, 1H), 6.76 (d, $J = 8.59$ Hz, 2H), 6.76 (s, 2H), 5.67–5.60 (m, 1H), 5.48–5.35 (m, $^1J_{\text{HF}} = 45.30$ Hz, 1H), 4.58–4.52 (m, 1H), 3.38–3.34 (m, 1H), 3.30–3.20 (m, 2H), 3.19–3.10 (m, 1H); ^{13}C NMR (150 MHz, $(\text{CD}_3)_2\text{SO}$) δ 201.5, 166.9, 165.9, 164.1, 161.5, 160.4, 153.3, 134.7, 132.4, 129.1, 129.0, 128.9, 124.5, 121.8 (d, $^1J_{\text{CF}} = 251.98$ Hz), 120.0, 119.7, 114.9, 113.7, 107.4, 89.4 (dd, $J = 186.95$ ($^1J_{\text{CF}}$), 25.49 ($^2J_{\text{CF}}$) Hz), 72.0 (d, $^2J_{\text{CF}} = 22.64$ Hz), 63.0 (d, $^2J_{\text{CF}} = 34.43$ Hz), 49.5, 48.4; HRMS (ESI): $[\text{M} + \text{H}]^+$, *m/z* calcd for $\text{C}_{28}\text{H}_{24}\text{F}_3\text{N}_2\text{O}_{10}$ 605.1383, found 605.1389.

C. References

- [1] A. Fürstner, O. R. Thiel, *J. Org. Chem.* **2000**, *65*, 1738-1742.
- [2] J. W. Lampe, P. F. Hughes, C. K. Biggers, S. H. Smith, H. Hu, *J. Org. Chem.* **1994**, *59*, 5147-5148.
- [3] K. C. Nicolaou, K. Koide, M. E. Bunnage, *Chem. –Eur. J.* **1995**, *1*, 454-466.
- [4] a) A. R. Patel, F. Liu, *Tetrahedron* **2013**, *69*, 744-752; b) A. R. Patel, G. Ball, L. Hunter, F. Liu, *Org Biomol Chem* **2013**, *11*, 3781-3785; c) A. R. Patel, L. Hunter, M. M. Bhadbhade, F. Liu, *Eur J Org Chem* **2014**, *2014*, 2584-2593.

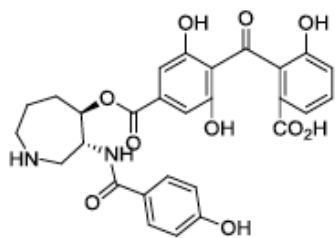
D. NMR spectra of 1, 3a–3e, 3.1a–3.1e, and 1a–1e.

S13 ^1H NMR spectrum of **1**

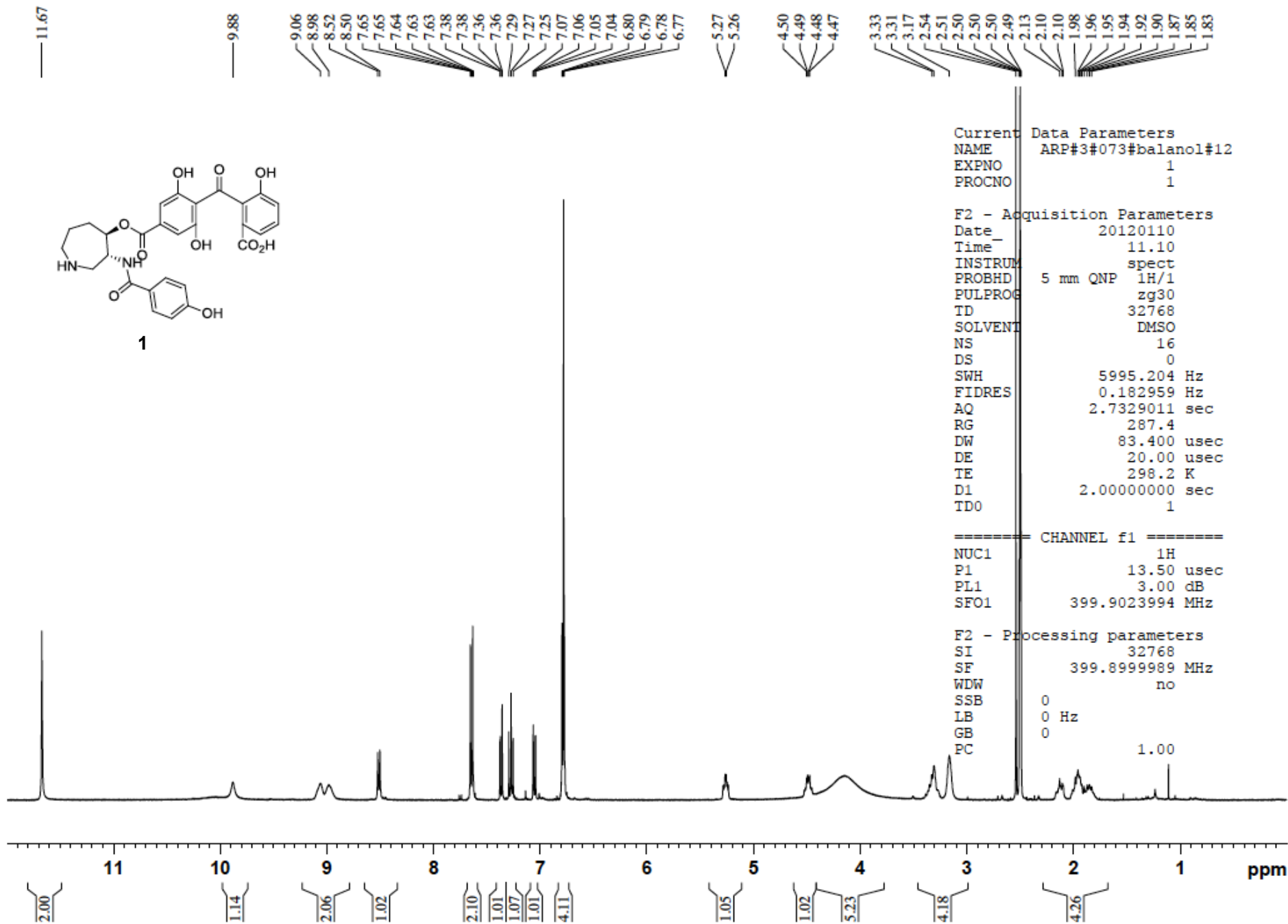
S14-23 ^1H and ^{13}C NMR spectra of NMR spectra of **3a–3e**

S24-33 ^1H and ^{13}C NMR spectra of NMR spectra **3.1a–3.1e**

S34-43 ^1H and ^{13}C NMR spectra of NMR spectra **1a–1e**



1

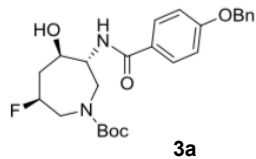


Current Data Parameters
 NAME ARP#3#073#balanol#12
 EXPNO 1
 PROCNO 1

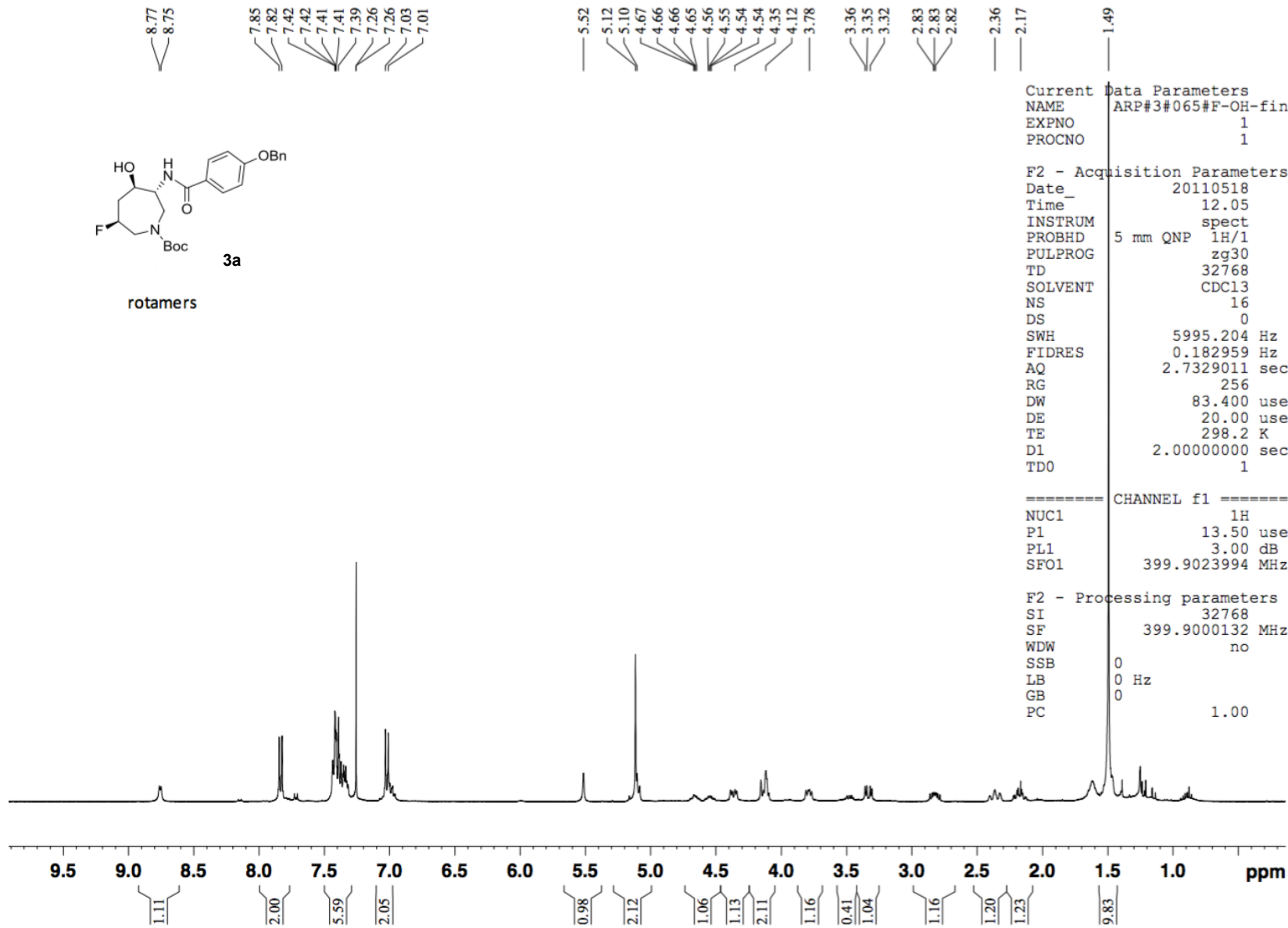
F2 - Acquisition Parameters
 Date_ 20120110
 Time_ 11.10
 INSTRUM spect
 PROBHD 5 mm QNP 1H/1
 PULPROG zg30
 TD 32768
 SOLVENT DMSO
 NS 16
 DS 0
 SWH 5995.204 Hz
 FIDRES 0.182959 Hz
 AQ 2.7329011 sec
 RG 287.4
 DW 83.400 usec
 DE 20.00 usec
 TE 298.2 K
 D1 2.00000000 sec
 TD0 1

CHANNEL f1
 NUC1 1H
 P1 13.50 usec
 PL1 3.00 dB
 SFO1 399.9023994 MHz

F2 - Processing parameters
 SI 32768
 SF 399.8999989 MHz
 WDW no
 SSB 0
 LB 0 Hz
 GB 0
 PC 1.00

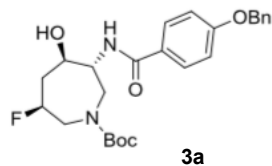


rotamers



Current Data Parameters
 NAME ARP#3#065#F-OH-final azp#fra 12-23
 EXPNO 4
 PROCNO 1

F2 - Acquisition Parameters
 Date_ 20110518
 Time_ 12.17
 INSTRUM spect
 PROBHD 5 mm QNP 1H/1
 PULPROG zgpg
 TD 66560
 SOLVENT CDC13
 NS 2000
 DS 2
 SWH 25125.629 Hz
 FIDRES 0.377488 Hz
 AQ 1.3245940 sec
 RG 4597.6
 DW 19.900 usec
 DE 20.00 usec
 TE 298.2 K
 D1 2.00000000 sec
 d11 0.03000000 sec
 DELTA 1.89999998 sec
 TD0 1

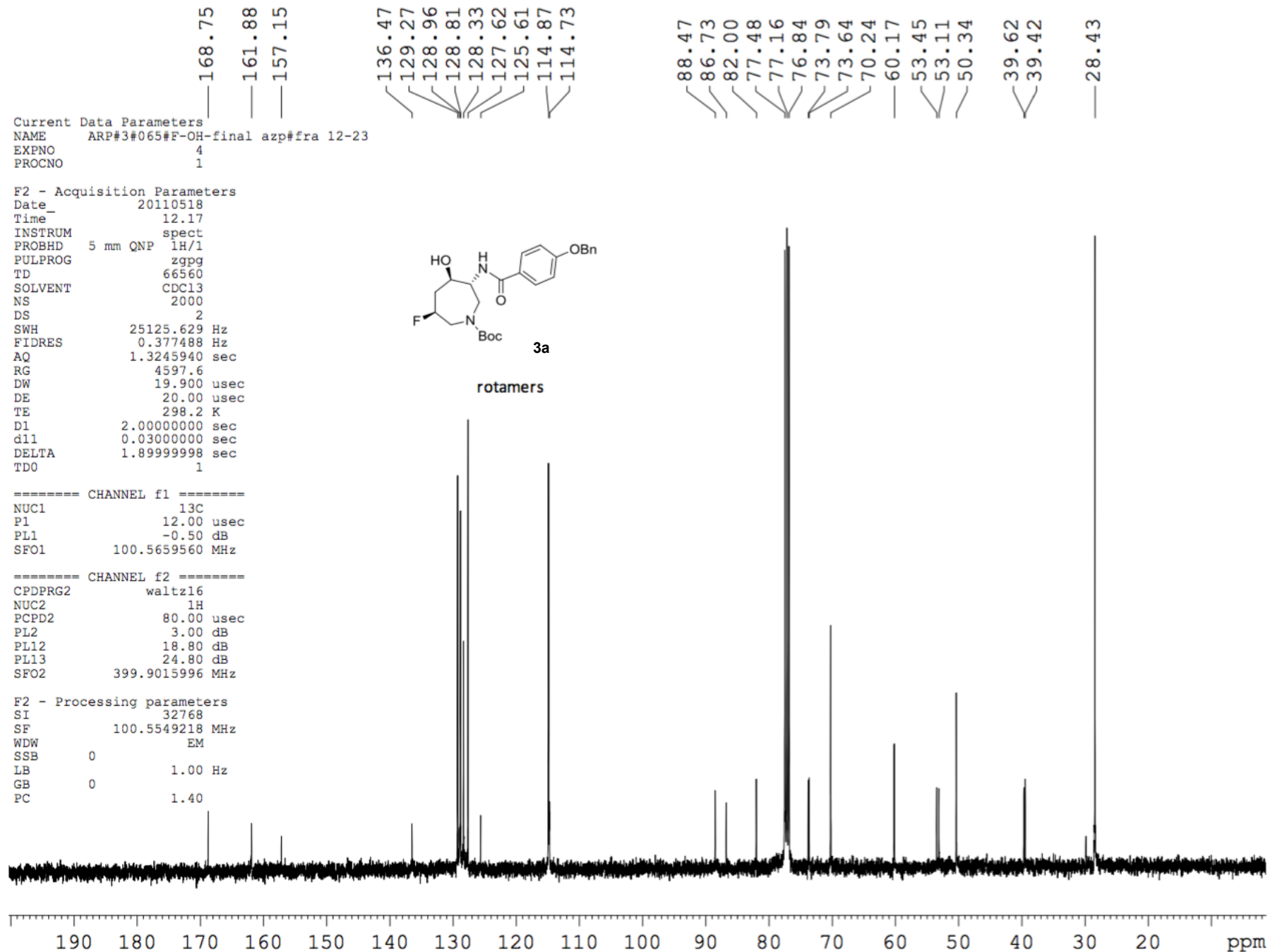


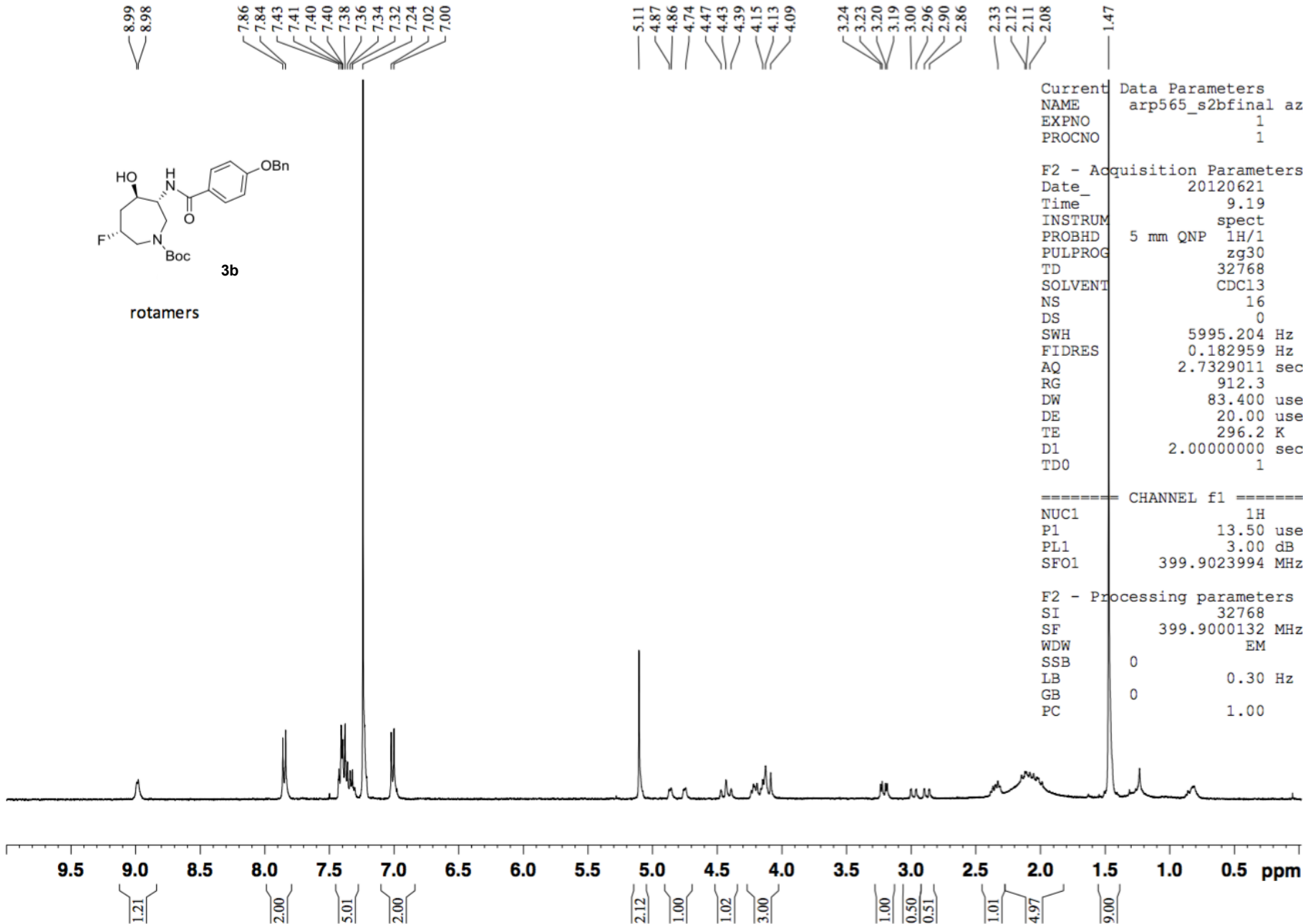
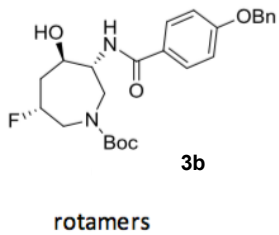
rotamers

==== CHANNEL f1 =====
 NUC1 13C
 P1 12.00 usec
 PL1 -0.50 dB
 SFO1 100.5659560 MHz

==== CHANNEL f2 =====
 CPDPRG2 waltz16
 NUC2 1H
 PCPD2 80.00 usec
 PL2 3.00 dB
 PL12 18.80 dB
 PL13 24.80 dB
 SFO2 399.9015996 MHz

F2 - Processing parameters
 SI 32768
 SF 100.5549218 MHz
 WDW EM
 SSB 0
 LB 1.00 Hz
 GB 0
 PC 1.40





```

Current Data Parameters
NAME      arp565_s2bfinal azp
EXPNO     1
PROCNO    1

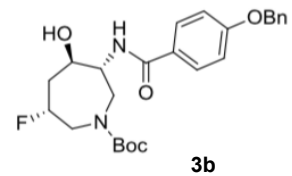
F2 - Acquisition Parameters
Date_     20120621
Time_     9.19
INSTRUM   spect
PROBHD    5 mm QNP 1H/1
PULPROG   zg30
TD         32768
SOLVENT   CDCl3
NS         16
DS         0
SWH        5995.204 Hz
FIDRES     0.182959 Hz
AQ         2.7329011 sec
RG         912.3
DW         83.400 usec
DE         20.00 usec
TE         296.2 K
D1         2.00000000 sec
TD0        1

----- CHANNEL f1 -----
NUC1      1H
P1        13.50 usec
PL1       3.00 dB
SFO1     399.9023994 MHz

F2 - Processing parameters
SI        32768
SF        399.9000132 MHz
WDW       EM
SSB       0
LB        0.30 Hz
GB        0
PC        1.00
  
```

Current Data Parameters
 NAME arp565_s2bfinal azp hplc_7B
 EXPNO 2
 PROCNO 1

F2 - Acquisition Parameters
 Date_ 20120621
 Time_ 9.30
 INSTRUM spect
 PROBHD 5 mm QNP 1H/1
 PULPROG zgpg
 TD 66560
 SOLVENT CDC13
 NS 3951
 DS 2
 SWH 25125.629 Hz
 FIDRES 0.377488 Hz
 AQ 1.3245940 sec
 RG 4597.6
 DW 19.900 usec
 DE 20.00 usec
 TE 296.2 K
 D1 2.00000000 sec
 d11 0.03000000 sec
 DELTA 1.89999998 sec
 TD0 1

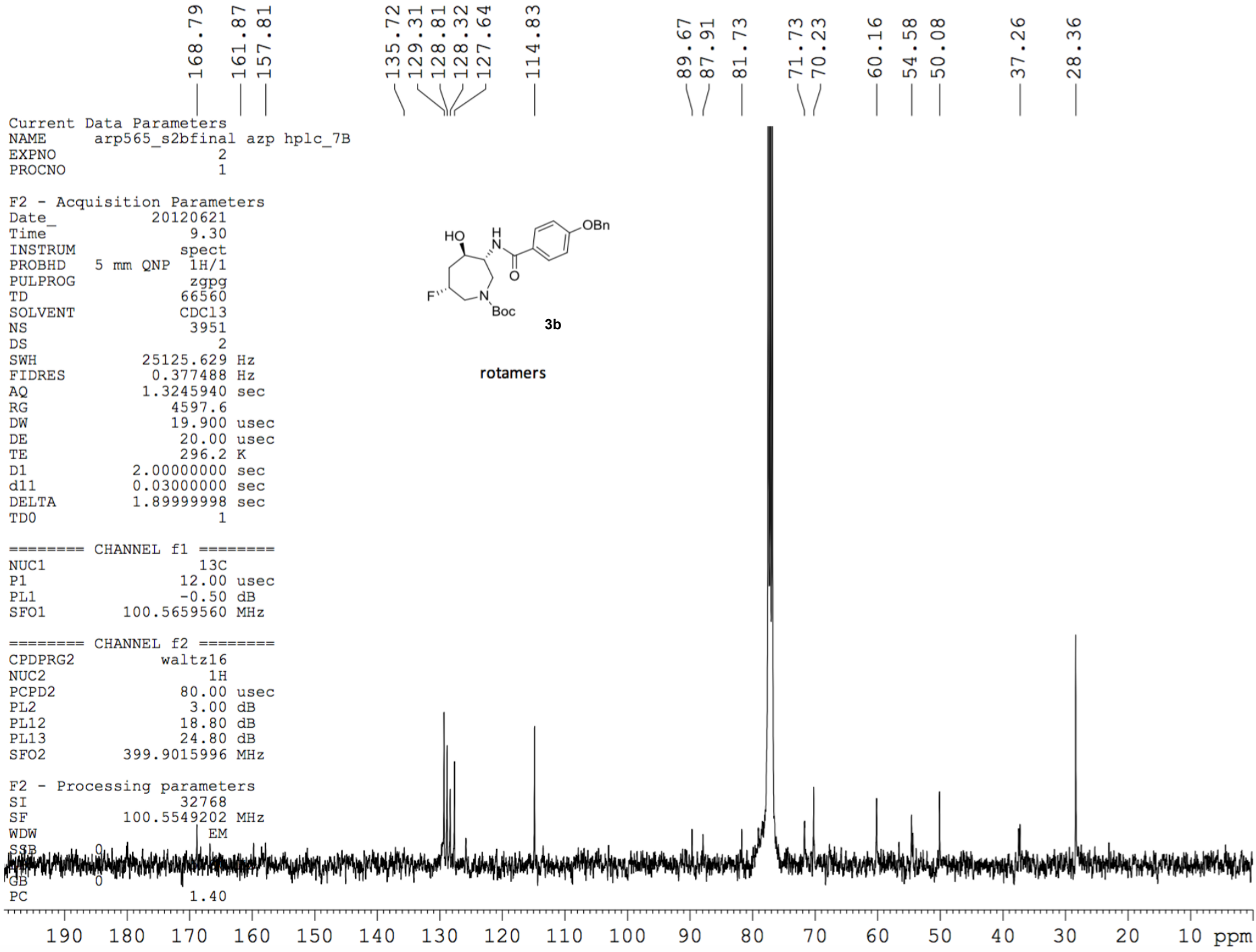


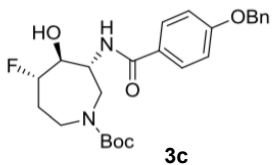
rotamers

==== CHANNEL f1 =====
 NUC1 13C
 P1 12.00 usec
 PL1 -0.50 dB
 SFO1 100.5659560 MHz

==== CHANNEL f2 =====
 CPDPRG2 waltz16
 NUC2 1H
 PCPD2 80.00 usec
 PL2 3.00 dB
 PL12 18.80 dB
 PL13 24.80 dB
 SFO2 399.9015996 MHz

F2 - Processing parameters
 SI 32768
 SF 100.5549202 MHz
 WDW EM
 SSB 0
 GB 0
 PC 1.40





rotamers

8.36
8.35
7.80
7.78
7.40
7.38
7.36
7.34
7.32
7.24
7.00
6.98

5.09
4.79
4.77
4.75
4.67
4.65
4.63
4.13
4.01
3.99
3.97

3.26
3.25
3.22
3.01
2.97

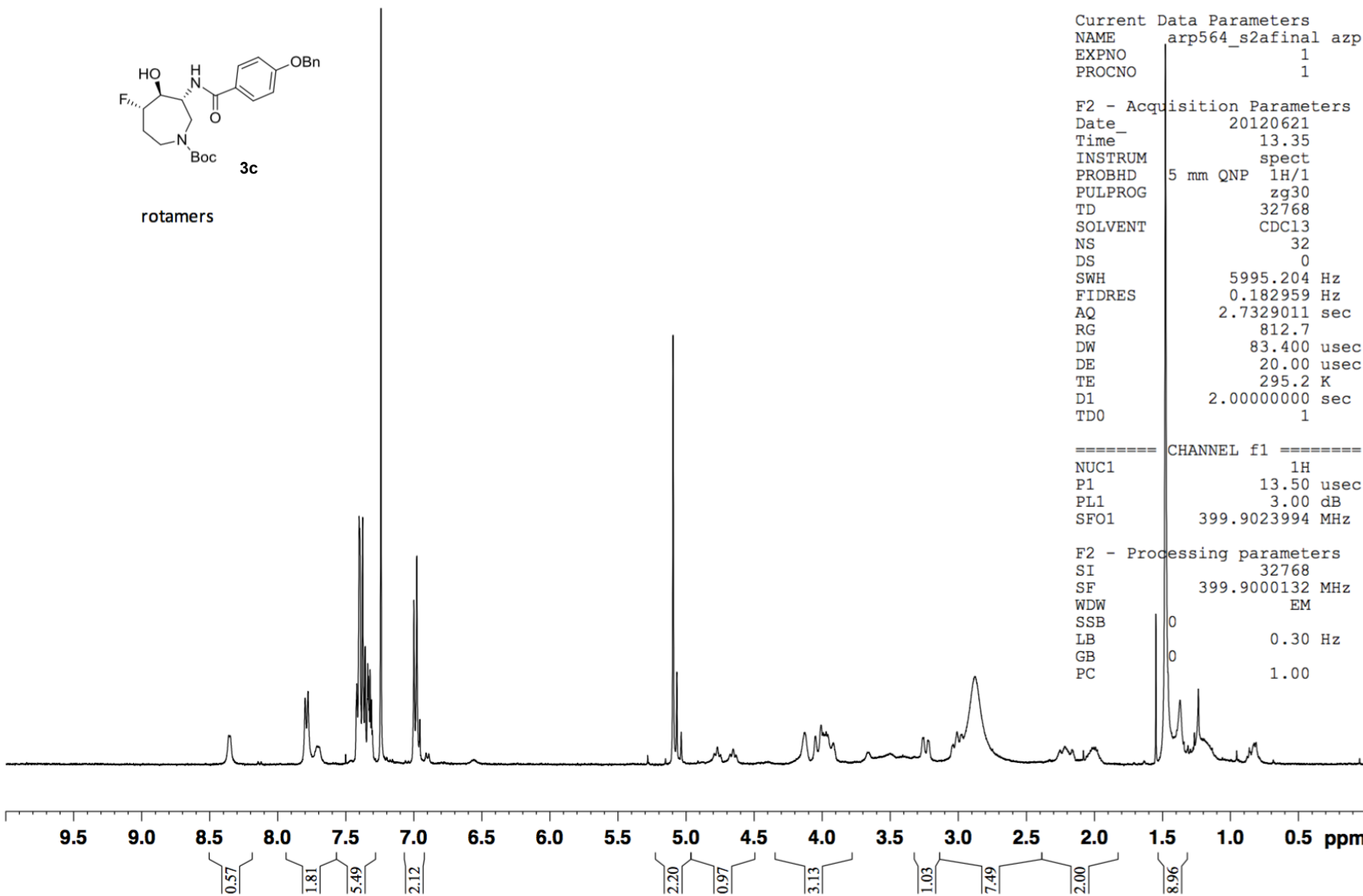
2.22
2.02
1.99
1.48

Current Data Parameters
NAME arp564_s2afinal azp
EXPNO 1
PROCNO 1

F2 - Acquisition Parameters
Date_ 20120621
Time 13.35
INSTRUM spect
PROBHD 5 mm QNP 1H/1
PULPROG zg30
TD 32768
SOLVENT CDCl3
NS 32
DS 0
SWH 5995.204 Hz
FIDRES 0.182959 Hz
AQ 2.7329011 sec
RG 812.7
DW 83.400 usec
DE 20.00 usec
TE 295.2 K
D1 2.00000000 sec
TDO 1

===== CHANNEL f1 =====
NUC1 1H
P1 13.50 usec
PL1 3.00 dB
SFO1 399.9023994 MHz

F2 - Processing parameters
SI 32768
SF 399.9000132 MHz
WDW EM
SSB 0
LB 0.30 Hz
GB 0
PC 1.00

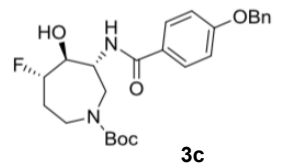


Current Data Parameters
 NAME arp564_s2a1001 hplc_10A
 EXPNO 1
 PROCNO 1

F2 - Acquisition Parameters
 Date_ 20120621
 Time_ 13.46
 INSTRUM spect
 PROBHD 5 mm QNP 1H/1
 PULPROG zgpg
 TD 66560
 SOLVENT CDC13
 NS 19671
 DS 2
 SWH 25125.629 Hz
 FIDRES 0.377488 Hz
 AQ 1.3245940 sec
 RG 18390.4
 DW 19.900 usec
 DE 20.00 usec
 TE 295.2 K
 D1 2.00000000 sec
 d11 0.03000000 sec
 DELTA 1.89999998 sec
 TD0 1

136.66
 129.55
 129.07
 128.61
 127.89
 125.81
 115.13

93.08
 91.34
 81.79
 78.64
 78.47
 70.50
 57.72
 47.76
 44.66
 33.14
 32.92
 28.73



rotamers

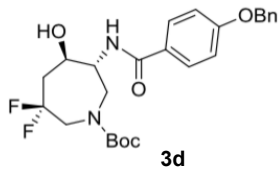
==== CHANNEL f1 =====
 NUC1 13C
 P1 12.00 usec
 PL1 -0.50 dB
 SFO1 100.5659560 MHz

==== CHANNEL f2 =====
 CPDPRG2 waltz16
 NUC2 1H
 PCPD2 80.00 usec
 PL2 3.00 dB
 PL12 18.80 dB
 PL13 24.80 dB
 SFO2 399.9015996 MHz

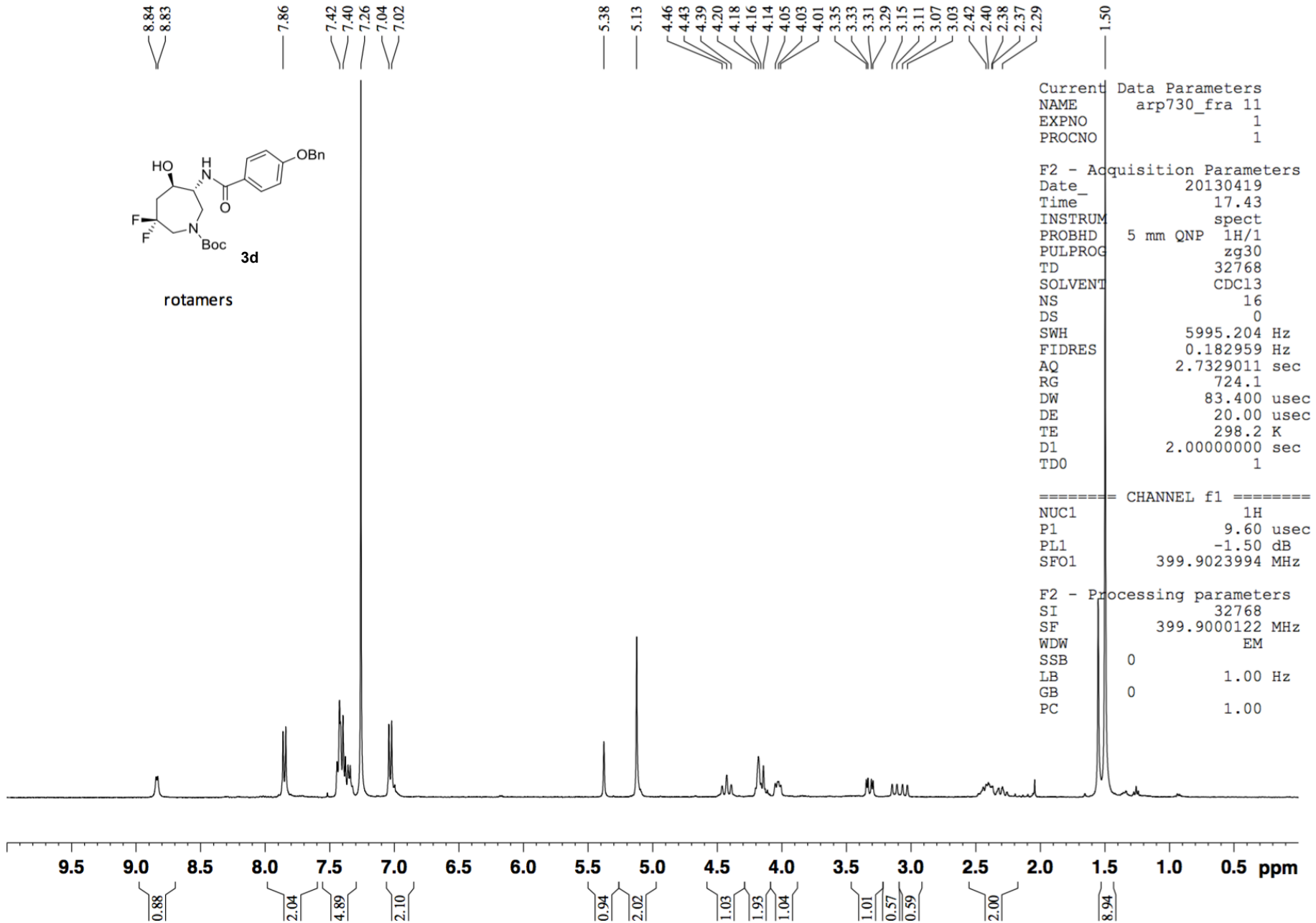
F2 - Processing parameters
 SI 32768
 SF 100.5548950 MHz
 WDW GM
 SSB 0
 LB -1.00 Hz
 GB 0.01
 PC 1.40



190 180 170 160 150 140 130 120 110 100 90 80 70 60 50 40 30 20 10 ppm

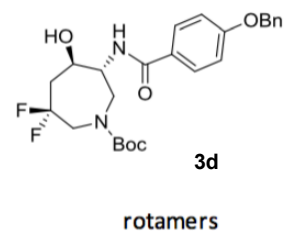


rotamers



Current Data Parameters
 NAME arp730_fra 11
 EXPNO 2
 PROCNO 1

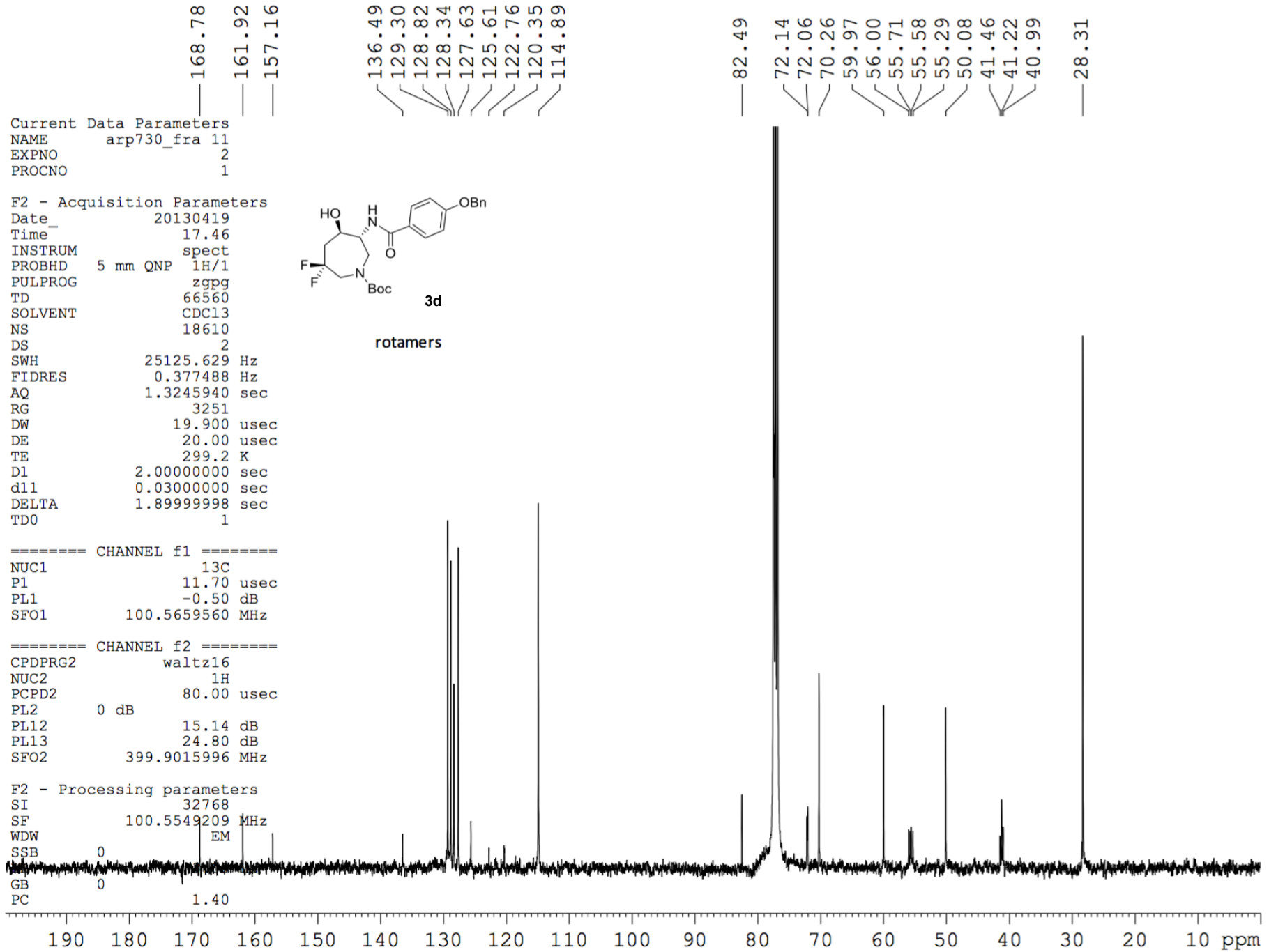
F2 - Acquisition Parameters
 Date_ 20130419
 Time_ 17.46
 INSTRUM spect
 PROBHD 5 mm QNP 1H/1
 PULPROG zgpg
 TD 66560
 SOLVENT CDCl3
 NS 18610
 DS 2
 SWH 25125.629 Hz
 FIDRES 0.377488 Hz
 AQ 1.3245940 sec
 RG 3251
 DW 19.900 usec
 DE 20.00 usec
 TE 299.2 K
 D1 2.00000000 sec
 d11 0.03000000 sec
 DELTA 1.89999998 sec
 TD0 1

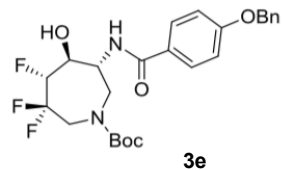


===== CHANNEL f1 =====
 NUC1 13C
 P1 11.70 usec
 PL1 -0.50 dB
 SFO1 100.5659560 MHz

===== CHANNEL f2 =====
 CPDPRG2 waltz16
 NUC2 1H
 PCPD2 80.00 usec
 PL2 0 dB
 PL12 15.14 dB
 PL13 24.80 dB
 SFO2 399.9015996 MHz

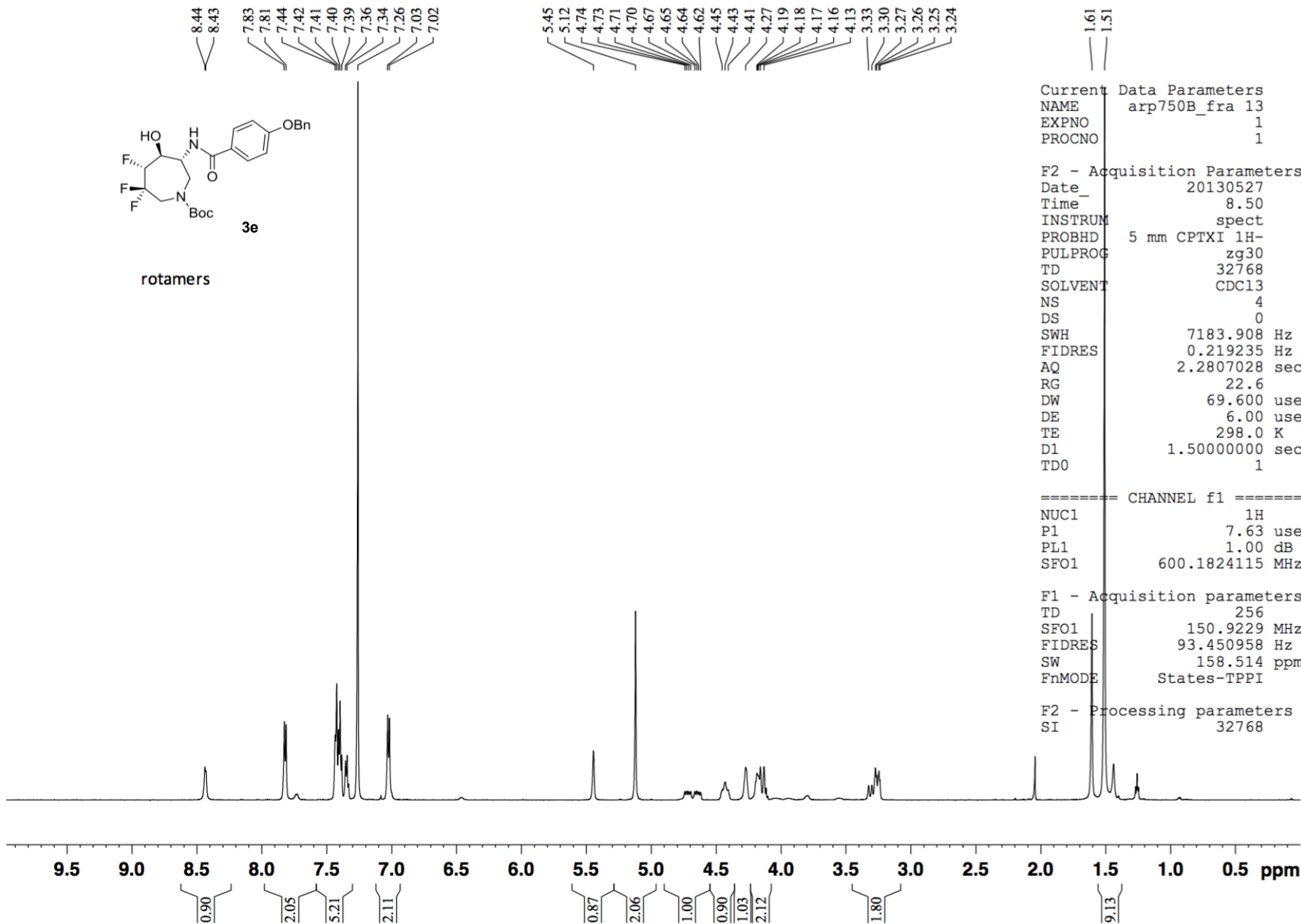
F2 - Processing parameters
 SI 32768
 SF 100.5549209 MHz
 WDW EM
 SSB 0
 GB 0
 PC 1.40





3e

rotamers



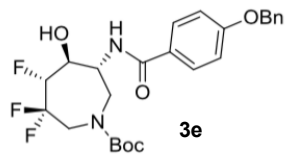
Current Data Parameters
 NAME arp750B_fra 13
 EXPNO 1
 PROCNO 1

F2 - Acquisition Parameters
 Date_ 20130527
 Time_ 8.50
 INSTRUM spect
 PROBHD 5 mm CPTXI 1H-
 PULPROG zg30
 TD 32768
 SOLVENT CDC13
 NS 4
 DS 0
 SWH 7183.908 Hz
 FIDRES 0.219235 Hz
 AQ 2.2807028 sec
 RG 22.6
 DW 69.600 usec
 DE 6.00 usec
 TE 298.0 K
 D1 1.5000000 sec
 TD0 1

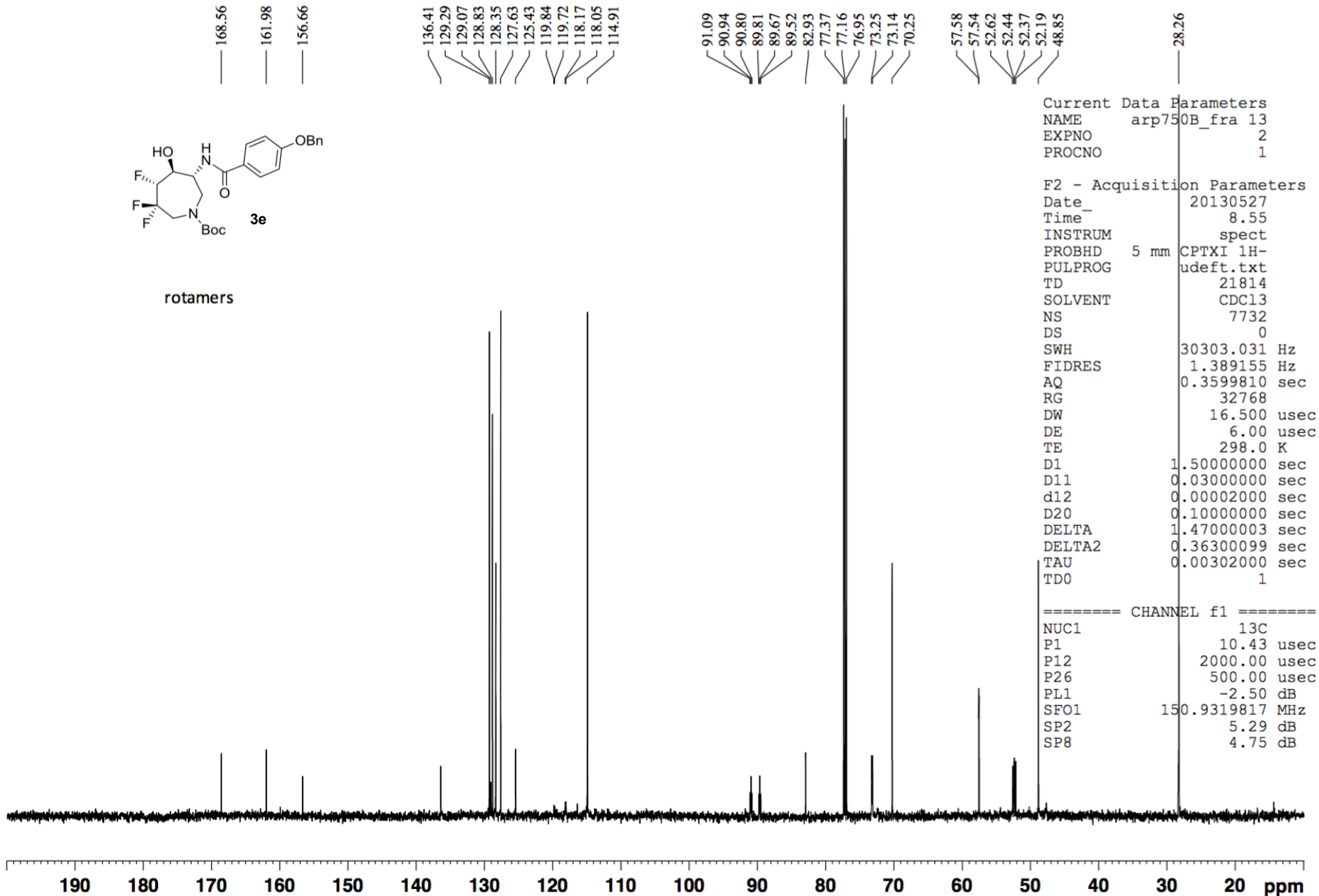
===== CHANNEL f1 =====
 NUC1 1H
 P1 7.63 usec
 PL1 1.00 dB
 SFO1 600.1824115 MHz

F1 - Acquisition parameters
 TD 256
 SFO1 150.9229 MHz
 FIDRES 93.450958 Hz
 SW 158.514 ppm
 FnMODE States-TPPI

F2 - Processing parameters
 SI 32768



rotamers



Current Data Parameters
 NAME arp750B_fra 13
 EXPNO 2
 PROCNO 1

F2 - Acquisition Parameters
 Date_ 20130527
 Time_ 8.55
 INSTRUM spect
 PROBHD 5 mm CPTXI 1H-
 PULPROG udeflt.txt
 TD 21814
 SOLVENT CDC13
 NS 7732
 DS 0
 SWH 30303.031 Hz
 FIDRES 1.389155 Hz
 AQ 0.3599810 sec
 RG 32768
 DW 16.500 usec
 DE 6.00 usec
 TE 298.0 K
 D1 1.5000000 sec
 D11 0.0300000 sec
 d12 0.0000200 sec
 D20 0.1000000 sec
 DELTA 1.4700003 sec
 DELTA2 0.36300099 sec
 TAU 0.0030200 sec
 TD0 1

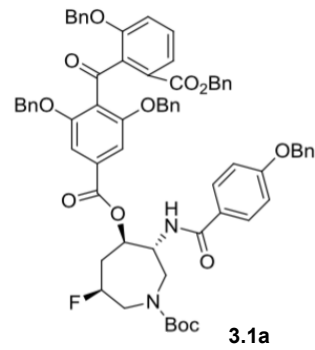
===== CHANNEL f1 =====
 NUC1 13C
 P1 10.43 usec
 P12 2000.00 usec
 P26 500.00 usec
 PL1 -2.50 dB
 SFO1 150.9319817 MHz
 SP2 5.29 dB
 SP8 4.75 dB

Current Data Parameters
 NAME arp559_protected F-balanol spot 3
 EXPNO 2
 PROCNO 1

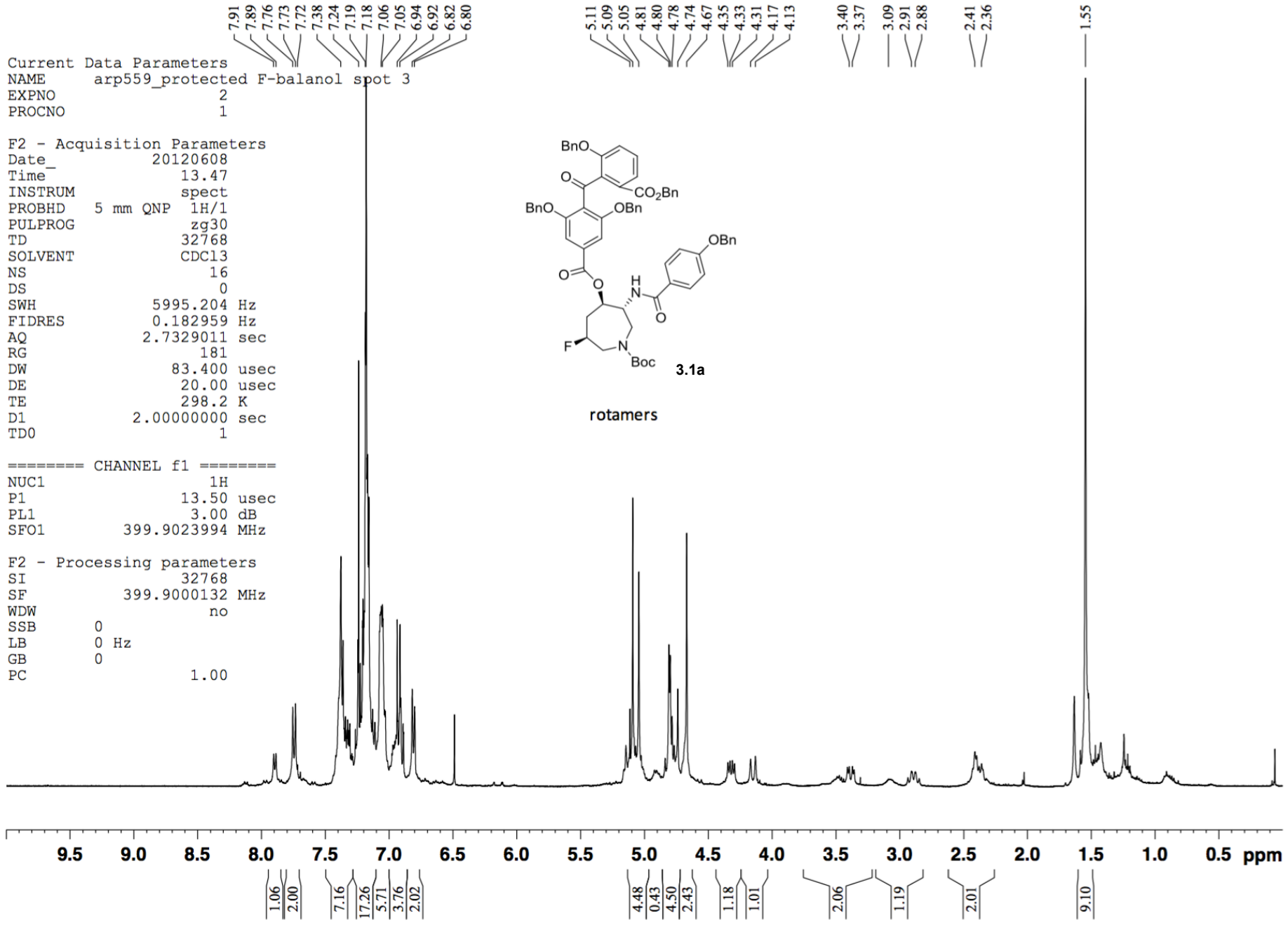
F2 - Acquisition Parameters
 Date_ 20120608
 Time_ 13.47
 INSTRUM spect
 PROBHD 5 mm QNP 1H/1
 PULPROG zg30
 TD 32768
 SOLVENT CDCl3
 NS 16
 DS 0
 SWH 5995.204 Hz
 FIDRES 0.182959 Hz
 AQ 2.7329011 sec
 RG 181
 DW 83.400 usec
 DE 20.00 usec
 TE 298.2 K
 D1 2.0000000 sec
 TD0 1

===== CHANNEL f1 =====
 NUC1 1H
 P1 13.50 usec
 PL1 3.00 dB
 SFO1 399.9023994 MHz

F2 - Processing parameters
 SI 32768
 SF 399.9000132 MHz
 WDW no
 SSB 0
 LB 0 Hz
 GB 0
 PC 1.00



rotamers

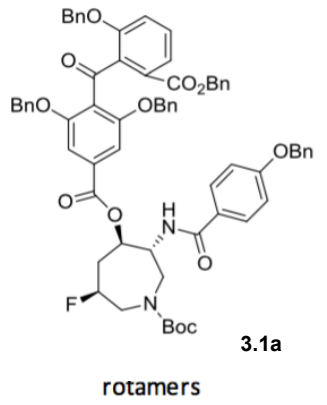


7.91, 7.89, 7.76, 7.73, 7.72, 7.38, 7.24, 7.19, 7.18, 7.06, 7.05, 6.94, 6.92, 6.82, 6.80, 5.11, 5.09, 5.05, 4.81, 4.80, 4.78, 4.74, 4.67, 4.65, 4.33, 4.31, 4.17, 4.13, 3.40, 3.37, 3.09, 2.91, 2.88, 2.41, 2.36, 1.55

192.00
 167.77
 166.50
 165.82
 161.88
 158.42
 157.43
 156.72
 136.75
 136.58
 136.18
 136.10
 133.18
 132.85
 130.87
 129.26
 129.06
 128.82
 128.71
 128.61
 128.31
 128.19
 127.91
 127.84
 127.61
 127.51
 126.76
 122.43
 115.72
 115.09
 107.43
 104.27
 88.67
 86.91
 82.18
 77.76
 77.44
 77.12
 72.63
 72.56
 70.88
 70.46
 67.46
 53.46
 53.23
 52.90
 51.61
 34.54
 34.33
 28.73

Current Data Parameters
 NAME arp559_protected F-balanol spot 3
 EXPNO 3
 PROCNO 1

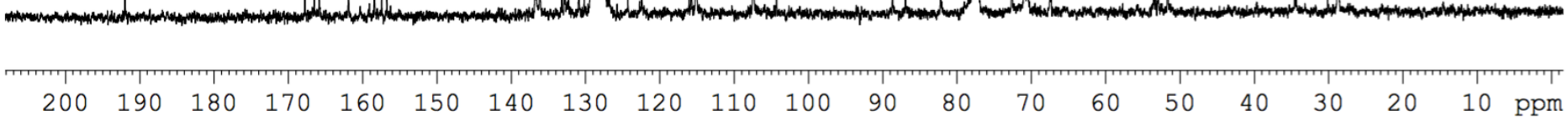
F2 - Acquisition Parameters
 Date_ 20120608
 Time_ 13.54
 INSTRUM spect
 PROBHD 5 mm QNP 1H/1
 PULPROG zgpg
 TD 66560
 SOLVENT CDC13
 NS 1291
 DS 2
 SWH 25125.629 Hz
 FIDRES 0.377488 Hz
 AQ 1.3245940 sec
 RG 20642.5
 DW 19.900 usec
 DE 20.00 usec
 TE 298.2 K
 D1 2.00000000 sec
 d11 0.03000000 sec
 DELTA 1.89999998 sec
 TD0 1



===== CHANNEL f1 =====
 NUC1 13C
 P1 12.00 usec
 PL1 -0.50 dB
 SFO1 100.5659560 MHz

===== CHANNEL f2 =====
 CPDPRG2 waltz16
 NUC2 1H
 PCPD2 80.00 usec
 PL2 3.00 dB
 PL12 18.80 dB
 PL13 24.80 dB
 SFO2 399.9015996 MHz

F2 - Processing parameters
 SI 32768
 SF 100.5548950 MHz
 WDW EM
 SSB 0
 LB 3.00 Hz
 GB 0
 PC 1.40

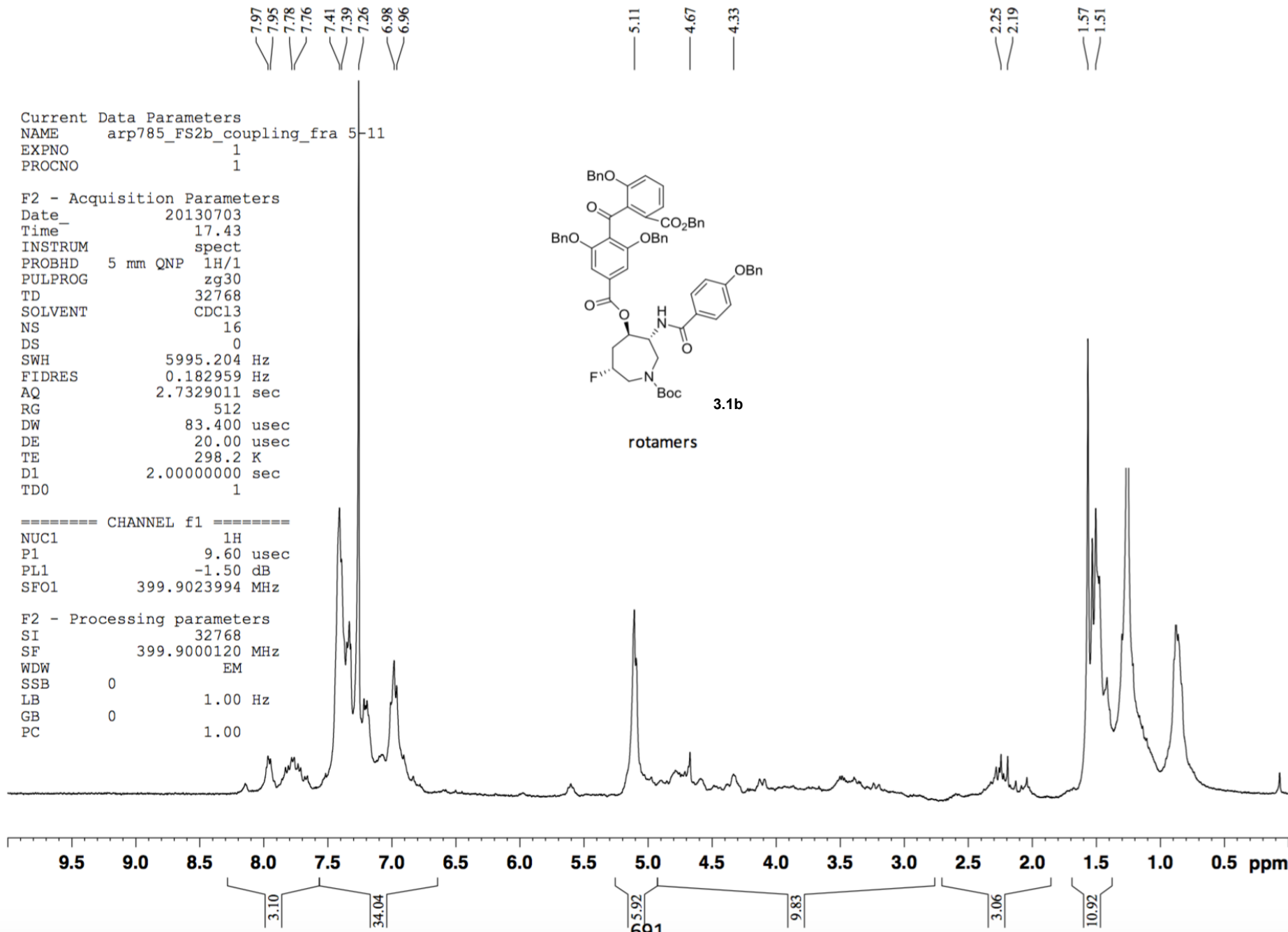
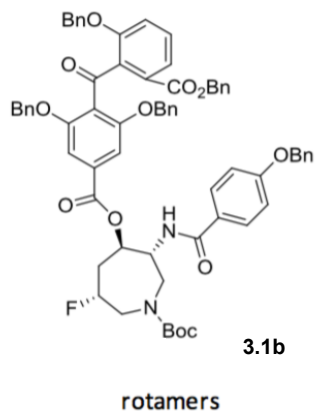


Current Data Parameters
 NAME arp785_FS2b_coupling_fra 5-11
 EXPNO 1
 PROCNO 1

F2 - Acquisition Parameters
 Date_ 20130703
 Time_ 17.43
 INSTRUM spect
 PROBHD 5 mm QNP 1H/1
 PULPROG zg30
 TD 32768
 SOLVENT CDCl3
 NS 16
 DS 0
 SWH 5995.204 Hz
 FIDRES 0.182959 Hz
 AQ 2.7329011 sec
 RG 512
 DW 83.400 usec
 DE 20.00 usec
 TE 298.2 K
 D1 2.00000000 sec
 TD0 1

===== CHANNEL f1 =====
 NUC1 1H
 P1 9.60 usec
 PL1 -1.50 dB
 SFO1 399.9023994 MHz

F2 - Processing parameters
 SI 32768
 SF 399.9000120 MHz
 WDW EM
 SSB 0
 LB 1.00 Hz
 GB 0
 PC 1.00

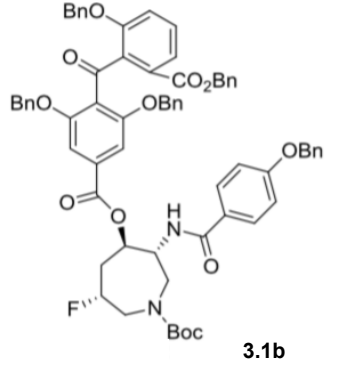


162.37
162.29
162.22
162.17
157.57
137.95
132.56
132.47
130.03
129.97
129.76
129.34
129.08
128.97
128.91
128.78
128.55
128.49
122.63
122.59
116.20
115.31
115.23

92.80
91.67
90.66
89.54
81.64
81.36
80.63
79.65
76.27
71.46
70.57
67.51
59.89
54.00
53.24
53.02
50.86
50.51
46.71
46.14
42.93
30.23
30.10
29.97
29.84
29.72
29.58
29.46
28.58
28.45

```
Current Data Parameters
NAME      arp797_Fs2bprobal
EXPNO     3
PROCNO    1

F2 - Acquisition Parameters
Date_     20130909
Time      17.20
INSTRUM   spect
PROBHD    5 mm CPTXI 1H-
PULPROG   zgpg30
TD         36696
SOLVENT   Acetone
NS         22080
DS         0
SWH        33333.332 Hz
FIDRES     0.908364 Hz
AQ         0.5504400 sec
RG         2050
DW         15.000 usec
DE         18.00 usec
TE         300.7 K
D1         2.00000000 sec
D11        0.03000000 sec
TD0        1
```

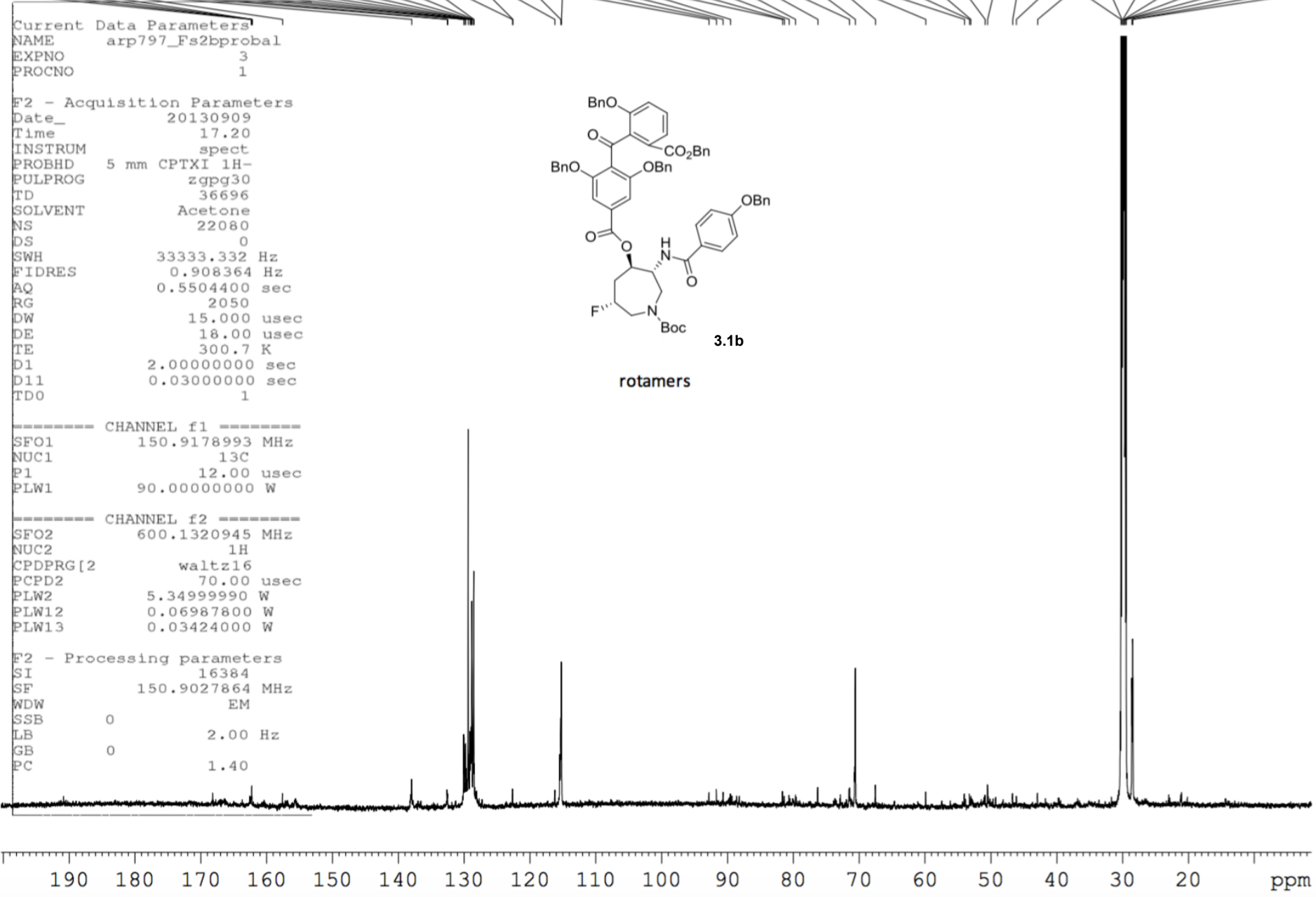


rotamers

```
----- CHANNEL f1 -----
SFO1      150.9178993 MHz
NUC1       13C
P1         12.00 usec
PLW1       90.00000000 W

----- CHANNEL f2 -----
SFO2      600.1320945 MHz
NUC2       1H
CPDPRG[2]  waltz16
PCPD2     70.00 usec
PLW2       5.34999990 W
PLW12     0.06987800 W
PLW13     0.03424000 W
```

```
F2 - Processing parameters
SI         16384
SF         150.9027864 MHz
WDW        EM
SSB        0
LB         2.00 Hz
GB         0
PC         1.40
```



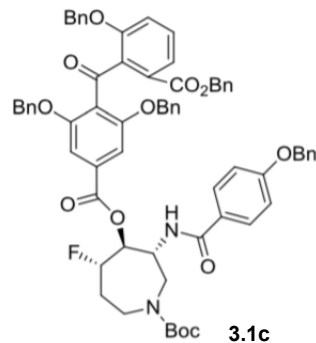
Current Data Parameters
 NAME arp785_FN3S2A_proba
 EXPNO 1
 PROCNO 1

F2 - Acquisition Parameters
 Date_ 20130722
 Time_ 18.49
 INSTRUM spect
 PROBHD 5 mm CPTXI 1H-
 PULPROG zg30
 TD 32768
 SOLVENT CDCl3
 NS 16
 DS 0
 SWH 8389.262 Hz
 FIDRES 0.256020 Hz
 AQ 1.9530228 sec
 RG 14.3
 DW 59.600 usec
 DE 6.00 usec
 TE 298.0 K
 D1 1.5000000 sec
 TD0 1

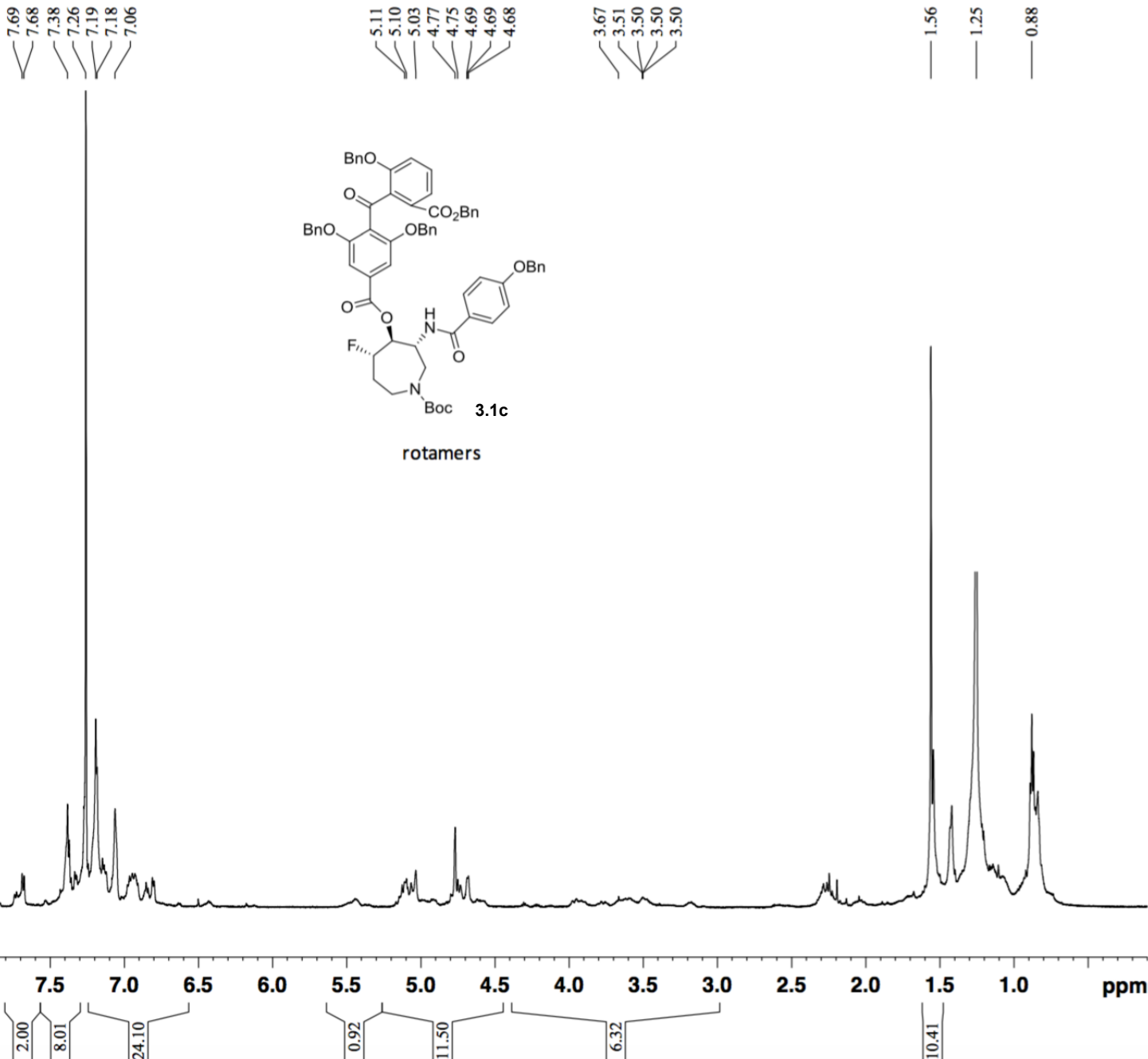
==== CHANNEL f1 =====
 NUC1 1H
 P1 8.40 usec
 PL1 1.00 dB
 SFO1 600.1822721 MHz

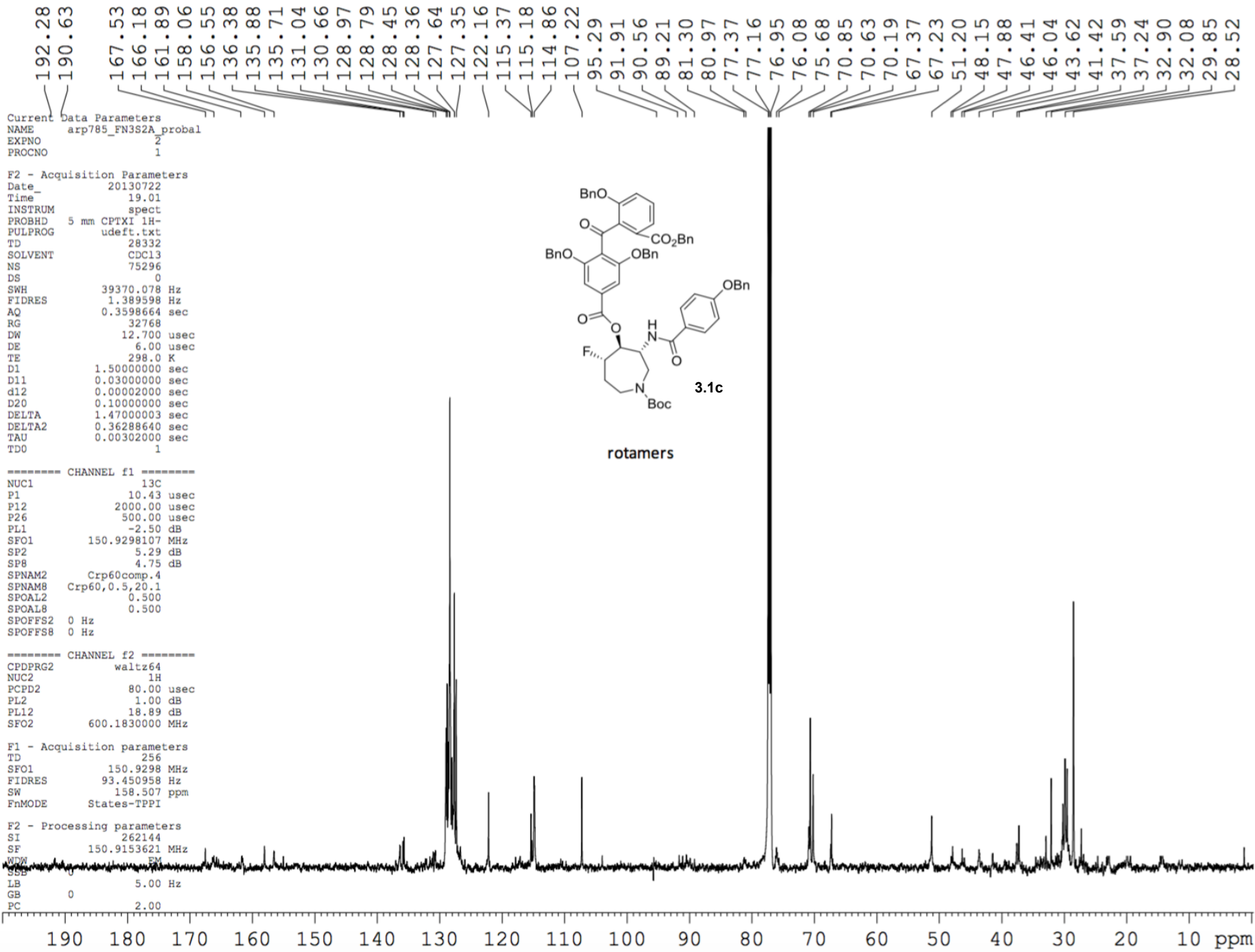
F1 - Acquisition parameters
 TD 256
 SFO1 150.9229 MHz
 FIDRES 93.450958 Hz
 SW 158.514 ppm
 EnMODE States-TPPI

F2 - Processing parameters
 SI 65536



rotamers





8.00
7.98
7.80
7.78
7.42
7.40
7.39
7.35
7.33
7.26
7.24
7.22
7.21
7.19
7.12
7.08
7.07
6.98
6.96

5.15
5.12
5.09
4.80
4.79
4.71
4.40
4.21
4.17

3.47
3.46
3.43
3.32
3.31
3.28
3.27

2.60
2.57

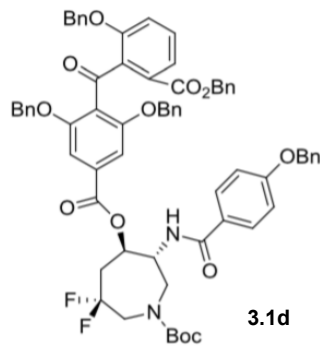
1.62
1.56

Current Data Parameters

NAME arp781_pro bal_ C6FF_fra 10-19
EXPNO 1
PROCNO 1

F2 - Acquisition Parameters

Date_ 20130624
Time_ 17.45
INSTRUM spect
PROBHD 5 mm QNP 1H/1
PULPROG zg30
TD 32768
SOLVENT CDC13
NS 64
DS 0
SWH 5995.204 Hz
FIDRES 0.182959 Hz
AQ 2.7329011 sec
RG 228.1
DW 83.400 usec
DE 20.00 usec
TE 298.2 K
D1 2.00000000 sec
TD0 1



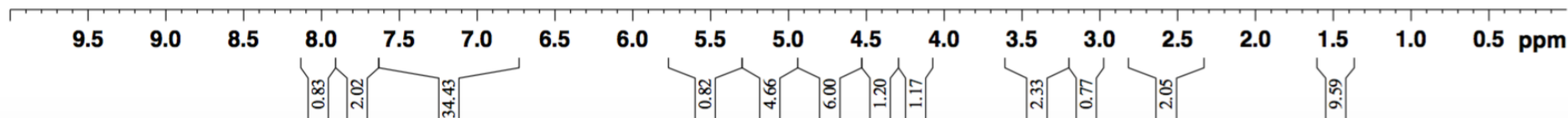
rotamers

==== CHANNEL f1 =====

NUC1 1H
P1 9.60 usec
PL1 -1.50 dB
SFO1 399.9023994 MHz

F2 - Processing parameters

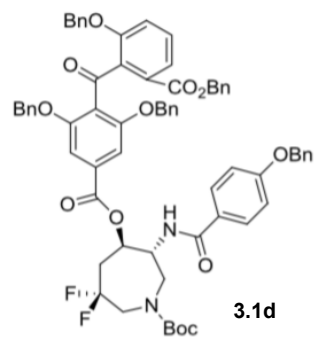
SI 32768
SF 399.9000121 MHz
WDW EM
SSB 0
LB 1.00 Hz
GB 0
PC 1.00



191.69
 167.52
 166.50
 164.89
 161.73
 158.13
 157.09
 136.45
 135.90
 135.81
 132.27
 130.70
 129.06
 128.79
 128.59
 128.37
 127.60
 127.22
 126.26
 122.18
 114.86
 114.72
 107.16
 82.43
 77.48
 77.16
 76.84
 76.07
 70.88
 70.62
 70.21
 69.89
 67.38
 67.23
 55.80
 55.54
 53.64
 53.44
 50.61
 36.39
 36.13
 28.29

Current Data Parameters
 NAME arp781_C6FFprobal_13C
 EXPNO 10
 PROCNO 1

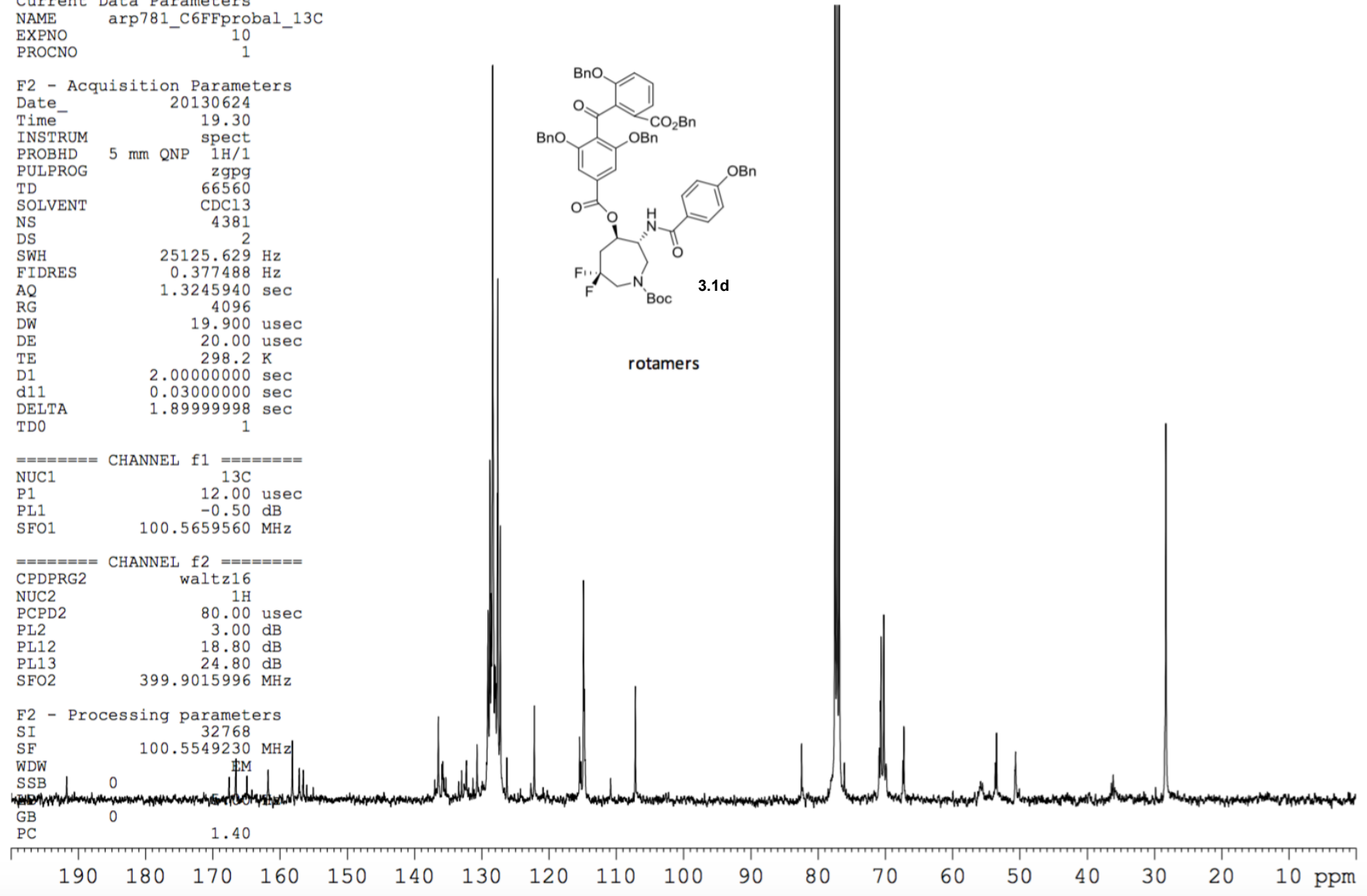
F2 - Acquisition Parameters
 Date_ 20130624
 Time_ 19.30
 INSTRUM spect
 PROBHD 5 mm QNP 1H/1
 PULPROG zgpg
 TD 66560
 SOLVENT CDCl3
 NS 4381
 DS 2
 SWH 25125.629 Hz
 FIDRES 0.377488 Hz
 AQ 1.3245940 sec
 RG 4096
 DW 19.900 usec
 DE 20.00 usec
 TE 298.2 K
 D1 2.00000000 sec
 d11 0.03000000 sec
 DELTA 1.89999998 sec
 TD0 1



==== CHANNEL f1 =====
 NUC1 13C
 P1 12.00 usec
 PL1 -0.50 dB
 SFO1 100.5659560 MHz

==== CHANNEL f2 =====
 CPDPRG2 waltz16
 NUC2 1H
 PCPD2 80.00 usec
 PL2 3.00 dB
 PL12 18.80 dB
 PL13 24.80 dB
 SFO2 399.9015996 MHz

F2 - Processing parameters
 SI 32768
 SF 100.5549230 MHz
 WDW EM
 SSB 0
 GB 0
 PC 1.40



7.73
7.71
7.69
7.39
7.37
7.24
7.23
7.21
7.19
7.06
7.05
6.95
6.88
6.86
6.84
6.82
6.80

5.66

5.14
5.11
5.06
5.05
4.76

4.38

4.08
4.04

3.47

Current Data Parameters

NAME arp780_pro bal_ triF_fra 12-21
EXPNO 1
PROCNO 1

F2 - Acquisition Parameters

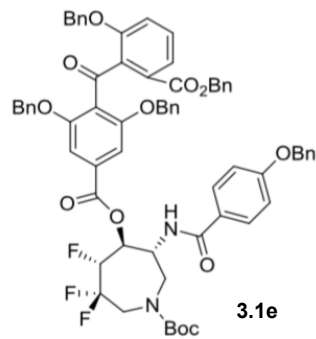
Date_ 20130624
Time 17.32
INSTRUM spect
PROBHD 5 mm QNP 1H/1
PULPROG zg30
TD 32768
SOLVENT CDCl3
NS 64
DS 0
SWH 5995.204 Hz
FIDRES 0.182959 Hz
AQ 2.7329011 sec
RG 574.7
DW 83.400 usec
DE 20.00 usec
TE 298.2 K
D1 2.00000000 sec
TDO 1

==== CHANNEL f1 =====

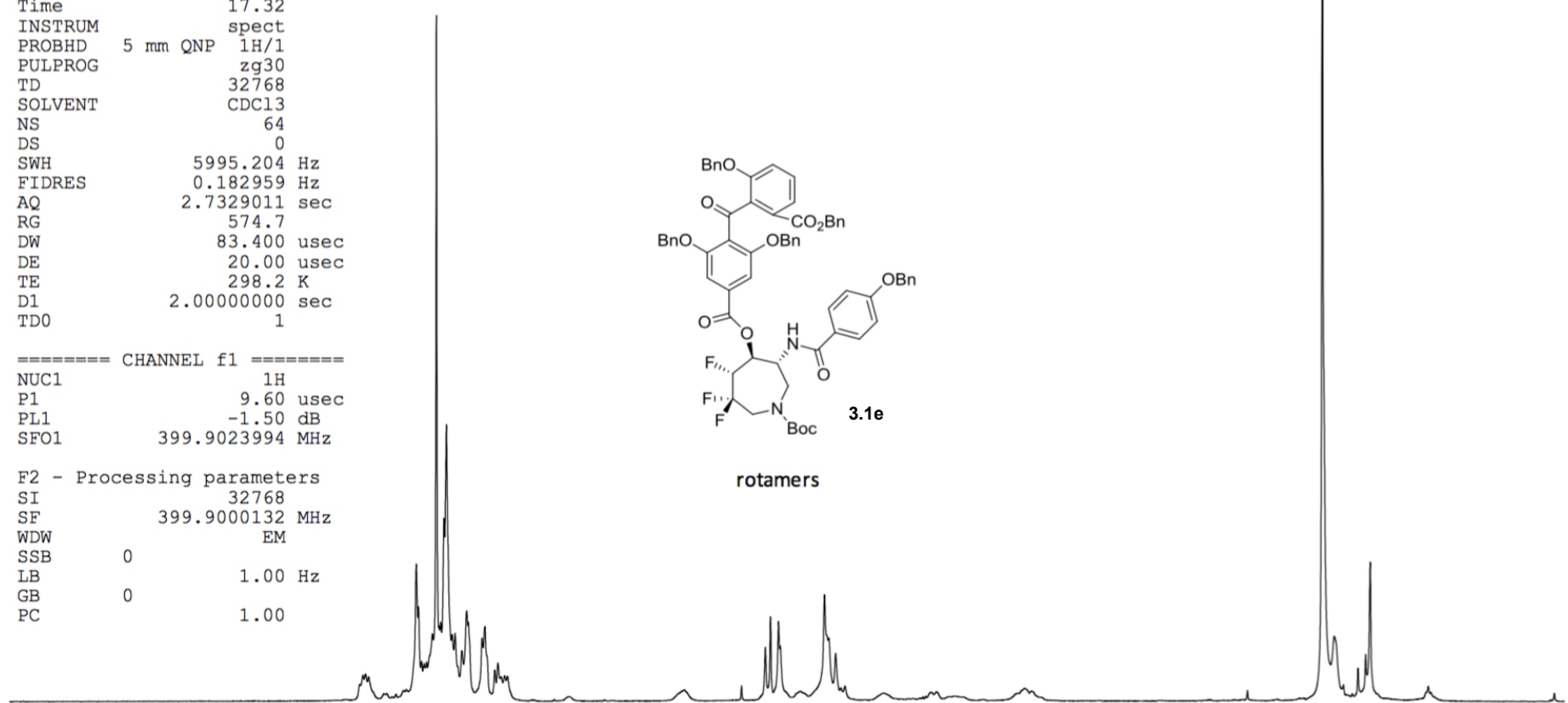
NUC1 1H
P1 9.60 usec
PL1 -1.50 dB
SFO1 399.9023994 MHz

F2 - Processing parameters

SI 32768
SF 399.9000132 MHz
WDW EM
SSB 0
LB 1.00 Hz
GB 0
PC 1.00

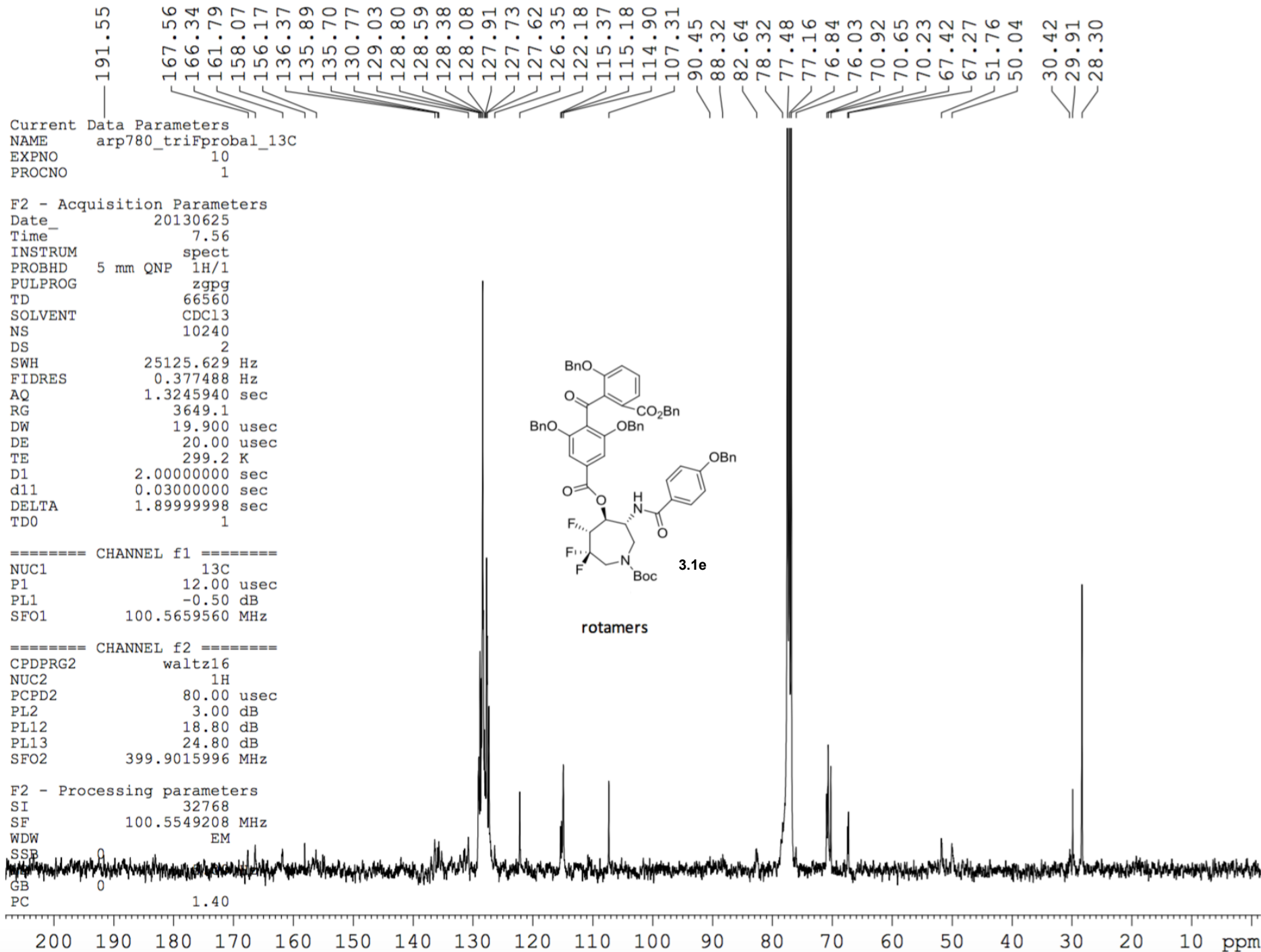


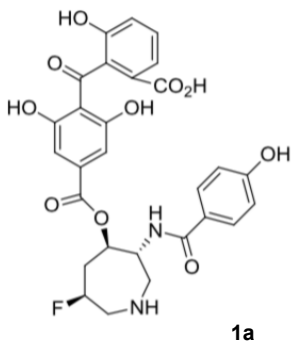
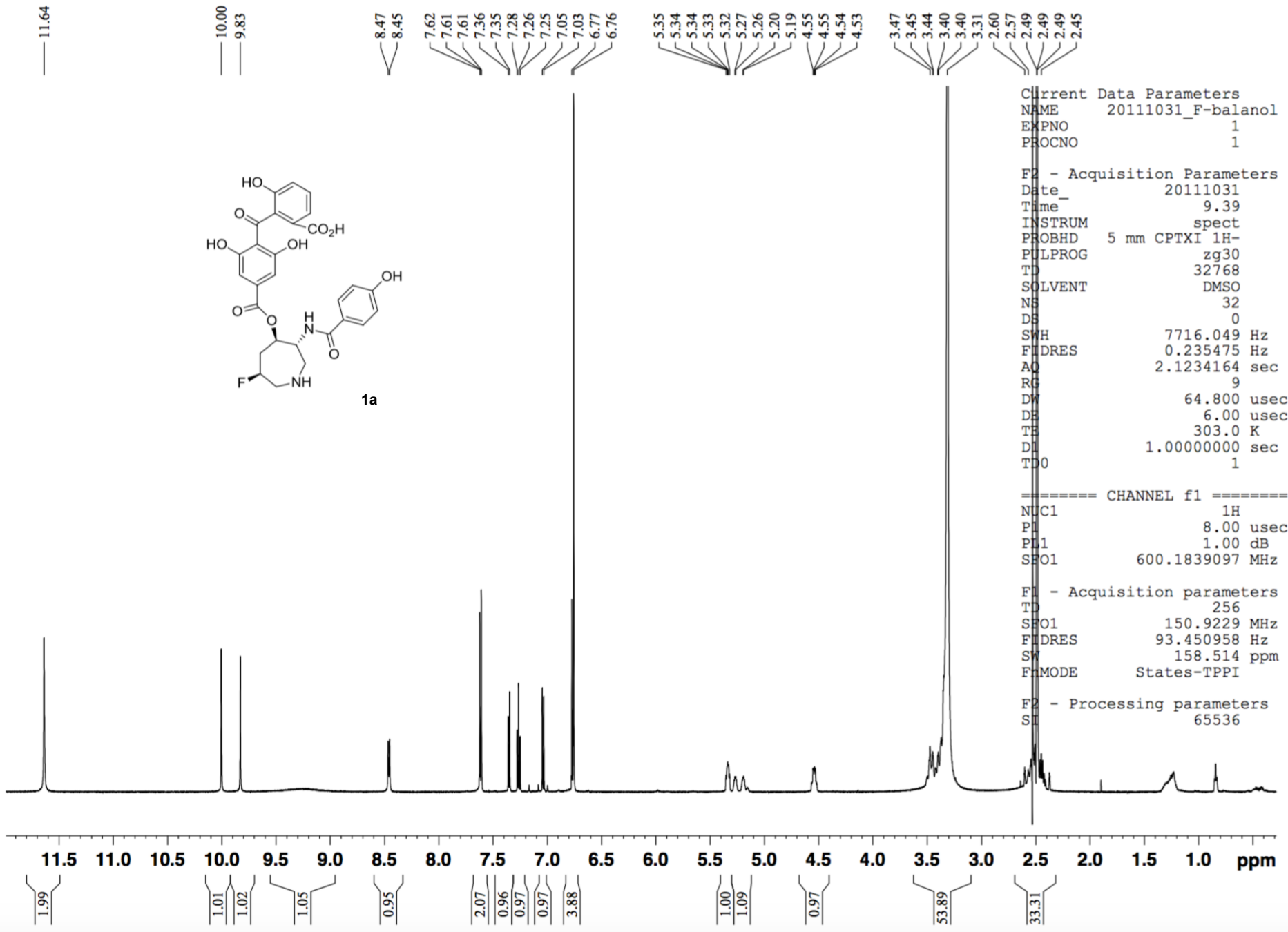
rotamers



9.5 9.0 8.5 8.0 7.5 7.0 6.5 6.0 5.5 5.0 4.5 4.0 3.5 3.0 2.5 2.0 1.5 1.0 0.5 ppm

2.05 33.39 1.23 4.30 6.81 1.01 1.06 0.93 2.00 10.53





Current Data Parameters
 NAME 20111031_F-balanol
 EXPNO 1
 PROCNO 1

F2 - Acquisition Parameters
 Date_ 20111031
 Time_ 9.39
 INSTRUM spect
 PROBHD 5 mm CPTXI 1H-
 PULPROG zg30
 TD 32768
 SOLVENT DMSO
 NS 32
 DS 0
 SWH 7716.049 Hz
 FIDRES 0.235475 Hz
 AQ 2.1234164 sec
 RG 9
 DW 64.800 usec
 DE 6.00 usec
 TE 303.0 K
 DL 1.00000000 sec
 TDO 1

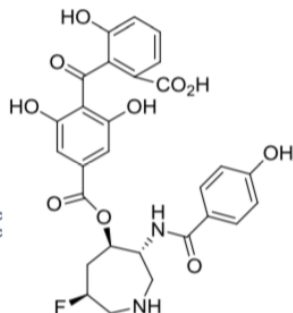
==== CHANNEL f1 =====
 NUC1 1H
 P1 8.00 usec
 PL1 1.00 dB
 SFO1 600.1839097 MHz

F1 - Acquisition parameters
 TD 256
 SFO1 150.9229 MHz
 FIDRES 93.450958 Hz
 SW 158.514 ppm
 FMODE States-TPPI

F2 - Processing parameters
 SI 65536

Current Data Parameters
NAME 20111031_F-balanol
EXPNO 3
PROCNO 1

F2 - Acquisition Parameters
Date_ 20111031
Time 11.33
INSTRUM spect
PROBHD 5 mm CPTXI 1H-
PULPROG udef.txt
TD 21814
SOLVENT DMSO
NS 10888
DS 0
SWH 30303.031 Hz
FIDRES 1.389155 Hz
AQ 0.3599810 sec
RG 16384
DW 16.500 usec
DE 6.00 usec
TE 303.0 K
D1 1.50000000 sec
D11 0.03000000 sec
d12 0.00002000 sec
D20 0.10000000 sec
DELTA 1.47000003 sec
DELTA2 0.36300099 sec
TAU 0.00302000 sec
TDO 1

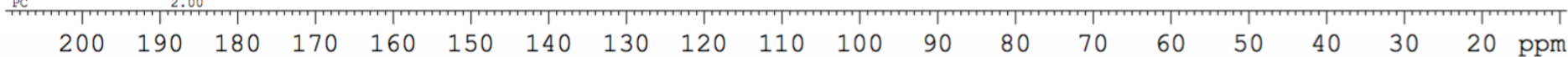


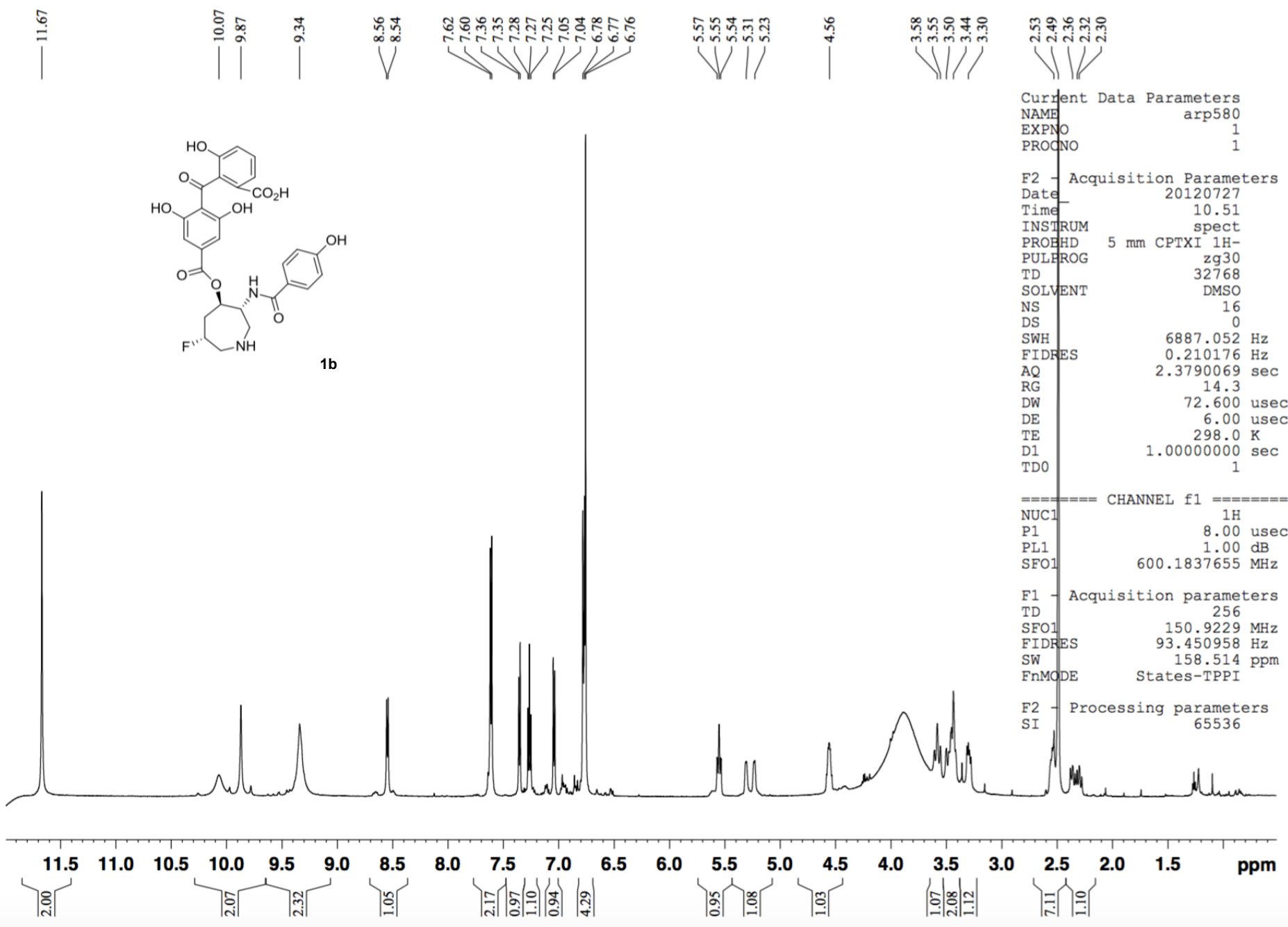
----- CHANNEL f1 -----
NUC1 13C
P1 10.43 usec
P12 2000.00 usec
P26 500.00 usec
PL1 -2.50 dB
SFO1 150.9319817 MHz
SP2 5.29 dB
SP8 4.75 dB
SPNAM2 Crp60comp.4
SPNAM8 Crp60,0.5,20.1
SPOAL2 0.500
SPOAL8 0.500
SPOFFS2 0 Hz
SPOFFS8 0 Hz

----- CHANNEL f2 -----
CPDPRG2 waltz64
NUC2 1H
PCPD2 80.00 usec
PL2 1.00 dB
PL12 18.64 dB
SFO2 600.1830000 MHz

F1 - Acquisition parameters
TD 256
SFO1 150.932 MHz
FIDRES 93.450958 Hz
SW 158.505 ppm
FnMODE States-TPPI

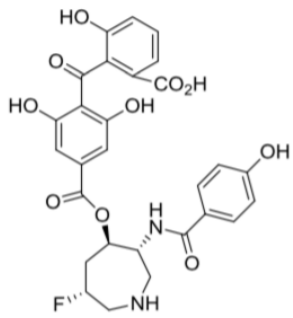
F2 - Processing parameters
SI 262144
SF 150.9154585 MHz
AQ 0.3599810 sec
LB 10.00 Hz
GB 0
PC 2.00





Current Data Parameters
 NAME arp580
 EXPNO 3
 PROCNO 1

F2 - Acquisition Parameters
 Date_ 20120727
 Time_ 23.35
 INSTRUM spect
 PROBHD 5 mm CPTXI 1H-
 PULPROG udeflt.txt
 TD 21814
 SOLVENT DMSO
 NS 20000
 DS 0
 SWH 30303.031 Hz
 FIDRES 1.389155 Hz
 AQ 0.3599810 sec
 RG 16384
 DW 16.500 usec
 DE 6.00 usec
 TE 298.0 K
 D1 1.50000000 sec
 D11 0.03000000 sec
 d12 0.00002000 sec
 D20 0.10000000 sec
 DELTA 1.47000003 sec
 DELTA2 0.36300099 sec
 TAU 0.00302000 sec
 TD0 1



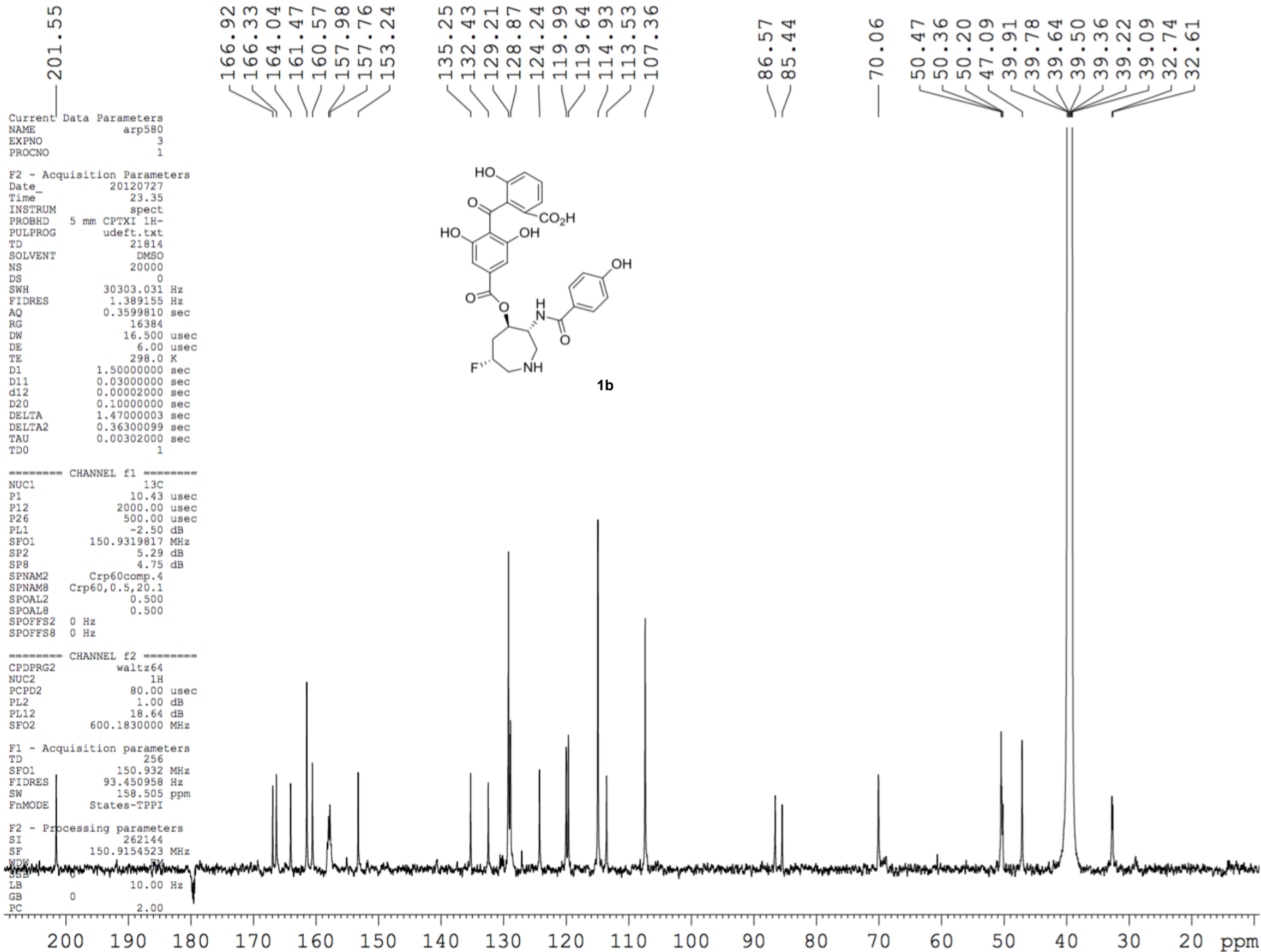
1b

----- CHANNEL f1 -----
 NUC1 13C
 P1 10.43 usec
 P12 2000.00 usec
 P26 500.00 usec
 PL1 -2.50 dB
 SFO1 150.9319817 MHz
 SP2 5.29 dB
 SP8 4.75 dB
 SPNAM2 Crp60comp.4
 SPNAM8 Crp60,0.5,20.1
 SPOAL2 0.500
 SPOAL8 0.500
 SPOFFS2 0 Hz
 SPOFFS8 0 Hz

----- CHANNEL f2 -----
 CPDPRG2 waltz64
 NUC2 1H
 PCPD2 80.00 usec
 PL2 1.00 dB
 PL12 18.64 dB
 SFO2 600.1830000 MHz

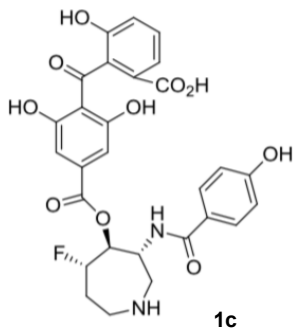
F1 - Acquisition parameters
 TD 256
 SFO1 150.932 MHz
 FIDRES 93.450958 Hz
 SW 158.505 ppm
 FnMODE States-TPPI

F2 - Processing parameters
 SI 262144
 SF 150.9154523 MHz
 DS 4
 LB 10.00 Hz
 GB 0
 PC 2.00



Current Data Parameters
 NAME arp786a_FN3S2A
 EXPNO 1
 PROCNO 4

F2 - Acquisition Parameters
 Date_ 20130730
 Time 14.35
 INSTRUM spect
 PROBHD 5 mm CPTXI 1H-
 PULPROG zg30
 TD 32768
 SOLVENT CD3CN
 NS 124
 DS 0
 SWH 6887.052 Hz
 FIDRES 0.210176 Hz
 AQ 2.3790069 sec
 RG 12.7
 DW 72.600 usec
 DE 6.00 usec
 TE 298.0 K
 D1 1.00000000 sec
 TD0 1

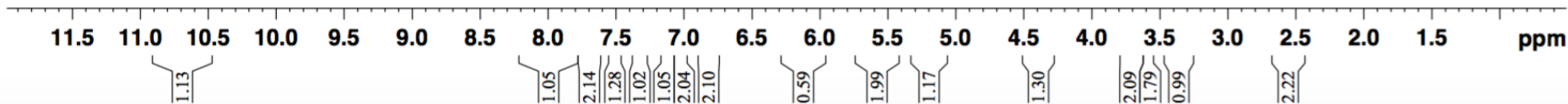


8.00 7.99 7.69 7.67 7.52 7.50 7.34 7.33 7.32 7.12 7.10 7.02 6.84 6.82
 5.50 5.49 5.48 5.27 5.26 5.20 5.19 5.19
 4.41
 3.69 3.67 3.65 3.57 3.53 3.41 3.41 3.39 3.37
 2.56 2.53 2.51 1.94 1.94 1.94 1.93

==== CHANNEL f1 =====
 NUC1 1H
 P1 7.90 usec
 PL1 1.00 dB
 SFO1 600.1837655 MHz

F1 - Acquisition parameters
 TD 256
 SFO1 150.9229 MHz
 FIDRES 93.450958 Hz
 SW 158.514 ppm
 FnMODE States-TPPI

F2 - Processing parameters
 SI 65536



Current Data Parameters
 NAME arp786a_FN3S2A
 EXPNO 3
 PROCNO 1

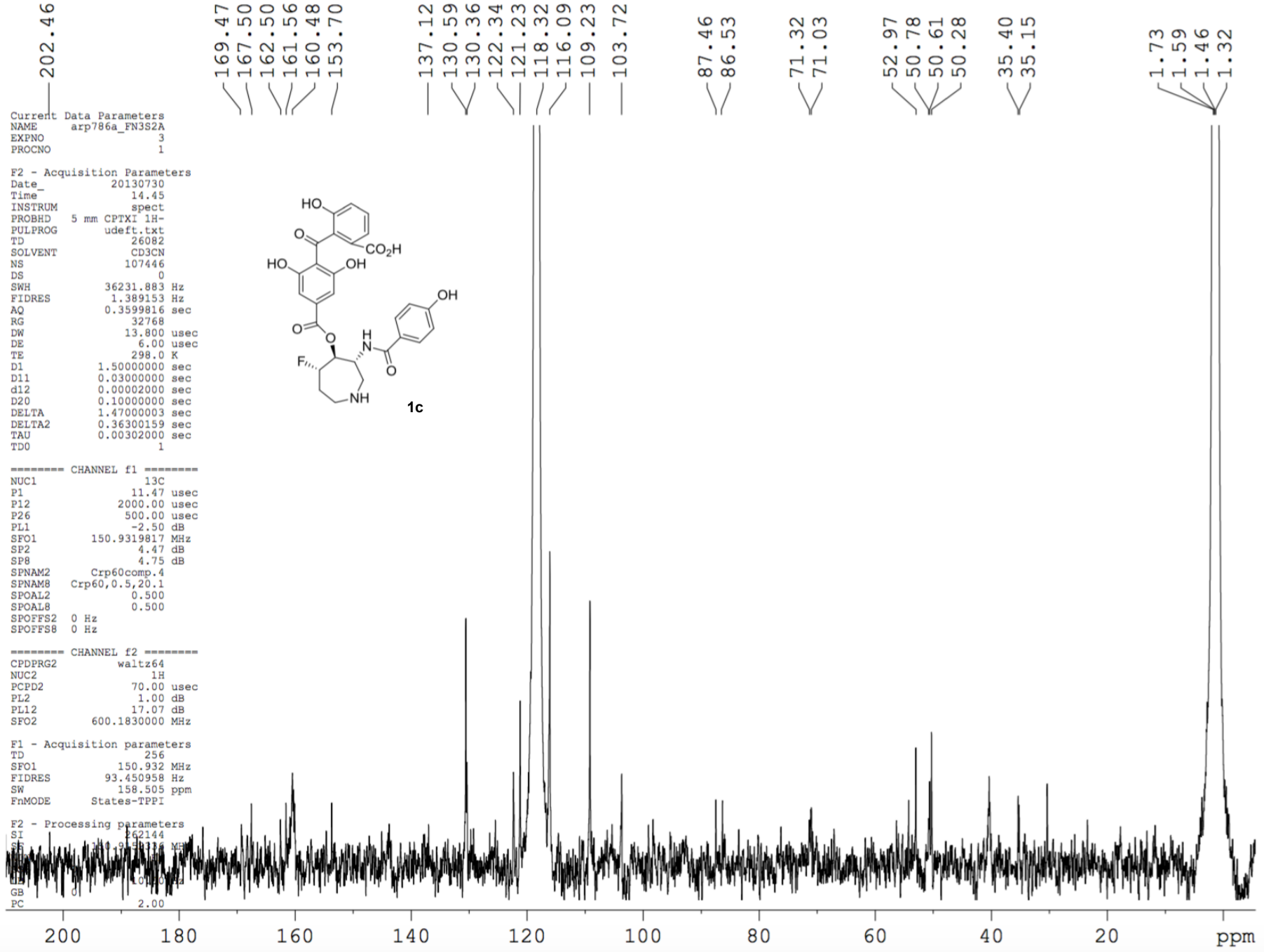
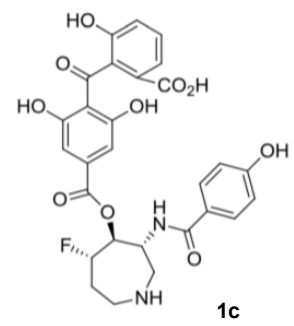
F2 - Acquisition Parameters
 Date_ 20130730
 Time_ 14.45
 INSTRUM spect
 PROBHD 5 mm CPTXI 1H-
 PULPROG udeflt.txt
 TD 26082
 SOLVENT CD3CN
 NS 107446
 DS 0
 SWH 36231.883 Hz
 FIDRES 1.389153 Hz
 AQ 0.3599816 sec
 RG 32768
 DW 13.800 usec
 DE 6.00 usec
 TE 298.0 K
 D1 1.50000000 sec
 D11 0.03000000 sec
 d12 0.00002000 sec
 D20 0.10000000 sec
 DELTA 1.47000003 sec
 DELTA2 0.36300159 sec
 TAU 0.00302000 sec
 TD0 1

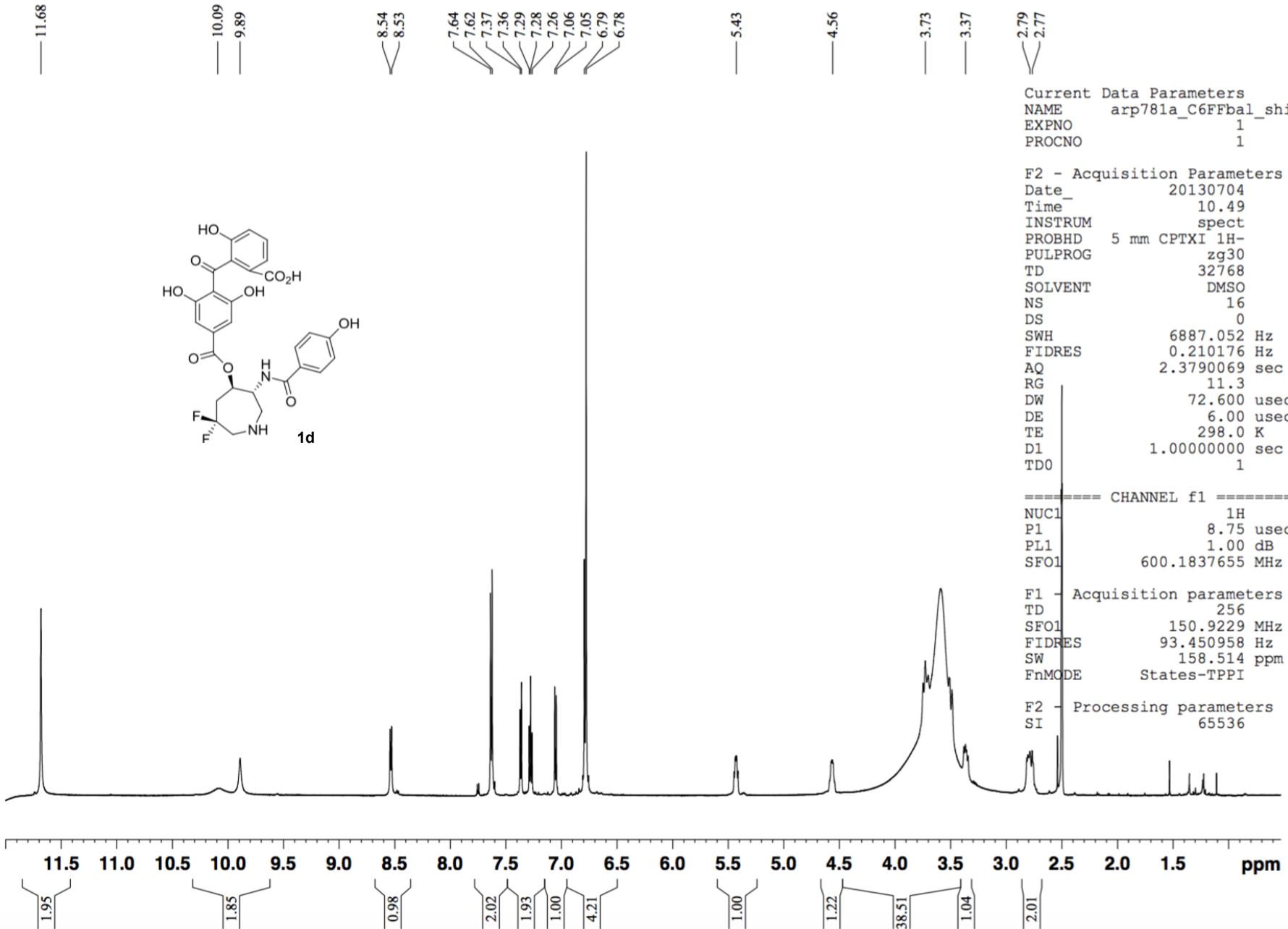
===== CHANNEL f1 =====
 NUC1 13C
 P1 11.47 usec
 P12 2000.00 usec
 P26 500.00 usec
 PL1 -2.50 dB
 SFO1 150.9319817 MHz
 SP2 4.47 dB
 SP8 4.75 dB
 SPNAM2 Crp60comp.4
 SPNAM8 Crp60,0.5,20.1
 SPOAL2 0.500
 SPOAL8 0.500
 SPOFFS2 0 Hz
 SPOFFS8 0 Hz

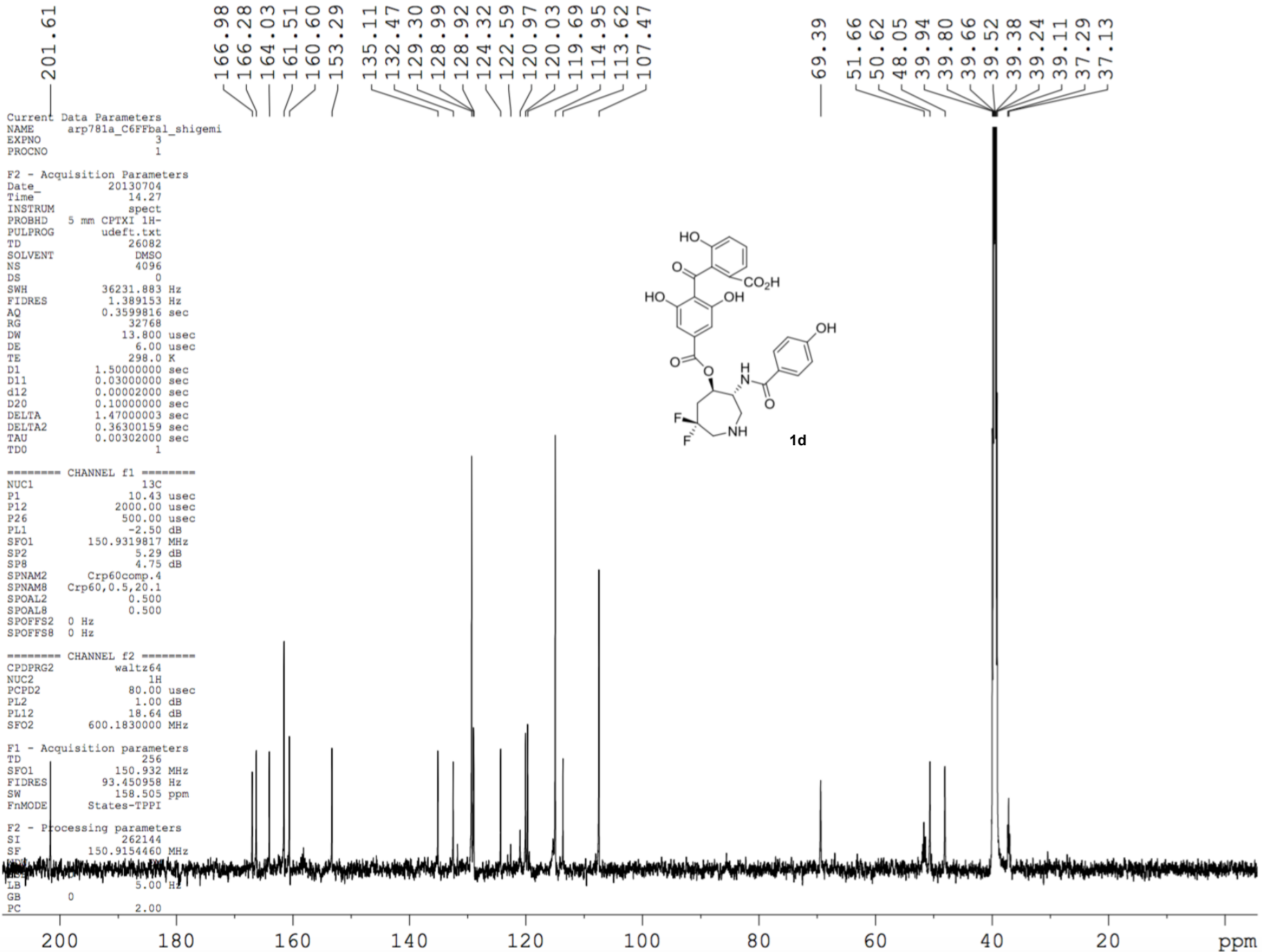
===== CHANNEL f2 =====
 CPDPRG2 waltz64
 NUC2 1H
 PCPD2 70.00 usec
 PL2 1.00 dB
 PL12 17.07 dB
 SFO2 600.1830000 MHz

F1 - Acquisition parameters
 TD 256
 SFO1 150.932 MHz
 FIDRES 93.450958 Hz
 SW 158.505 ppm
 FnMODE States-TPPI

F2 - Processing parameters
 SI 262144
 SF 200.9319817 MHz
 DF 101.000 MHz
 GB 0
 PC 2.00







Current Data Parameters
 NAME arp781a_C6FFbal_shigemi
 EXPNO 3
 PROCNO 1

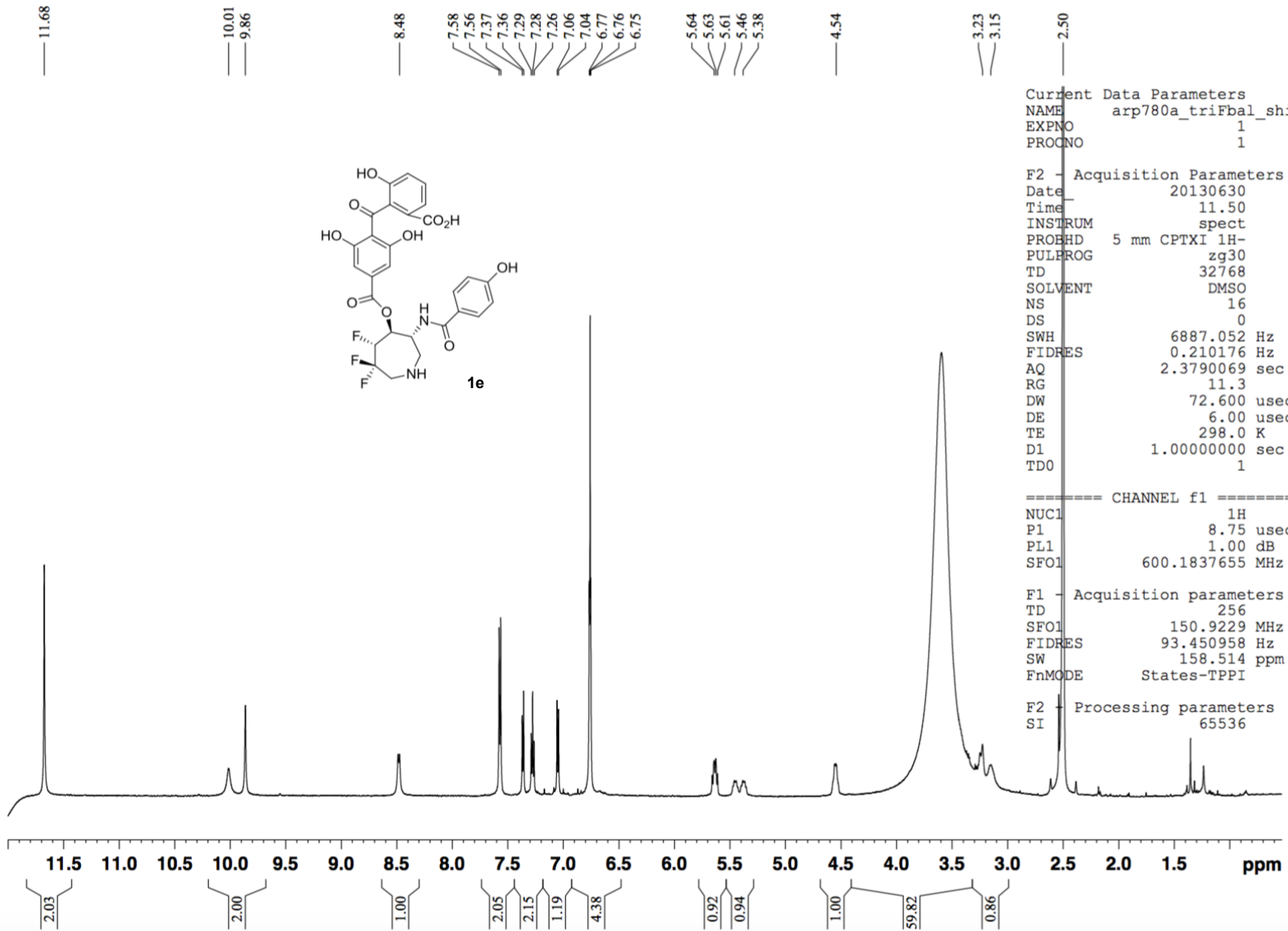
F2 - Acquisition Parameters
 Date_ 20130704
 Time_ 14.27
 INSTRUM spect
 PROBHD 5 mm CPTXI 1H-
 PULPROG udeflt.txt
 TD 26082
 SOLVENT DMSO
 NS 4096
 DS 0
 SWH 36231.883 Hz
 FIDRES 1.389153 Hz
 AQ 0.3599816 sec
 RG 32768
 DW 13.800 usec
 DE 6.00 usec
 TE 298.0 K
 D1 1.50000000 sec
 D11 0.03000000 sec
 d12 0.00002000 sec
 D20 0.10000000 sec
 DELTA 1.47000003 sec
 DELTA2 0.36300159 sec
 TAU 0.00302000 sec
 TD0 1

----- CHANNEL f1 -----
 NUC1 13C
 P1 10.43 usec
 P12 2000.00 usec
 P26 500.00 usec
 PL1 -2.50 dB
 SFO1 150.9319817 MHz
 SP2 5.29 dB
 SP8 4.75 dB
 SPNAM2 Crp60comp.4
 SPNAM8 Crp60,0.5,20.1
 SPOAL2 0.500
 SPOAL8 0.500
 SPOFFS2 0 Hz
 SPOFFS8 0 Hz

----- CHANNEL f2 -----
 CPDPRG2 waltz64
 NUC2 1H
 PCPD2 80.00 usec
 PL2 1.00 dB
 PL12 18.64 dB
 SFO2 600.1830000 MHz

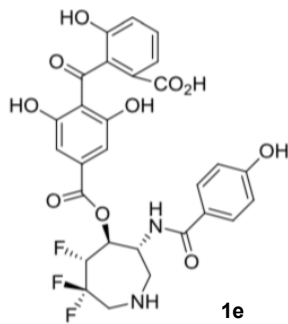
F1 - Acquisition parameters
 TD 256
 SFO1 150.932 MHz
 FIDRES 93.450958 Hz
 SW 158.505 ppm
 FNAME States-TPPI

F2 - Processing parameters
 SI 262144
 SF 150.9154460 MHz
 LB 5.00 Hz
 GB 0
 PC 2.00



Current Data Parameters
 NAME arp780a_triFbal_shigemi
 EXPNO 3
 PROCNO 1

F2 - Acquisition Parameters
 Date_ 20130630
 Time_ 19.36
 INSTRUM spect
 PROBHD 5 mm CPTXI 1H-
 PULPROG udeflt.txt
 TD 26082
 SOLVENT DMSO
 NS 43008
 DS 0
 SWH 36231.883 Hz
 FIDRES 1.389153 Hz
 AQ 0.3599816 sec
 RG 32768
 DW 13.800 usec
 DE 6.00 usec
 TE 298.0 K
 D1 1.50000000 sec
 D11 0.03000000 sec
 d12 0.00002000 sec
 D20 0.10000000 sec
 DELTA 1.47000003 sec
 DELTA2 0.36300159 sec
 TAU 0.00302000 sec
 TD0 1



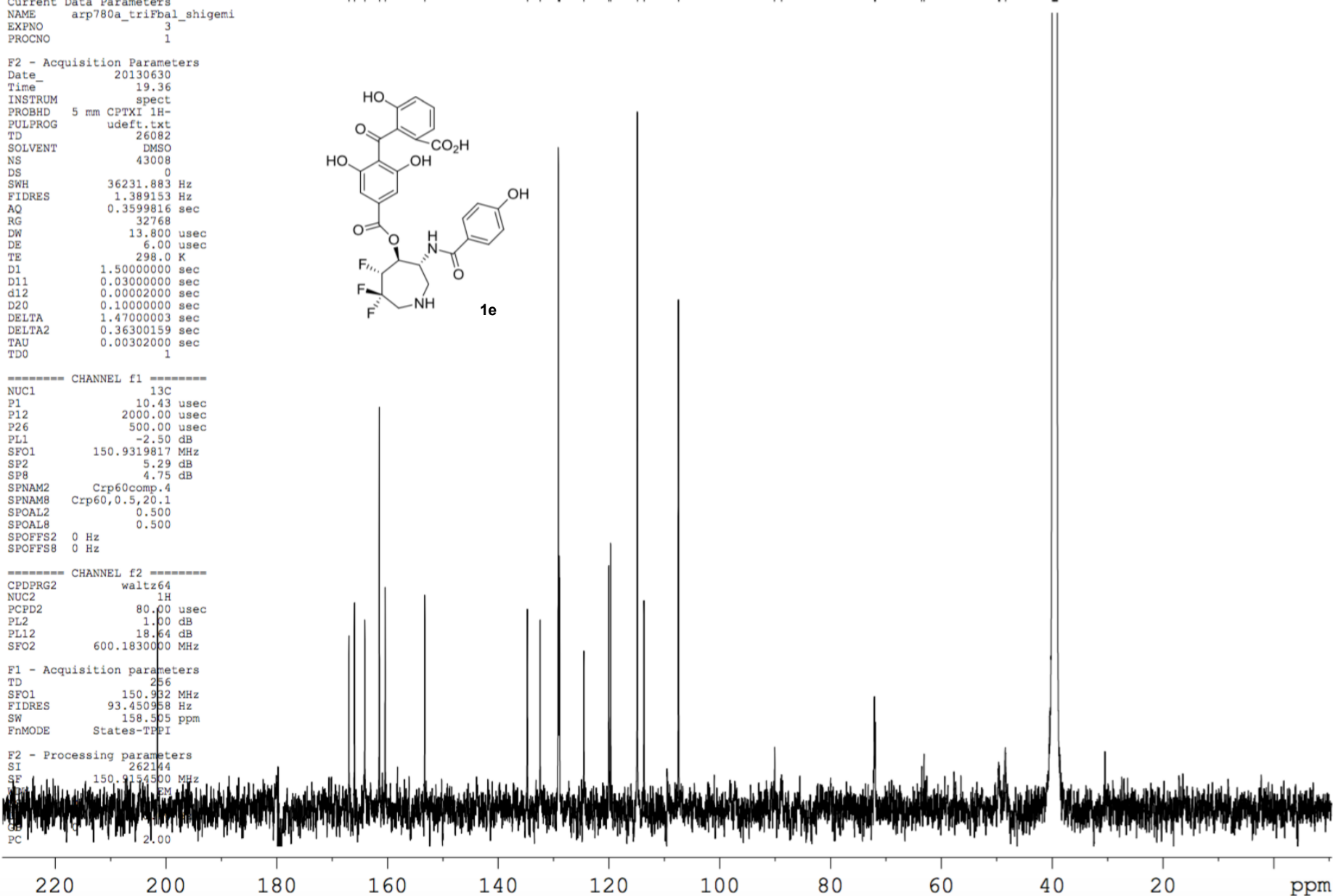
----- CHANNEL f1 -----
 NUC1 13C
 P1 10.43 usec
 P12 2000.00 usec
 P26 500.00 usec
 PL1 -2.50 dB
 SFO1 150.9319817 MHz
 SP2 5.29 dB
 SP8 4.75 dB
 SPNAM2 Crp60comp.4
 SPNAM8 Crp60,0.5,20.1
 SPOAL2 0.500
 SPOAL8 0.500
 SPOFFS2 0 Hz
 SPOFFS8 0 Hz

----- CHANNEL f2 -----
 CPDPRG2 waltz64
 NUC2 1H
 PCPD2 80.00 usec
 PL2 1.00 dB
 PL12 18.64 dB
 SFO2 600.1830000 MHz

F1 - Acquisition parameters
 TD 256
 SFO1 150.932 MHz
 FIDRES 93.450958 Hz
 SW 158.505 ppm
 FmMODE States-TFPI

F2 - Processing parameters
 SI 262144
 SF 150.9154500 MHz
 F2 600.1377500 MHz
 GB 1.00
 PC 2.00

166.94
 165.94
 164.09
 161.45
 160.41
 153.26
 134.72
 132.41
 129.14
 128.98
 128.90
 124.52
 120.00
 119.67
 114.87
 113.66
 107.44
 90.15
 88.85
 72.05
 71.90
 63.58
 63.09
 49.61
 49.46
 48.43
 39.94
 39.80
 39.66
 39.52
 39.38
 39.24
 39.10



II. Binding affinity measurements.

A. Binding assay for balanol and balanoids.

Compounds were tested by DiscoverRx, USA using the assay KINOMEscan™.^[1]

KINOMEscan™ is a competition-binding assay with quantitative measurement of the ability of a compound to compete with an immobilized, active-site directed ligand. The assay utilizes three components: a DNA-tagged kinase; an immobilized ligand; and a test compound. The ability of the test compound to compete with the immobilized ligand is measured via quantitative PCR of the DNA tag.

KINOMEscan™ Assay Principle

Compounds that bind the kinase active site and directly (sterically) or indirectly (allosterically) prevent kinase binding to the immobilized ligand and consequently reduce the amount of kinase captured on the solid support (A & B). Conversely, test molecules that do not bind the kinase have no effect on the amount of kinase captured on the solid support (C) (Figure 6.2). The dissociation constants (K_d 's) for test compound-kinase interactions are calculated by measuring the amount of kinase captured on the solid support as a function of the test compound concentration by using a quantitative, precise and ultra-sensitive qPCR method that detects the associated DNA label (D).

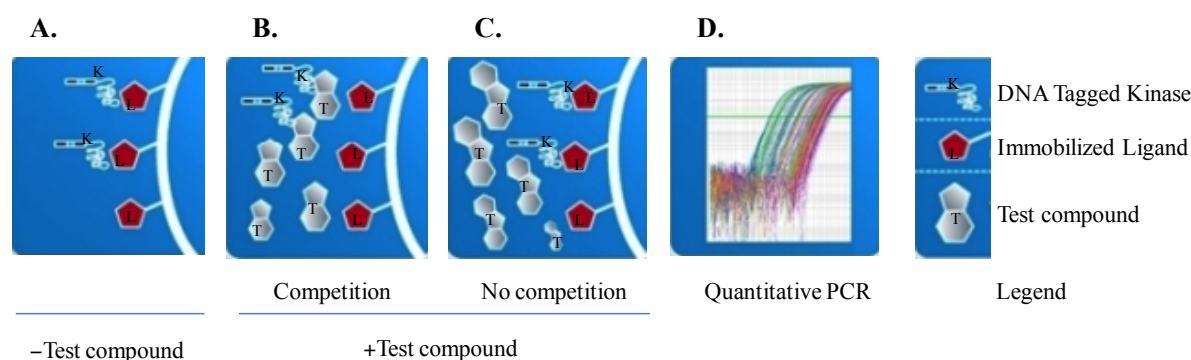


Figure S2.1. KINOMEscan™ assay schematic representation as provided by DiscoverX.^[1]

KINOMEscan™ Assay Protocol (as provided by DiscoverRx)

For most assays, kinase-tagged T7 phage strains were grown in parallel in 24-well blocks in an *E. coli* host derived from the BL21 strain. *E. coli* were grown to log-phase and infected with T7 phage from a frozen stock (multiplicity of infection = 0.4) and incubated with shaking at 32°C until lysis (90-150 minutes). The lysates were centrifuged (6,000 x g) and filtered (0.2µm) to remove

cell debris. The remaining kinases were produced in HEK-293 cells and subsequently tagged with DNA for qPCR detection. Streptavidin-coated magnetic beads were treated with biotinylated small molecule ligands for 30 minutes at room temperature to generate affinity resins for kinase assays. The liganded beads were blocked with excess biotin and washed with blocking buffer (SeaBlock (Pierce), 1 % BSA, 0.05 % Tween 20, 1 mM DTT) to remove unbound ligand and to reduce non-specific phage binding. Binding reactions were assembled by combining kinases, liganded affinity beads, and test compounds in 1x binding buffer (20 % SeaBlock, 0.17x PBS, 0.05 % Tween 20, 6 mM DTT). Test compounds were prepared as 40x stocks in 100% DMSO and directly diluted into the assay. All reactions were performed in polypropylene 384-well plates in a final volume of 0.04 ml. The assay plates were incubated at room temperature with shaking for 1 hour and the affinity beads were washed with wash buffer (1x PBS, 0.05 % Tween 20). The beads were then re-suspended in elution buffer (1x PBS, 0.05 % Tween 20, 0.5 μ M non-biotinylated affinity ligand) and incubated at room temperature with shaking for 30 minutes. The kinase concentration in the eluates was measured by qPCR.

Binding Affinities (K_d 's)

The binding constants (K_d 's) were calculated with a standard dose–response curve using the Hill equation:

$$\text{Response} = \frac{\text{Signal} - \text{Background}}{1 + (K_d^{\text{Hill Slope}}/\text{Dose}^{\text{Hill Slope}})}$$

The Hill Slope was set to -1 . Curves were fitted using a non–linear least square fit with the Levenberg–Marquardt algorithm.

References

- [1] M. A. Fabian, W. H. Biggs, D. K. Treiber, C. E. Atteridge, M. D. Azimioara, M. G. Benedetti, T. A. Carter, P. Ciceri, P. T. Edeen, M. Floyd, J. M. Ford, M. Galvin, J. L. Gerlach, R. M. Grotzfeld, S. Herrgard, D. E. Insko, M. A. Insko, A. G. Lai, J.-M. Lelias, S. A. Mehta, Z. V. Milanov, A. M. Velasco, L. M. Wodicka, H. K. Patel, P. P. Zarrinkar, D. J. Lockhart, *Nat Biotech* **2005**, *23*, 329-336.

B. Full set of binding constants and curves measured for balanol **1** and balanoids **1a–1e** against PKA/C isozymes.

The compounds were tested in duplicate experiments (Figure S2.2). The binding constants are tabulated in Table S2.1. The cross-references of compound/protein names and the assay codes are listed in Table S2.2.

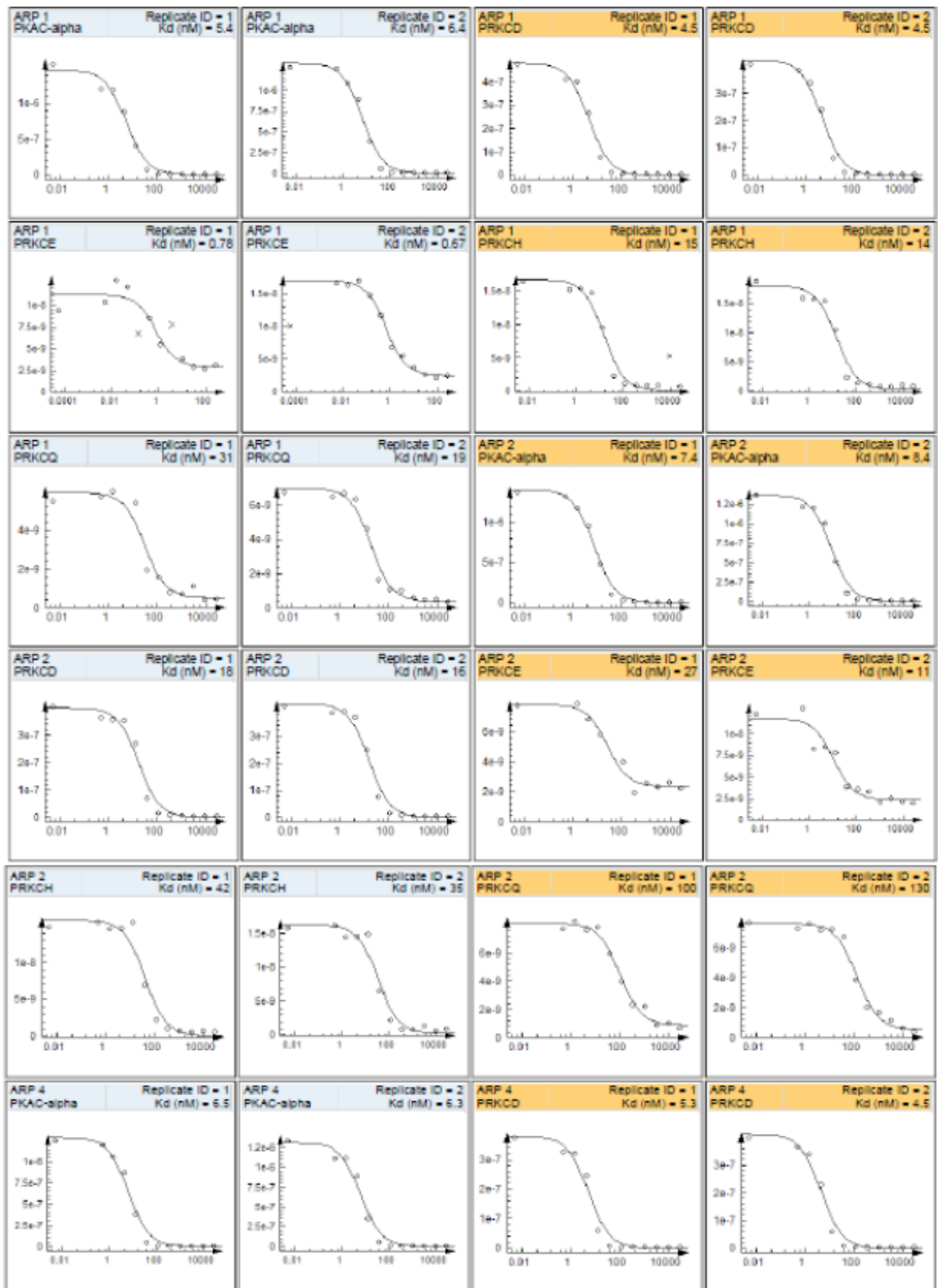
Table S2.1. K_d (nM) values of **1** and **1a–1e** against PKA and PKC isozymes in duplicate experiments.

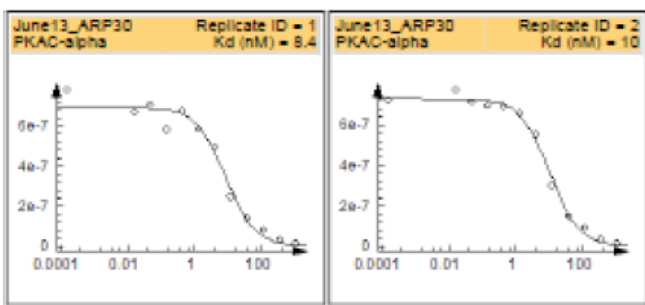
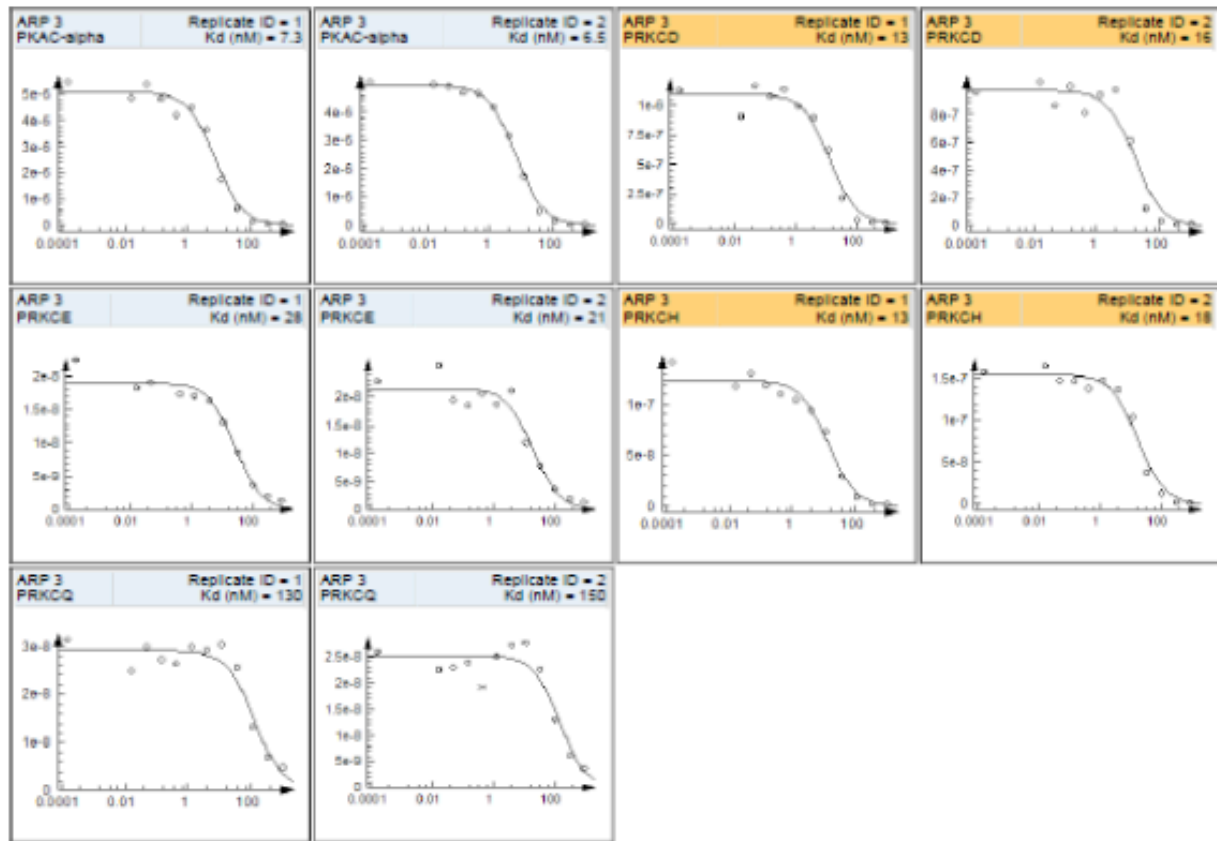
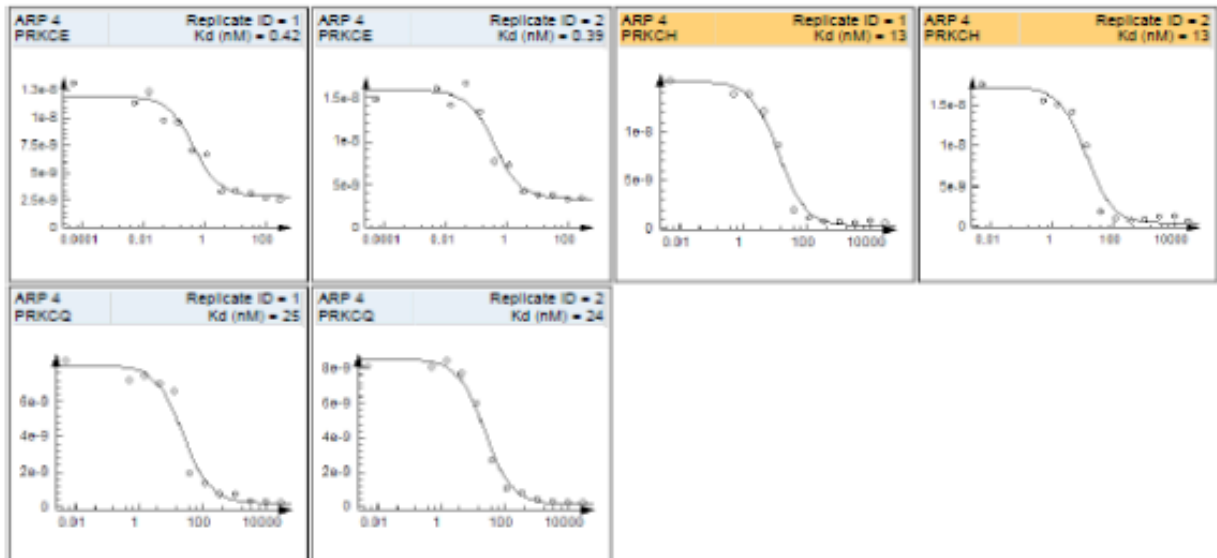
Compound	K_d (nM)				
	PKA	PKC δ	PKC ϵ	PKC η	PKC θ
1	5.4	4.5	0.78	15	31
1	6.4	4.5	0.78	14	19
1a	7.4	18	27	42	100
1a	8.4	16	11	35	130
1b	7.3	13	28	13	150
1b	6.5	16	21	18	130
1c	6.5	5.3	0.42	13	25
1c	6.3	4.5	0.39	13	24
1d	8.4	19	130	19	640
1d	10	20	93	20	520
1e	40	19	49	10	770
1e	47	18	26	14	930

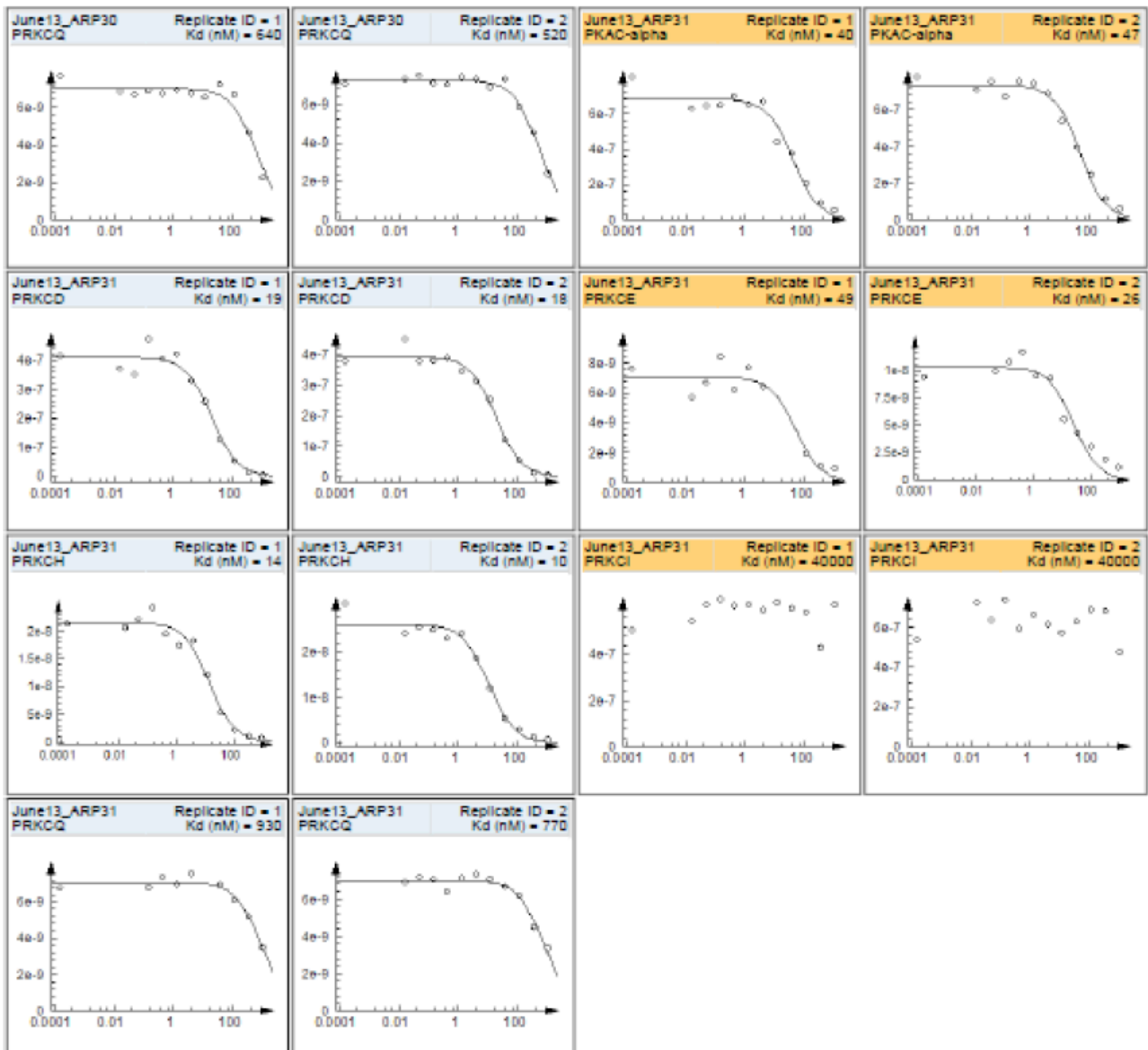
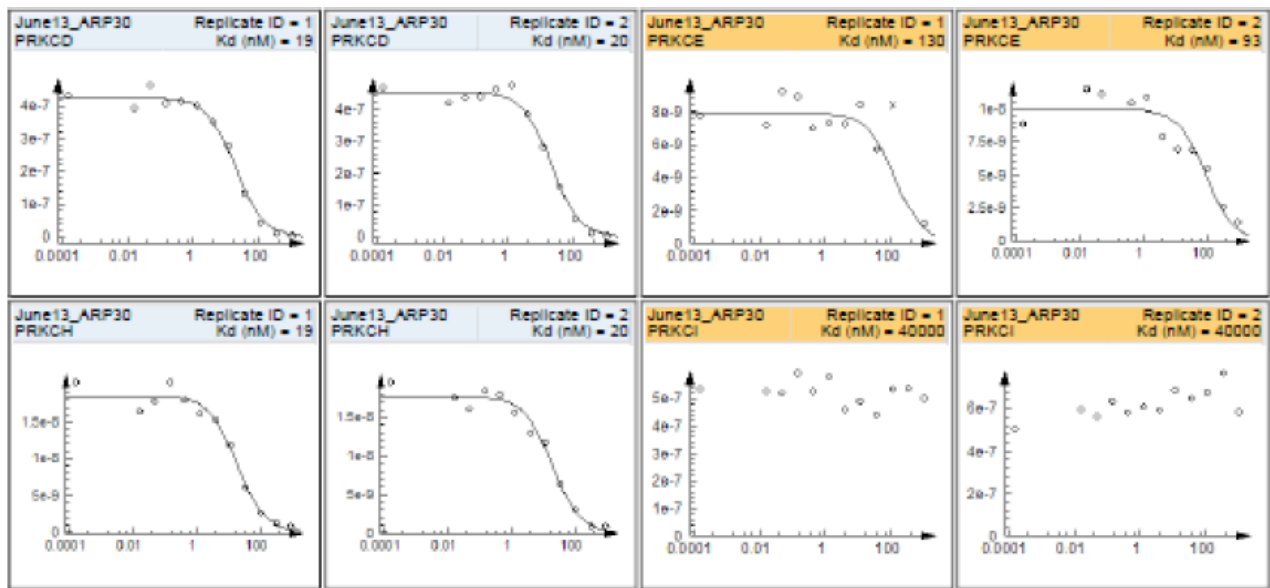
Table S2.2. Cross-references of compound/protein names and assay codes.

Compound	Assay code	Proteins	Protein code
1	ARP1	PKA	PKAC-alpha
1a	ARP2	PKCδ	PRKCD
1b	ARP3	PKCϵ	PRKCE
1c	ARP4	PKCη	PRKCH
1d	ARP30	PKCθ	PRKCQ
1e	ARP31	PKCι	PRKCI

Figure S2.2. Binding curve images of compounds **1** and **1a–1e** provided by DiscoverX.







III. Docking analysis.

A. Development of docking protocols using the balanol-PKA X-ray crystal structure 1BX6.

In order to find the optimum docking procedure which would reproduce the observed conformation of the balanol docked to PKA (1BX6), a few re-docking procedures were performed using the Molsoft ICM 3.7-2a Package (Neves et al. 2012). ICM exploits a Biased Probability Monte Carlo (BPMC) simulation (Abagyan & Totrov 1994) to find docking solutions. This Monte Carlo simulation globally optimizes internal coordinates of ligand within grid potential maps of a receptor binding site. The simulation involves four stages: (1) a random move which is applied to either the rotational, translational or conformational variables of the ligand in the binding pocket; (2) a minimization of differentiable terms of energy function; (3) a calculation of desolvation energy; and (4) a Metropolis selection criterion to accept or reject final minimized conformation. The stages are iteratively run until reaching the maximal number of steps. For the scoring function, ICM uses a weighted sum of ligand-receptor van der Waals interactions (with coefficients α_1 to α_5) of H-bond interactions (ΔE_{Hbond}), hydrogen bond donor-acceptor desolvation energy ($\Delta E_{HBDdesol}$), solvation electrostatic energy upon ligand binding (ΔE_{SolEl}), hydrophobic free energy gain (ΔE_{HPhob}) and a size correction term proportional to the number of ligand atoms (Q_{Size}) together with an internal force field energy of the ligand (ΔE_{IntEF}) and free energy changes due to conformational energy loss upon ligand binding ($T\Delta S_{Tor}$), (Neves et al. 2012). The scoring function is expressed as follows:

$$\Delta G = \Delta E_{IntFF} + T\Delta S_{Tor} + \alpha_1 \Delta E_{HBond} + \alpha_2 \Delta E_{HBDdesol} + \alpha_3 \Delta E_{SolEl} + \alpha_4 \Delta E_{HPhob} + \alpha_5 Q_{Size}$$

ICM also provides an option for semi-flexible docking through ligand and receptor complex refinement. The docking involves a two-step docking process. The first step is the docking of a flexible ligand and a rigid receptor and is followed by a refinement of the entire ligand-receptor complex. The procedure allows the side chains of the receptor to be fully flexible (Neves et al. 2012).

Before performing docking, molecules were assigned MMFF atom types for ligands and partial charges of protein atoms from library of ECEPP/3 residue templates. In addition, molecules were globally optimized to avoid steric clashes (Neves et al. 2012).

During the preliminary step of re-docking of balanol was carried out using two different approaches. In the first group of procedures (labelled group I), the approach of flexible ligand/rigid

receptor was used, while in the second (referred to as group II), the approach was to use flexible ligand/semi-flexible receptor docking simulation in which the side chain amino acid residues interacting with ligand were allowed to be flexible.

In group I docking, we investigated flexible ligand/rigid receptor docking simulations with or without water molecules as shown in the crystal structure, as well as running the simulation with different grid box size (25.09 x 26.63 x 24.07 Å or 32 x 32 x 32 Å). Docking simulations with and without water molecules were also conducted for the second group but without using the larger grid box size as the results from group I indicated that a smaller grid box size would be more reliable, which were then used exclusively for group II (flexible ligand and receptor side chain simulation). Seven replications were conducted for each simulation. The lowest root mean squared deviation (RMSD) for heavy atoms of the re-docked balanol conformation in each simulation were listed in Table S3.1.

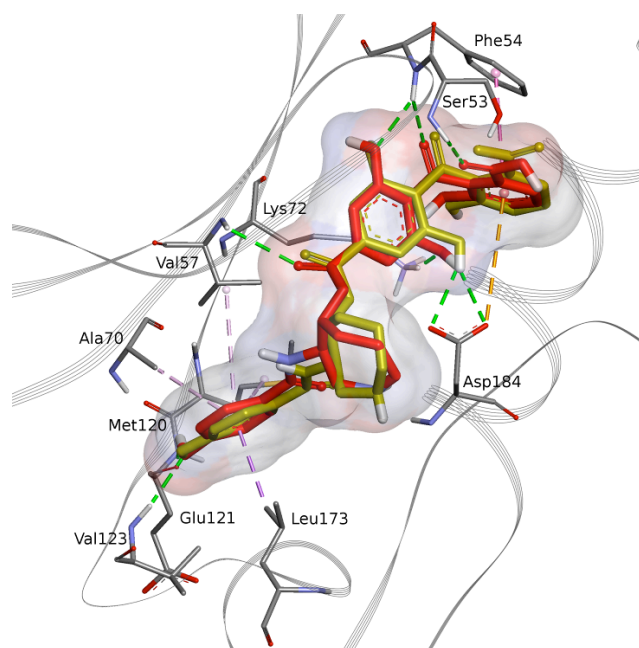
Table S3.1. The lowest RMSD for heavy atoms of balanol in 1BX6 obtained by various docking protocols.

Docking simulation procedures tested	The lowest RMSD from heavy atoms of balanol (Å)
<i>Group I: Flexible ligand and rigid receptor</i>	
In the presence of water molecules (25.09 x 26.63 x 24.07 Å)	1.01
In the absence of water molecules (25.09 x 26.63 x 24.07 Å)	1.03
Bigger size of grid box size (32 x 32 x 32 Å)	1.44
<i>Group II: Flexible ligand and flexible side chain residues of the receptor interacting with ligand</i>	
In the presence of water molecules (25.09 x 26.63 x 24.07 Å)	0.74
In the absence of water molecules (25.09 x 26.63 x 24.07 Å)	0.73

The lowest RMSD values are 0.74 and 0.73 Å for group II procedures with or without water molecules respectively, suggesting that flexible ligand/semi-flexible receptor docking procedure would be more appropriate for assessing balanol binding to PKA. This is comparable to existing methods that have also found that inclusion of flexibility is important for optimal docking (Wong et al. 2005; Rezácová et al. 2008). Docking simulation with or without water molecules appeared to give comparable results, which is consistent with the observation that no water molecule appear in the key interactions identified in the crystallographic structure of balanol and PKA complex.

The least RMSD value of 0.73 Å without water molecules was the best outcome for method validation. The overlay of the X-ray complex structure 1BX6 and this docking simulated structure of balanol-PKA is shown in Figure S3.1. The docking method reproduced the binding mode of balanol with very slight changes in the azepane and benzophenone conformations.

A



B

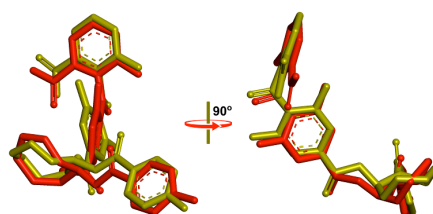


Figure S3.1. Structural comparison between 1BX6 and docking simulated structure of balanol bound to PKA. (A) The X-ray structure of balanol in the ATP site from 1BX6 (balanol in red) overlaid with the docking simulation structure for the same site with balanol (balanol in gold). The protein backbone is shown in grey ribbons and the amino acid sidechains are shown in sticks. (B) Overlay of the two balanol structures alone (balanol from 1BX6 in red and balanol from docking simulation in gold).

B. Construction of the PKC ϵ structural homology model (from PDB 3TXO and 1BX6).

X-Ray crystal structure for the human PKC ϵ (Q02156) is unavailable yet, although there is a crystal structure (PDB: 3TXO) for human PKC η with naphthyridine bound in the adenine subsite of the ATP pocket. BLAST analysis (<http://blast.ncbi.nlm.nih.gov/Blast.cgi>) indicated 83.2% primary sequence homology (69.8 % identity) between PKC ϵ and PKC η . Likewise, mouse PKA (PDB: 1BX6) and human PKC ϵ showed 54.1% primary sequence homology (36.4% identity by CLUSTAL 2.1, <http://www.ebi.ac.uk/Tools/msa/clustalo/>) (McWilliam et al. 2013). The alignment of three proteins is shown in Figure S3.2.

CLUSTAL 2.1 multiple sequence alignment

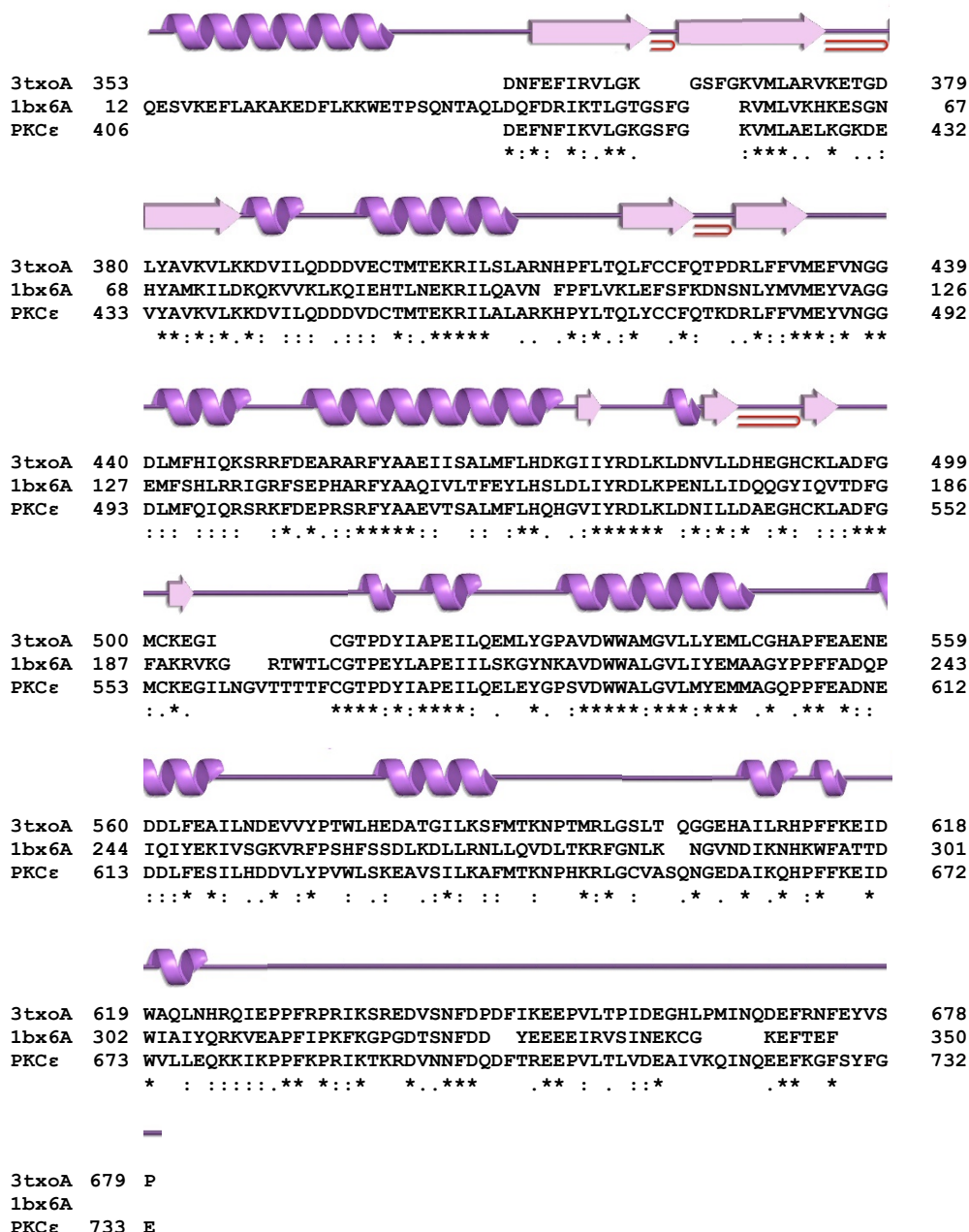


Figure S3.2. Human PKC η (P24723), PKA mouse (P05132) and PKC ϵ human (Q02156) alignment using CLUSTAL 2.1. “*” - identical residue; “:” - one of the following 'strong' groups is fully conserved residue; “.” - one of the following 'weaker' groups is fully conserved.

The catalytic domain of protein kinases have two forms with either “open” or “closed” conformation, both of which can be bound to a ligand in the ATP site. The structure 3TXO shows the naphthyridine ligand bound in the “closed” conformation of the receptor, while in 1BX6, balanol is bound to the “open” conformation. PKC ϵ is likely to bind to balanol in a conformation analogous to that of PKA with balanol bound (Narayana et al. 1999). Hence, 1BX6 was used as the

main structural template to model the open conformation of PKC ϵ around the ligand and 3TXO as a template for the rest of the protein.

Firstly, 3TXO and 1BX6 were structurally aligned using jCE algorithm (Prlic et al. 2010) to examine the equivalency of both structures. The result showed that the RMSD of their structures is 1.65 Å and they share identity and similarity at 34.23% and 51.35%, respectively. Next, the sequence of human PKC ϵ was aligned with the sequences of 3TXO and 1BX6 using CLUSTAL 2.1 and also edited manually to maintain the “open” conformation at the glycine-rich loop (GXGXXG) in 3TXO (Taylor et al. 2011).

The three dimensional model of human PKC ϵ with bound balanol was built using Modeller 9.14 (Eswar et al. 2008). The resulting models were ranked using the DOPE score (Shen & Sali 2006). The score represents the quality of the model and the lower the score, the more native-like the corresponding model. The model was further assessed (Table S3.2) using Ramachandran plot on PROCHECK webserver (Laskowski et al. 2001).

Table S3.2. Statistics of Ramachandran plot of the PKC ϵ structure homology model with balanol bound.

	Number of residues	%
Residues in most favoured regions	271	91.8
Residues in additional allowed regions	16	5.5%
Residues in generously allowed regions	6	2.0%
Residues in disallowed regions	2	0.7%

PROCHECK has suggested that a good quality model would be expected to have over 90% in the most favoured regions, based on an analysis of 118 structures of at least 2.0 Å resolution and R-factor no greater than 20%, (Laskowski et al. 2001). Thereby, the selected PKC ϵ model can be considered of good quality, with a score of 91.8% in the most favoured regions.

The docking simulated structure of balanol bound to PKC ϵ is compared to the crystal structure of balanol bound to PKA in Figure S3.3. The close contact between the benzophenone and the glycine-rich loop is similar in these two structures, and the key backbone H-bonding between the *p*-hydroxybenzamide phenol to the conserved Glu amino acid residue (Glu 121 in PKA and Glu 487 in PKC ϵ) is also maintained in both. However, the azepane conformation in these two structures is significantly different, with the azepane ring making more H-bonding interactions in the case of the PKC ϵ model. The key ligand-protein interactions in both structures are tabulated in Table S3.3.

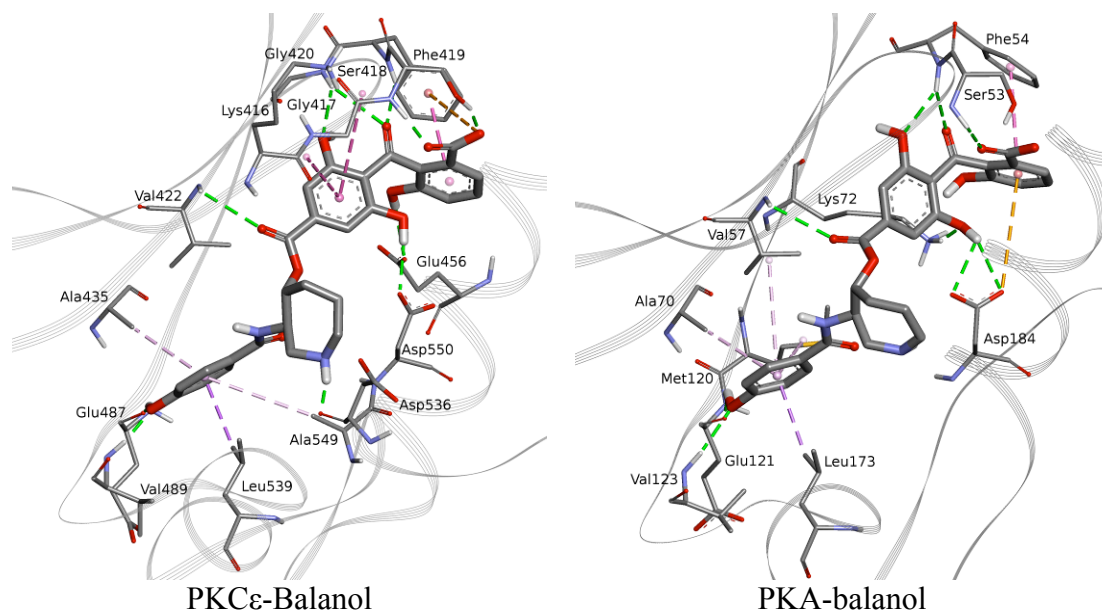


Figure S3.3. The docking simulated structure of balanol bound to PKC ϵ is compared to the crystal structure of balanol bound to PKA.

Table S3.3. Key amino acid residue contact comparison for balanol binding to mouse PKA (1BX6) and human PKC ϵ (from docking simulation). These amino acid residues are important in balanol binding in the ATP site according to 1BX6.

Key ATP binding contact

Glycine rich loop
Catalytic lysine
Activation loop

PKA ⁴⁷KTLGTGSFGRVMLVKHKESGNHYAMK⁷²...¹²⁰MEYVAGGEMF¹²⁹...¹⁸⁴DFG

PKC ϵ ⁴¹²KVLGKGSFGKVMLAELKKGKDEVYAVK⁴³⁷...⁴⁸⁶MEYVNGGDLMF⁴⁹⁶...⁵⁵⁰DFG

PKC ϵ residues	Balanol motifs	Type ^a	Subtype ^a	Matching PKA residues	Balanol motifs	Type	Subtype
Lys416 [^]	C2'-C7' ring	π - π	BB				
Gly417 [^]	C2'-C7' ring	π - π	BB				
Ser418 [#]	C15''- CO ₂ H	H-bond	BB	Ser53	C15''- CO ₂ H	H-bond	BB
Phe419 [#]	C15''- CO ₂ H	π -Anion	SC	Phe54	C4''-OH	H-bond	BB
Phe419 [#]	C9''- C14'' ring	π - π Stacking	SC	Phe54	C9''- C14'' ring	π - π Stacking	SC
Phe419 [^]	C8'=O	H-bond	BB	Phe54	C8''=O	H-bond	BB
Gly420 [^]	C8'=O	H-bond	BB				
Gly420 [#]	C4''-OH	H-bond	BB				
Val422 [#]	C1''=O	H-bond	BB	Val57	C1''=O	H-bond	BB
				Val57	C2'-C7' ring	π -Alkyl	SC
Ala435 [^]	C2'-C7' ring	π -Alkyl	SC	Ala70	C2'-C7' ring	π -Alkyl	SC
				Lys72	C6''-OH	H-bond	SC
Glu456 [#]	C10''-OH	H-bond	SC				
				Met120	C2'-C7' ring	π -Alkyl	SC
Glu487 [^]	C5'-OH	H-bond	BB	Glu121	C5'-OH	H-bond	BB
Val489 [^]	C5'-OH	H-bond	BB	Val123	C5'-OH	H-bond	BB
Leu539 [^]	C2'-C7' ring	π - σ	SC	Leu173	C2'-C7' ring	π - σ	SC
Asp550 [#]	C6''-OH	H-bond	SC	Asp184	C6''-OH	H-bond	SC
				Asp184	C9''- C14'' ring	π -Anion	SC
Asp536 [*]	N1	H-bond	BB				
Ala549 [^]	C2'-C7' ring	π - σ	SC				

^a H-bond: hydrogen bond; BB : backbone; SC : side chain

[^] p-Hydroxybenzamide moiety binding interactions

^{*} Azepan moiety binding interactions

[#] Benzophenone moiety binding interactions

C. Docking simulation of balanoids to PKA/C using optimized docking simulation procedure.

Balanoids (**1a**, **1c**, and **1d**) were used for docking analysis using the mouse PKA crystal structure (1BX6) and the PKC ϵ structural homology model (Figure S3.4). These balanoids were built by adding fluorine atoms at particular positions of the seven-membered azepane ring of the natural

balanol. Each balanoid was subjected to the optimised docking procedure and docked into PKA (see section A) with seven replication each. The simulation indicates that all balanoids have highly similar conformations and occupy the ATP site of PKA in similar positions and binding orientations (Figure S3.5).

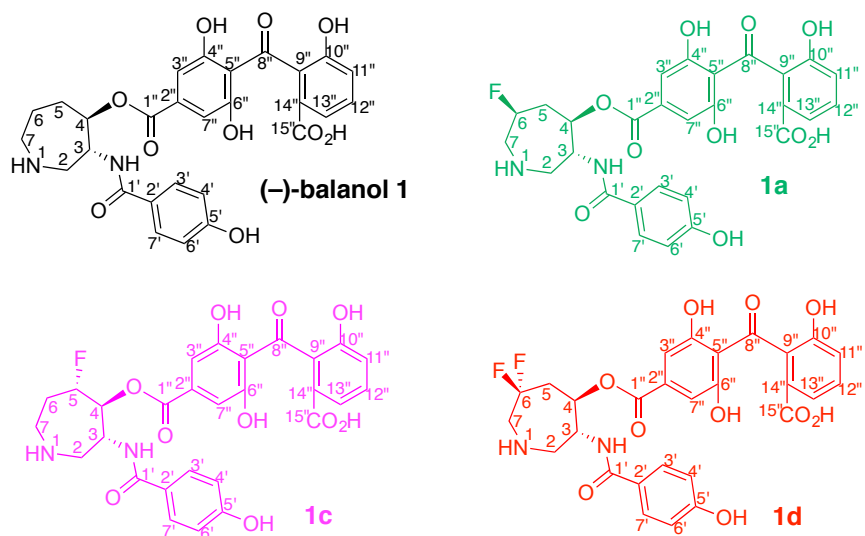


Figure S3.4. Structures of balanol (**1**) and balanoids (**1a**, **1c**, and **1d**) used for docking analysis. Balanol **1**: black; **1a**: green; **1c**: pink; and **1d**: red. The colour codes are used throughout the section.

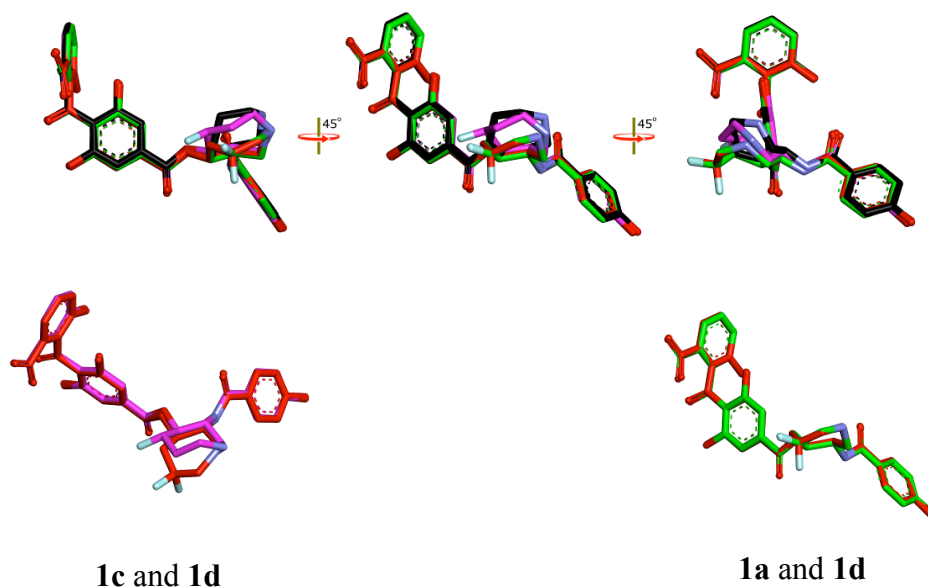


Figure S3.5. An overlay of the bound form of balanol with balanoids **1a**, **1c**, and **1d** in PKA (according to the same color codes as in Figure S3., Balanol **1**: black; **1a**: green; **1c**: pink; and **1d**: red) viewed from multiple angles. Pairwise overlay of the bound conformations of balanoids are also shown to highlight the similarities and differences in their conformations.

In particular, the benzophenone binding conformations are similar across balanol and the balanoids, which is consistent with the experimental observations that these compounds have similar binding affinities to PKA. In addition, the *p*-hydroxybenzamide binding conformations of these compounds

are also very similar, and the azepane moiety is the only part of that undergoes noticeable conformational changes. These results again suggest good correlation between the measure binding affinities and interaction profiles identified by the docking analysis.

Likewise, each balanoid was subjected to the optimised docking procedure (section B) with seven replicates each. The grid maps derived from the PKC ϵ structure homology model was used for the docking simulation. The calculated binding energies (ΔG°) were listed along with the experimental K_d in Table S3.4.

Table S3.4. Experimental K_d values of the balanoids binding to PKC ϵ and their calculated ΔG° obtained from docking simulation.

Balanoids	K_d (nM)	$\ln K_d$	Calculated ΔG°
1	0.73	-21.04	-26.11
7 1a	19	-17.78	-23.75
9 1c	0.4	-21.64	-26.36
12 1d	110	-16.02	-21.44

Graphical plotting between $\ln K_d$ of the balanoids and calculated ΔG° showed good linear correlation (Figure 3.6).

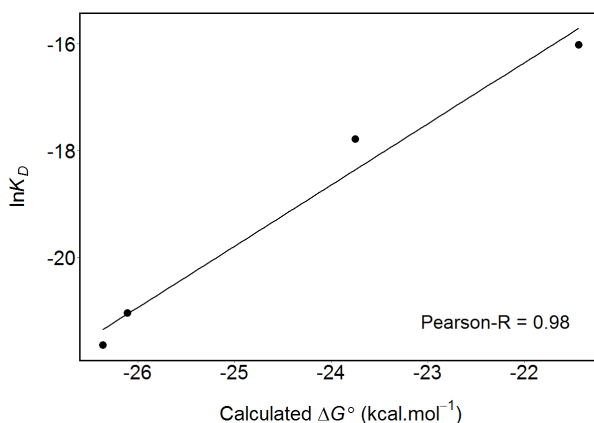


Figure S3.6. Correlation between $\ln K_d$ and calculated ΔG° of binding between the balanoids and PKC ϵ .

As was the case with PKA, the bound ligand conformation to PKC ϵ is similar across the panel. In particular, the binding interactions of the benzophenone moiety appeared to be very conserved across all members. Larger conformational differences of the azepane ring appeared in the ribose-binding subsite and the *p*-hydroxybenzamide motif in the adenine subsite, with **1**, **1a**, and **1c** being comparable, and **1d** different from the other three (Figure 3.7).

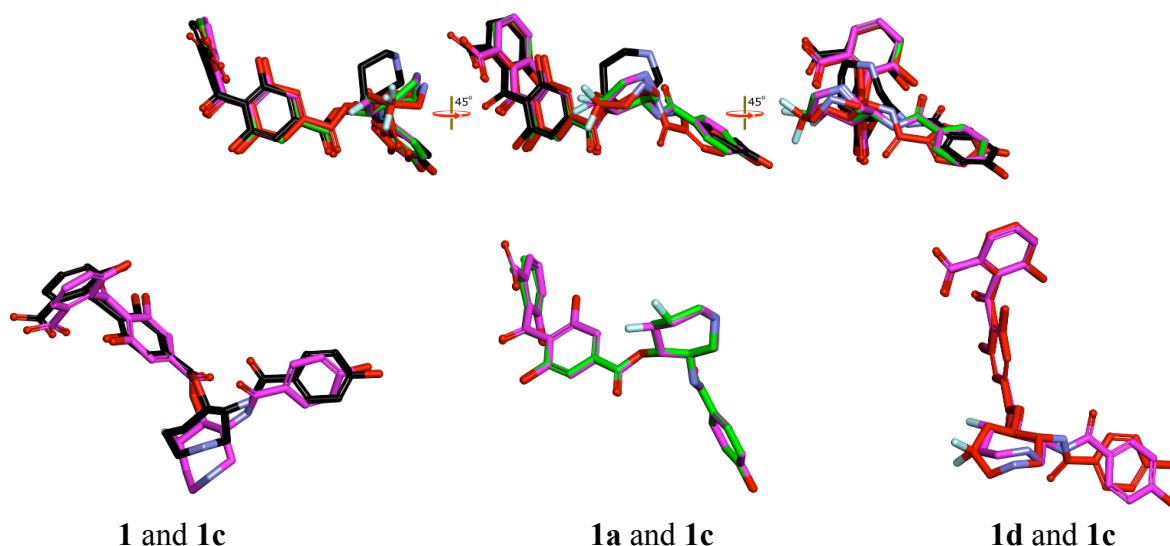


Figure S3.7. An overlay of bound balanol/balanoids conformations in PKCε (according to the same color codes as in Figure S3., Balanol **1**: black; **1a**: green; **1c**: pink; and **1d**: red). Pairwise overlay of the bound conformations of balanoids are also shown to highlight the similarities and differences in their conformations.

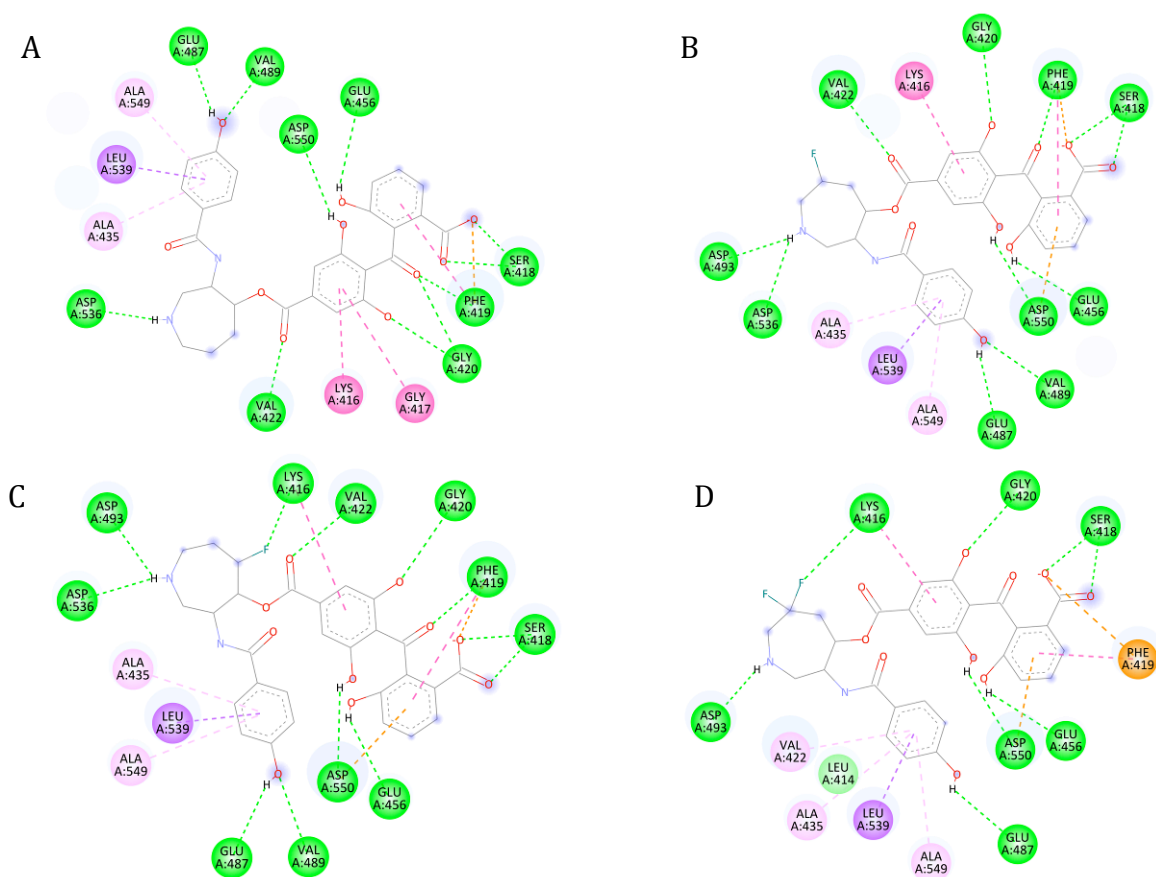


Figure S3.8. Two-dimensional graphical representations of ligand-receptor interactions of balanoids (A) **1**, (B) **1a**, (C) **1c**, and (D) **1d** with PKCε. The interaction visualisation was generated using Discovery Studio Visualizer (Systeme 2016).

In general, the key interactions, as identified earlier in section I between the benzophenone motif of balanol and PKA, are preserved here in the case of balanoids **1**, **1a**, **1c** and **1d** with PKC ϵ (Table S3.5, Figure S3.8, and Figure S3.9). These include: hydrogen bonds with hydroxyl of Ser418 and carboxyl of Glu456. The first ring also interacted with Phe419 via π - π interaction. Meanwhile, the Gly420 backbone and the side chain of Asp550 made hydrogen bonds with the second ring of benzophenone moiety. Those interactions suggest stabilisation of the benzophenone moiety of balanol analogues at the ATP binding site of PKC ϵ .

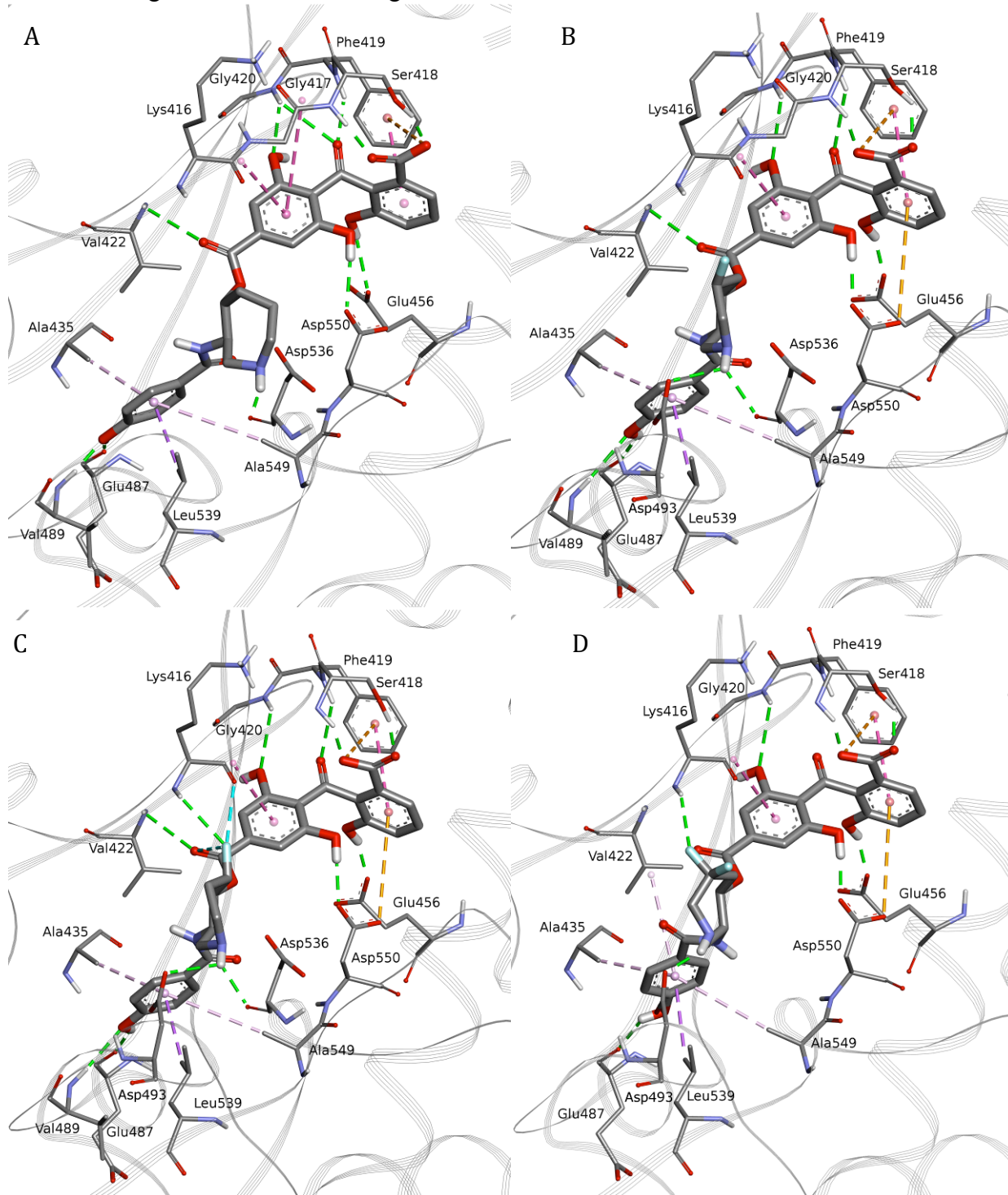


Figure S3.9. Ligand-receptor interactions of balanoids (A) **1**, (B) **1a**, (C) **1c**, and (D) **1d** with PKC ϵ .

Table S3.5. Comparison of ligand-receptor interactions of balanoids **1**, **1a**, **1c**, and **1d** with PKC ϵ .

Residues	Balanol1 (1)			Balanol7 (1a)			Balanol9 (1c)			Balanol12 (1d)		
	Balanol motifs	Type ^a	Subtype ^a	Balanol motifs	Type	Subtype	Balanol motifs	Type	Subtype	Balanol motifs	Type	Subtype
Lys416 [^]	C2'-C7' ring	π - π	BB	C2'-C7' ring	π - π	BB	C2'-C7' ring	π - π	BB	C2'-C7' ring	π - π	BB
Lys416 [*]							C5-F	H-bond	BB	C6-F	H-bond	BB
Gly417 [^]	C2'-C7' ring	π - π	BB									
Ser418 [#]	C15''- CO ₂ H	H-bond	BB	C15''- CO ₂ H	H-bond	BB	C15''- CO ₂ H	H-bond	BB	C15''- CO ₂ H	H-bond	BB
Ser418 [#]	C15''- CO ₂ H	H-bond	SC	C15''- CO ₂ H	H-bond	SC	C15''- CO ₂ H	H-bond	SC	C15''- CO ₂ H	H-bond	SC
Phe419 [#]	C15''- CO ₂ H	π -Anion	SC	C15''- CO ₂ H	π -Anion	SC	C15''- CO ₂ H	π -Anion	SC	C15''- CO ₂ H	π -Anion	SC
Phe419 [#]	C9''- C14'' ring	π - π Stacking	SC	C9''- C14'' ring	π - π Stacking	SC	C9''- C14'' ring	π - π Stacking	SC	C9''- C14'' ring	π - π Stacking	SC
Phe419 [^]	C8'=O	H-bond	BB	C8'=O	H-bond	BB	C8'=O	H-bond	BB			
Gly420 [^]	C8'=O	H-bond	BB									
Gly420 [#]	C4''-OH	H-bond	BB	C4''-OH	H-bond	BB	C4''-OH	H-bond	BB	C4''-OH	H-bond	BB
Val422 [#]	C1''=O	H-bond	BB	C1''=O	H-bond	BB	C1''=O	H-bond				
Ala435 [^]	C2'-C7' ring	π -Alkyl	SC	C2'-C7' ring	π -Alkyl	SC	C2'-C7' ring	π -Alkyl	SC	C2'-C7' ring	π -Alkyl	SC
Glu456 [#]	C10''-OH	H-bond	SC	C10''-OH	H-bond	SC	C10''-OH	H-bond	SC	C10''-OH	H-bond	SC
Glu487 [^]	C5'-OH	H-bond	BB	C5'-OH	H-bond	BB	C5'-OH	H-bond	BB	C5'-OH	H-bond	BB
Val489 [^]	C5'-OH	H-bond	BB	C5'-OH	H-bond	BB	C5'-OH	H-bond	BB			
Asp493 [*]				N1	H-bond	SC	N1	H-bond	SC	N1	H-bond	SC
Asp536 [*]	N1	H-bond	BB	N1	H-bond	BB	N1	H-bond	BB			
Leu539 [^]	C2'-C7' ring	π - σ	SC	C2'-C7' ring	π - σ	SC	C2'-C7' ring	π - σ	SC	C2'-C7' ring	π - σ	SC
Ala549 [^]	C2'-C7' ring	π - σ	SC	C2'-C7' ring	π - σ	SC	C2'-C7' ring	π - σ	SC	C2'-C7' ring	π - σ	SC
Asp550 [#]	C6''-OH	H-bond	SC	C6''-OH	H-bond	SC	C6''-OH	H-bond	SC	C6''-OH	H-bond	SC
				C9''- C14'' ring	π -Anion	SC	C9''- C14'' ring	π -Anion	SC	C9''- C14'' ring	π -Anion	SC

^a H-bond: hydrogen bond; BB: backbone; SC: side chain. [^] Benzamide moiety binding interactions. ^{*} Azepan moiety binding interactions. [#] Benzophenone moiety binding interactions

The details of H-bonds are presented in Table S3.6. The balanoid **1c** has the maximum H-bonds (12), followed closely by **1a** (with 11) and **1** (10), while **1d** has the least bonds (8). These are consistent with the $\ln K_d$ values shown in Table S3.4, where **1** has a higher affinity than **1a**, and **1d**. The interaction with Gly420 is specific to **1**, as balanoids interact with Asp493, which is not seen with **1**.

Table S3.6. H-bond distances among balanoids in PKC ϵ binding site.

	H-bond distances (Å)			
	Balanol1 (1)	Balanol7 (1a)	Balanol9 (1c)	Balanol12 (1d)
Lys416			2.90	2.73
Ser418	1.97	1.98	1.92	1.99
Ser418	1.86	1.86	1.75	1.84
Phe419	2.07	2.88	2.81	
Gly420	2.36			
Gly420	2.93	2.85	2.86	3.00
Val422	3.06	2.97	2.96	
Glu456	2.47	1.80	1.83	1.84
Glu487	1.85	2.13	2.07	2.48
Val489	1.77	2.50	2.41	
Asp493		2.37	2.50	1.78
Asp536	1.83	2.34	2.16	
Asp550	2.24	1.99	2.02	1.94

A comparison of **1c** bound to PKA and to PKC ϵ is informative in understanding interactions that are unique to each complex (Figure S3.10). We note that the H-bond of **1c** and Asp493 of PKC ϵ (which is conserved among all balanoids; Table S3.6) is the case of PKA, where this residue is replaced by Glu127, which is beyond H-bonding distance from N1H. Furthermore, the interaction between F (on C5) of **1c** and the backbone of Lys416 of PKC ϵ is replaced by a single interaction in PKA with the CO of equivalent residue, Thr51. A comparison of **1c** and **1d** bound to PKA is shown in Figure S3.7. The interactions in the azepane, benzophenone and the *p*-hydroxybenzyl regions are comparable for these two compounds.

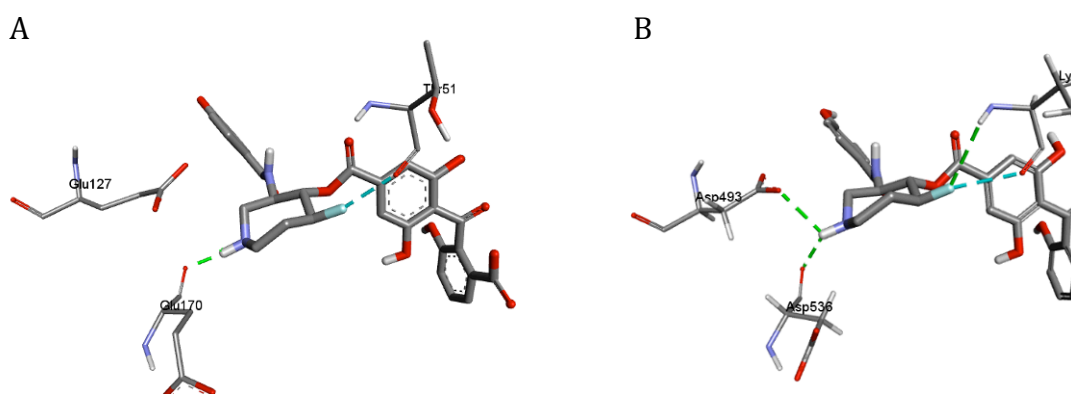


Figure S3.10. A comparison of **1c** docked on (A) PKA and (B) PKC ϵ . Two H-bonding interactions are missing in the complex of **1c** and PKA.

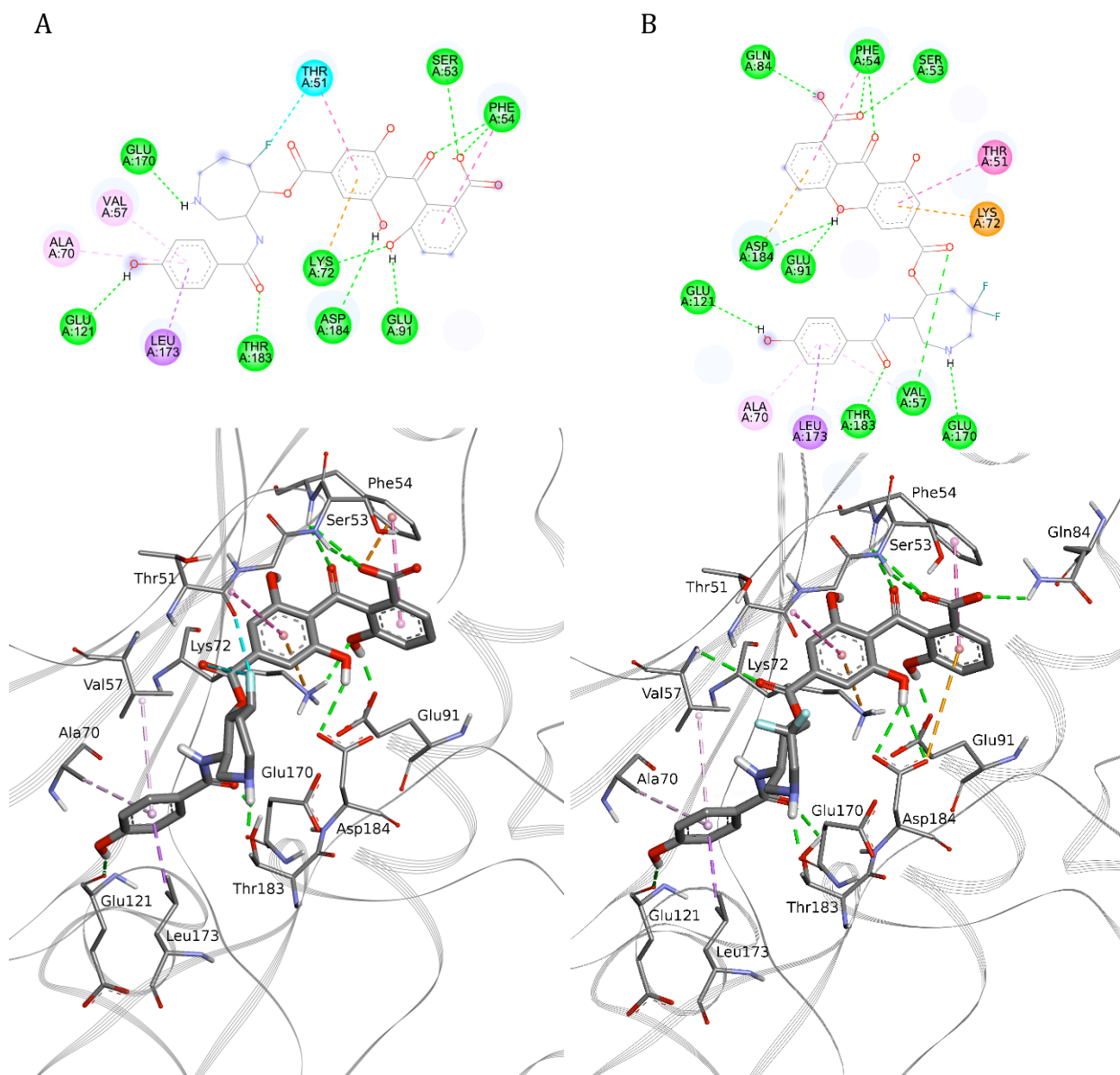


Figure S3.11. Ligand-receptor interactions of balanoids (A) **1c**, and (B) **1d** with PKA.

Table S3.7. Comparison of Non-covalent interaction of the balanoid **1c** and **1d** in PKA.

Residues	1c			1d		
	Balanol motifs	Type ^a	Subtype ^a	Balanol motifs	Type	Subtype
Thr51[#]	C2''-C7'' ring	π -Alkyl	BB	C2''-C7'' ring	π -Alkyl	BB
Ser53[#]	C15''- CO ₂ H	H-bond	BB	C15''- CO ₂ H	H-bond	BB
Phe54[#]	C15''- CO ₂ H	H-bond	BB	C15''- CO ₂ H	H-bond	BB
Phe54[#]	C15''- CO ₂ H	π -Anion	side chain			
Phe54[#]	C9''- C14'' ring	π - π Stacking	SC	C9''- C14'' ring	π - π Stacking	SC
Phe54[#]	C8''=O	H-bond	BB	C8''=O	H-bond	BB
Val57[^]	C2'-C7' ring	π -Alkyl	SC	C2'-C7' ring	π -Alkyl	SC
Val57[#]				C1''=O	H-bond	BB
Ala70[^]	C2'-C7' ring	π -Alkyl	SC	C2'-C7' ring	π -Alkyl	SC
Lys72[#]	C10''-OH	H-bond	SC			
Lys72[#]	C2''-C7'' ring	π -Cation	SC	C2''-C7'' ring	π - Cation	SC
Gln84[#]				C15''- CO ₂ H	H-bond	SC
Glu91[#]	C10''-OH	H-bond	SC	C10''-OH	H-bond	SC
Glu121[^]	C5'-OH	H-bond	BB	C5'-OH	H-bond	BB
Glu170[*]	N1	H-bond	BB	N1	H-bond	BB
Leu173[^]	C2'-C7' ring	π - σ	SC	C2'-C7' ring	π - σ	SC
Thr183[^]	C1'=O	H-bond	SC	C1'=O	H-bond	SC
Asp184[#]	C6''-OH	H-bond	SC	C6''-OH	H-bond	SC
Asp184[#]				C9''- C14'' ring	π -Anion	SC

^a H-bond: hydrogen bond; BB: backbone; SC: side chain.

[^] Benzamide moiety

^{*} Azepan moiety

[#] Benzophenone moiety

D. References

- Abagyan, R. & Totrov, M., 1994. Biased Probability Monte Carlo Conformational Searches and Electrostatic Calculations for Peptides and Proteins. *Journal of molecular biology*, 235(3), pp.983–1002.
- Eswar, N. et al., 2008. Protein Structure Modeling with MODELLER. In B. Kobe, M. Guss, & T. Huber, eds. *Structural Proteomics High-Throughput Methods*. Methods in Molecular Biology™. Humana Press, pp. 145–159. Available at: http://dx.doi.org/10.1007/978-1-60327-058-8_8.
- Laskowski, R.A., MacArthur, M.W. & Thornton, J.M., 2001. PROCHECK: validation of protein structure coordinates. In M. G. Rossmann & E. D. Arnold, eds. *International Tables of Crystallography, Volume F. Crystallography of Biological Macromolecules*. The Netherlands: Kluwer Academic Publishers, pp. 722–725.
- McWilliam, H. et al., 2013. Analysis Tool Web Services from the EMBL-EBI. *Nucleic acids research*, 41(Web Server issue), pp.597–600.
- Narayana, N. et al., 1999. Crystal Structure of the Potent Natural Product Inhibitor Balanol in Complex with the Catalytic Subunit of cAMP-Dependent Protein Kinase. *Biochemistry*, 38(8), pp.2367–2376. Available at: <http://dx.doi.org/10.1021/bi9820659>.
- Neves, M. a C., Totrov, M. & Abagyan, R., 2012. Docking and scoring with ICM: the benchmarking results and strategies for improvement. *Journal of computer-aided molecular design*, 26(6), pp.675–86. Available at: <http://www.pubmedcentral.nih.gov/articlerender.fcgi?artid=3398187&tool=pmcentrez&render type=abstract> [Accessed December 3, 2014].
- Prlic, A. et al., 2010. Pre-calculated protein structure alignments at the RCSB PDB website. *Bioinformatics (Oxford, England)*, 26(23), pp.2983–5. Available at: <http://www.pubmedcentral.nih.gov/articlerender.fcgi?artid=3003546&tool=pmcentrez&render type=abstract> [Accessed January 4, 2015].
- Rezácová, P. et al., 2008. Crystal structure and putative function of small Toprim domain-containing protein from *Bacillus stearothermophilus*. *Proteins*, 70(2), pp.311–319.
- Shen, M.-Y. & Sali, A., 2006. Statistical potential for assessment and prediction of protein structures. *Protein science : a publication of the Protein Society*, 15(11), pp.2507–24. Available at: <http://www.pubmedcentral.nih.gov/articlerender.fcgi?artid=2242414&tool=pmcentrez&render type=abstract> [Accessed September 29, 2014].
- Systèmes, D., 2016. Dassault Systèmes BIOVIA, Discovery Studio Modeling Environment, Release 2016.
- Taylor, S.S., Kornev, A.P. & Manuscript, A., 2011. Protein Kinases: Evolution of Dynamic Regulatory Proteins. *Trends in biochemical sciences*, 36(2), pp.65–77. Available at: <http://www.ncbi.nlm.nih.gov/pmc/articles/PMC3084033/>.
- Wong, C.F. et al., 2005. Molecular docking of balanol to dynamics snapshots of protein kinase A. *Proteins: Structure, Function and Genetics*, 61(4), pp.850–858.